University of New Hampshire
University of New Hampshire Scholars' Repository

Doctoral Dissertations | Student Scholarship

Spring 2022

N-HETEROCYCLIC CARBENE FUNCTIONALIZED SINGLE-CHAIN NANOPARTCLES AQUEOUS CATALYTIC PLATFORM

Xianggeng Liu
University of New Hampshire, Durham

Follow this and additional works at: https://scholars.unh.edu/dissertation

Recommended Citation

Liu, Xianggeng, "N-HETEROCYCLIC CARBENE FUNCTIONALIZED SINGLE-CHAIN NANOPARTCLES AQUEOUS CATALYTIC PLATFORM" (2022). *Doctoral Dissertations*. 2683.
https://scholars.unh.edu/dissertation/2683

This Dissertation is brought to you for free and open access by the Student Scholarship at University of New Hampshire Scholars' Repository. It has been accepted for inclusion in Doctoral Dissertations by an authorized administrator of University of New Hampshire Scholars' Repository. For more information, please contact Scholarly.Communication@unh.edu.

N-HETEROCYCLIC CARBENE FUNCTIONALIZED SINGLE-CHAIN NANOPARTCLES AQUEOUS CATALYTIC PLATFORM

BY

XIANGGENG LIU

B.S., Southern University of Science and Technology, 2015

DISSERTATION

Submitted to the University of New Hampshire
in Partial Fulfillment of
the Requirements for the Degree of

Doctor of Philosophy
in
Chemistry

May 2022

ALL RIGHTS RESERVED
© 2022
Xianggeng Liu

This dissertation was examined and approved in partial fulfillment of the requirements for the degree of Doctor of Philosophy in Chemistry by:

Dissertation Director, Erik Berda, Professor of Chemistry and Materials Science

John Tsavalas, Associate Professor of Chemistry and Materials Science

Marc Boudreau, Assistant Professor of Chemistry

Richard Johnson, Professor of Chemistry

Young Jo Kim, Assistant Professor of Chemical Engineering

On March 28th, 2020

Approval signatures are on file with the University of New Hampshire Graduate School.

Acknowledgements

Table of Contents

LIST OF FIGURES

LIST OF TABLES

LIST OF SCHEMES

ABSTRACT

N-HETEROCYCLIC CARBENE FUNCTIONALIZED SINGLE-CHAIN NANOPARTCLES AQUEOUS CATALYTIC PLATFORM

By

Xianggeng Liu

University of New Hampshire

Single-chain nanoparticles (SCNP) are a class of intramolecular cross-linked polymeric nanoparticles with a variety of applications including catalysis, sensors, nanomedicine, and nanoreactors. Such nanoparticles are synthesized by folding or collapsing single polymer molecules. By implementing a single-chain folding technique, the single-chain nanoparticles with uniform degrees of cross-linking are synthesized by parent polymer chains with similar chain lengths and polymer microstructure. Polymer chains that are synthesized by various controlled polymerization techniques can be converted to SCNPs through a variety of covalent chemistry and supramolecular interactions. Based on the expected cross-linking chemistry, related functional groups can be installed either during monomer synthesis or post-polymerization functionalization by utilizing a variety of methodologies.

With the goal of effecting catalysis of various organic reactions in aqueous system, we developed a series of ligand functionalized SCNPs with water-soluble pendent groups. N-heterocyclic carbene (NHC) ligands were designed and synthesized to immobilize transition metal cation on SCNPs for catalysis. By employing polymer functionalization strategy, amine-ended ligands, water soluble pendent groups, and cross-linkers were installed by substitution reaction on poly

(pentafluorophenyl acrylate) (PFPA) synthesized by reversible addition fragmentation transfer polymerization (RAFT), and the process of reaction can be monitored by F^{19} NMR conveniently. Moreover, to realize inverse temperature dependent controlling, the temperature sensitive water-soluble pendent groups were utilized, such as N-isopropyl amide, which can be installed by the addition of isopropylamine in the process of functionalization of poly (PFPA). Consequently, a variety of organic reactions could be possible in aqueous system catalyzed by combination of different transition metal cations and water-soluble NHC-functionalized SCNP platform.

Chapter 1. Introduction

Interest in polymeric nanoparticles have substantially risen over the past decades in both synthesis and application. Such nanoparticles are synthesized by folding polymer chains, where administration of functionality is more convenient during monomer synthesis and post-polymerization functionalization.[1] By implementing a single-chain folding technique, the single-chain nanoparticles (SCNP) with uniform degrees of cross-linking are synthesized by parent polymer chains with similar chain lengths, polydispersities.[2]

Controlled polymerizations afford polymers with various functional pendant groups in narrow molecular weight distribution. Based on the expected cross-linking chemistry, related functional groups can be installed by either monomer synthesis or post-polymerization functionalization by utilizing reported methodologies.[3] However, in most cases, the intramolecular cross-linking process occurrs in dilute solution (typically < 1 mg mL^{-1}). Lower concentration of polymer prevents the formation of polymer networks by intermolecular cross-linking, but also limits the application of several reactions in syntheses of SCNPs.[4] Hence, searching for suitable reactions has been one of the most vital challenges in the synthesis of SCNPs. In the last two decades, highly efficient reactions were explored in intramolecular cross-linking of polymers, such as “click” reactions.[5]

In order to extend the application of SCNPs in fields such as biomolecular mimicking and catalysis, SCNPs with more complex secondary structures or metal coordination have attracted more attention in the last decade.[4] As a key factor of folding biomacromolecules in nature, hydrogen

bonding is also utilized to fold SCNPs into architecturally defined nanostructures.[6-11] Additionally, the self-assembly of polymer coils into SCNPs via hydrophobic interactions provides more potential application of SCNPs in aqueous systems.[12-14] Moreover, for enzyme mimicking, various metal-ligand complexations were selected for cross-linking chemistries of SCNPs to provide catalytic activity.[15-20]

1.1 Polymer backbone synthesis and functionalization

To synthesize single-chain nanoparticles with similar size, the length of the polymer backbone should be controlled in a uniform distribution. Controlled chain-growth polymerizations have been applied to SCNP synthesis extensively, such as reversible addition-fragmentation chain-transfer polymerization (RAFT),[21] atom transfer radical polymerization (ATRP),[22] ring-opening metathesis polymerization (ROMP),[23] and nitroxide-mediated living free radical polymerization (NMP).[20]

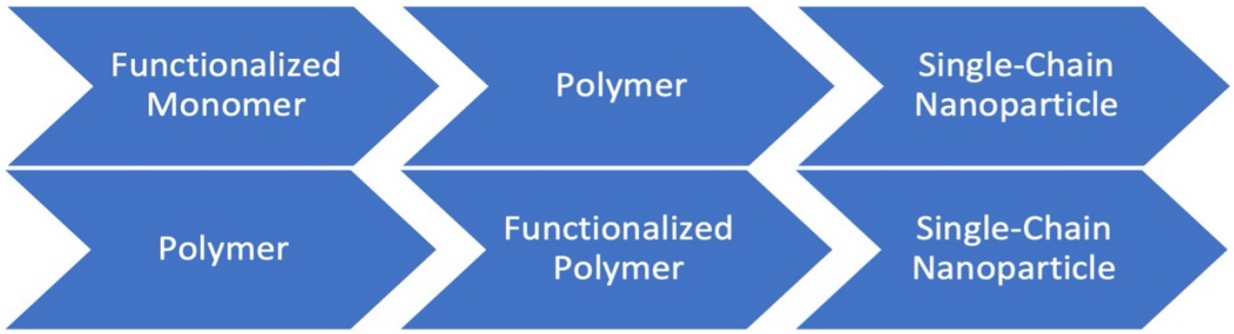

Figure 1 Synthetic pathway of SCNPs

When living free radical polymerizations (LFRP) were selected, acrylate or styrene derivatives are usually utilized as monomers because of their double bonds' extraordinary reactivity.[24] In these cases, the synthetic routes toward SCNPs can be divided into two pathways (Figure 1). There are two steps in the first approach, including the copolymerization of acrylates or styrene with their functionalized derivatives and cross-linking reactions. Since it is s rather straightforward process, the first pathway has been widely utilized in covalently cross-linked SCNPs. However, the

functionalized monomers need to have high radical tolerance, which limits their application in non-covalent cross-linked SCNPs. Hence, researchers began studying the second pathway, post-polymerization functionalization. In this case, monomers with the reactive groups are polymerized solely or co-polymerized with unreactive monomers.[25] For instance, activated esters, such as pentafluorophenyl esters and N-hydroxysuccinimide esters, have been proved to be capable of polymer functionalization (Scheme 1).[25] The pentafluorophenyl group can be substituted by amine at mild conditions, which provides flexibility in SCNP synthesis. Meijer and Palmans have reported a series of SCNPs synthesized by poly(pentafluorophenyl acrylate) post-polymerization functionalization.[9, 11] In these studies, various amine-end functional compounds were reacted with the polymer chains to form stable amide bonds. The whole process can be monitored by ^{19}F NMR.[9] Besides, azides[26] and halides[16] are other common reactive functional groups for CuAAC and SN2 reactions.

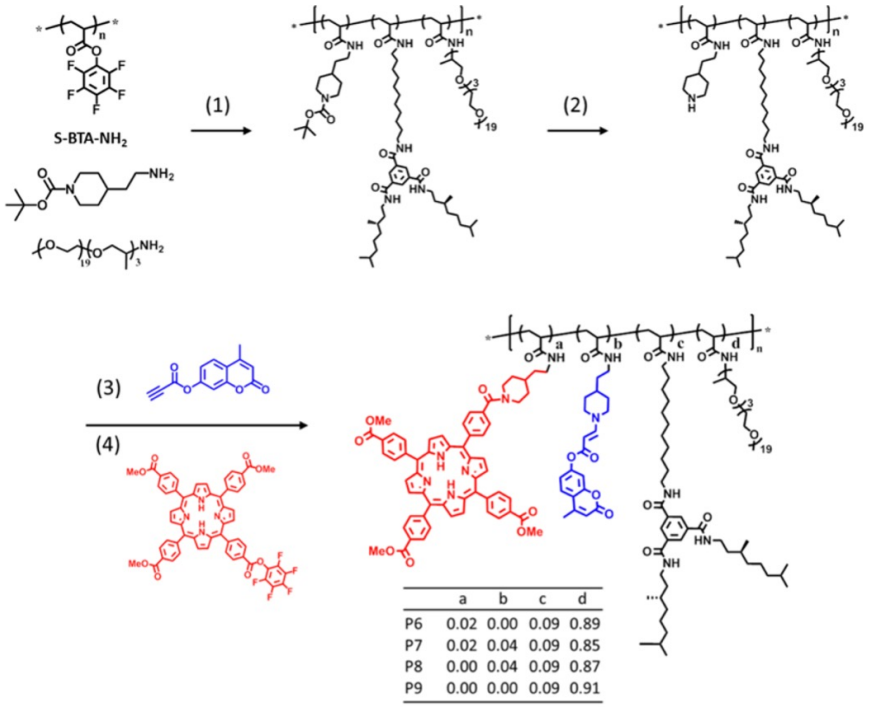

Scheme 1 Synthesis of SCNPs by poly (pentafluorophenyl acrylate) functionalization. Reprinted with permission from ref 7. Copyright 2015 American Chemical Society.

Through ROMP, norbornene and cyclooctadiene derivatives are also commonly used. ROMP has been an effective approach for SCNP formation due to the mild reaction conditions required and overall orthogonality with most reactions. Norbornene derivatives monomers are usually synthesized through the Diels—Alder reaction between cyclopentadiene and different maleimide derivatives or maleic anhydride.[27] By reacting with an anhydride group on the polymer chain, post-polymerization functionalization in this way is a common method towards successful SCNP formation.[28]

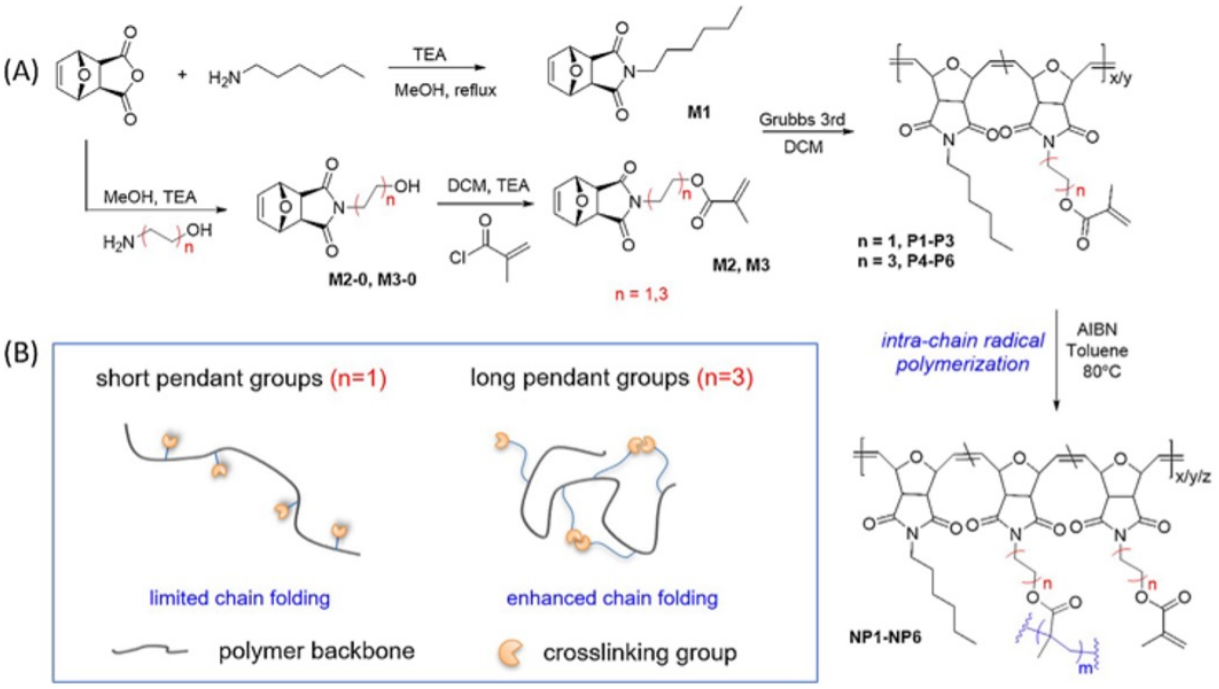

Scheme 2 (A) Synthesis of parent polymer by ROMP and SCNP by radical polymerization. (B) Cross-linking efficiency affected by pendant group length. Reprinted with permission from ref 27. Copyright 2019 Elsevier.

1.2 Crosslinking chemistry

Since Hawker defined single-chain nanoparticles in 2002,[29] various methodologies have been applied in intra-chain polymer cross-linking for the formation of SCNPs. Because SCNPs formation typically occurs in dilute solution to prevent inter-chain cross-linking, the cross-linking chemistries must be highly efficient and avoid the production of side product. In the last 20 years, covalent and non-covalent chemistries have been applied in the intra-chain cross-linking of SCNPs. Studies conducted in 2015 and earlier have been summarized in our previous review.[1] Therefore, this chapter focuses on the publications following 2015.

1.2.1 Covalent Chemistry

Many classic organic chemistry reactions have proved capable in intramolecular polymer cross-linking, such as Michael addition reaction and Diels—Alder reactions. These classic reactions have been developed over decades and described in textbooks specifically. Usually, these reactions are highly efficient without the use of precious metal and are not air or water sensitive. Since these reactions are well-studied and offer a great deal of convenience in experiments, they have been added to the library of SCNP cross-linking chemistries in a major way.

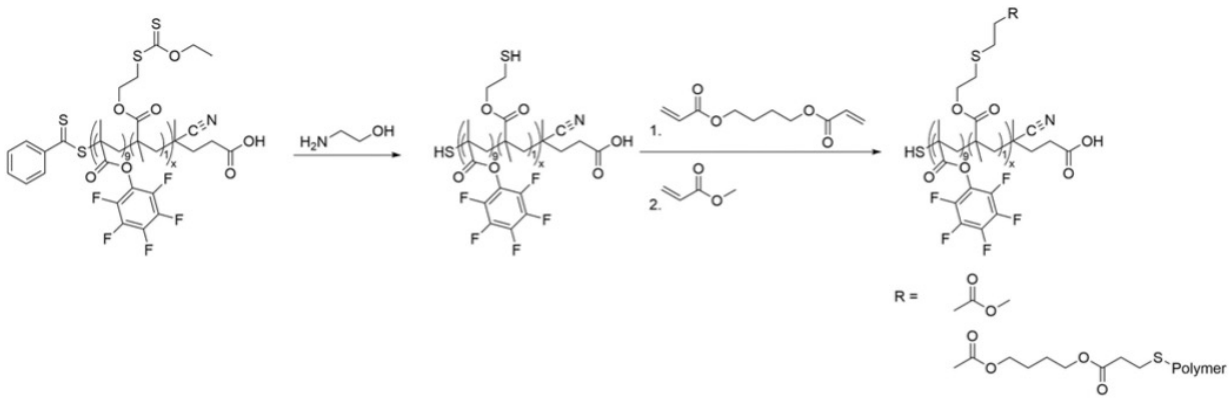

Scheme 3 Synthetic route of thiol-ene "click" reaction crosslinking SCNPs. Reprinted with permission from ref 33. Copyright 2020 The Royal Society of Chemistry.

Arbe and Colmenero reported the latest Michael addition cross-linked SCNP in 2020.[30] Trimethylolpropane triacrylate (TMT) was utilized as cross-linker to synthesize globular SCNPs. The cross-linking reaction was run at room temperature in presence of potassium hydroxide as the catalyst and completed in 3 days. Compared to a traditional Michael addition reaction, the thiol-ene Michael addition reaction, also known as the thiol-ene “click” reaction, became more popular in recent publications.[31-33] Because thiols are highly active in radical reactions, undesired side reactions during radical polymerization can occur,[31] especially in RAFT polymerizations. So protected thiol-functionalized monomers were utilized in polymer backbone synthesis. Paulusse and co-workers have shown that xanthate methacrylate monomers can work very well in polymer synthesis and are easily deprotected by aminolysis. Hydrazine was utilized in aminolysis in their studies because it not only reduces xanthate into thiol but also prevents disulfide formation.[31]

Isocyanate is another useful tool for SCNP folding, and cross-linking this way has worked very well in the conjunction with amines at room temperature.[34] In 2017, Diesendruck examined the reaction between alcohol and isocyanate catalyzed by dibutyltin dilaurate in intramolecular cross-linking.[35] In this study, IR was applied to provide direct evidence of urethane formation. The obvious difference of signal between original polymer, diisocyanate cross-linker, SCNPs at different temperatures, and model compounds were shown in the spectra. From the spectra, carbonyls in isocyanates, model urea, model urethane, and SCNPs shows an obvious difference from 2280 cm^{-1} to 1540 cm^{-1} (Figure 2).

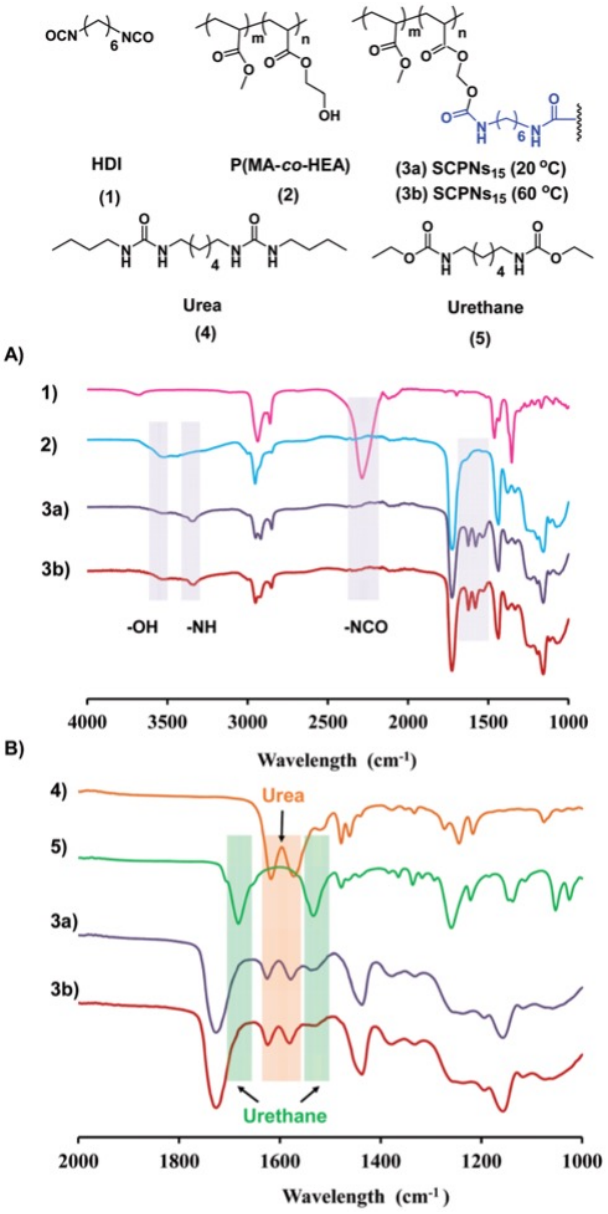

Figure 2 (A) Comparison of IR of diisocyanate cross-linker, parent polymer, and SCNPs. (B) Comparision of IR of urea, urethane, .and SCNPs. Reprinted with permission from ref 35. Copyright 2017 The Royal Society of Chemistry

Diels—Alder chemistry is another classic reaction applied in intramolecular cross-linking of SCNPs synthesis. The reaction has good oxygen and water tolerance, which provides much convenience in experiments. In 2017, our group explored the traditional thermal Diels—Alder chemistry in SCNPs synthesis.[36] In this study, self-

cross-linking and external cross-linker were both applied. In both strategies, the cross-linking reaction occurred between maleimide and furan. The first internal cross-linking strategy provided a new SCNP synthesis methodology utilizing the reversible reaction at different temperatures. The reaction was run in an open system to release furan from the solution so that the deprotected maleimide group tended to react with the furfuryl group on the polymers. A second external cross-linker strategy showed more possibilities in the structure of the cross-linker. The concentration of intramolecular cross-linking was increased up to 10 mg mL^{-1} by a continuous addition method. In the same year, the Barner-Kowollik group reported dynamic covalent SCNPs synthesized by hetero Diels-Alder chemistry.[37]

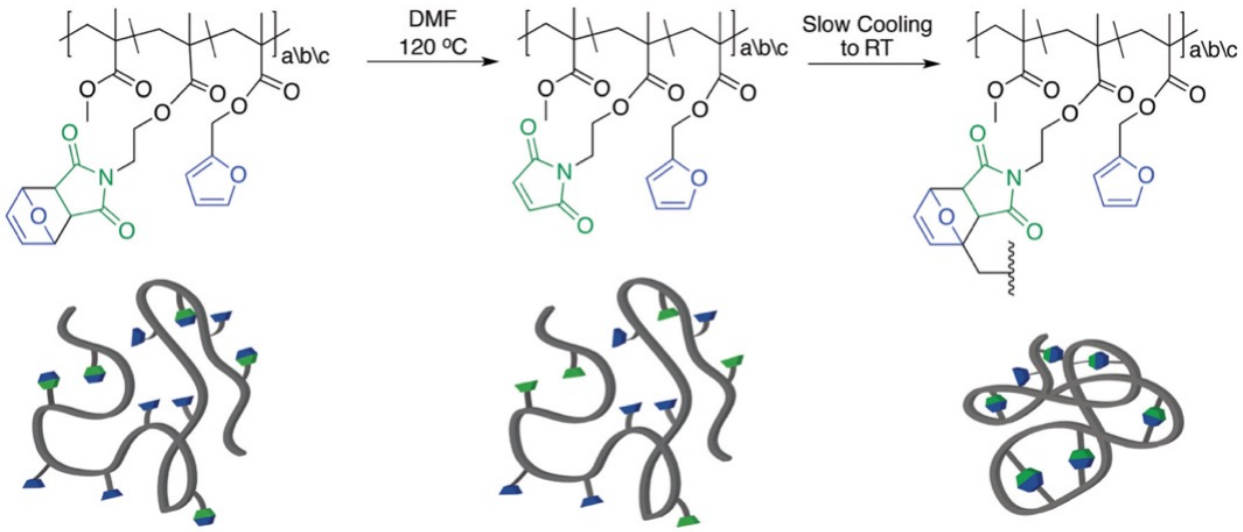

Scheme 4 Deprotection of maleimide pendant group and Diels-Alder chemistry cross-linking SCNPs. Reprinted with permission from ref 36. Copyright 2017 The Royal Society of Chemistry.

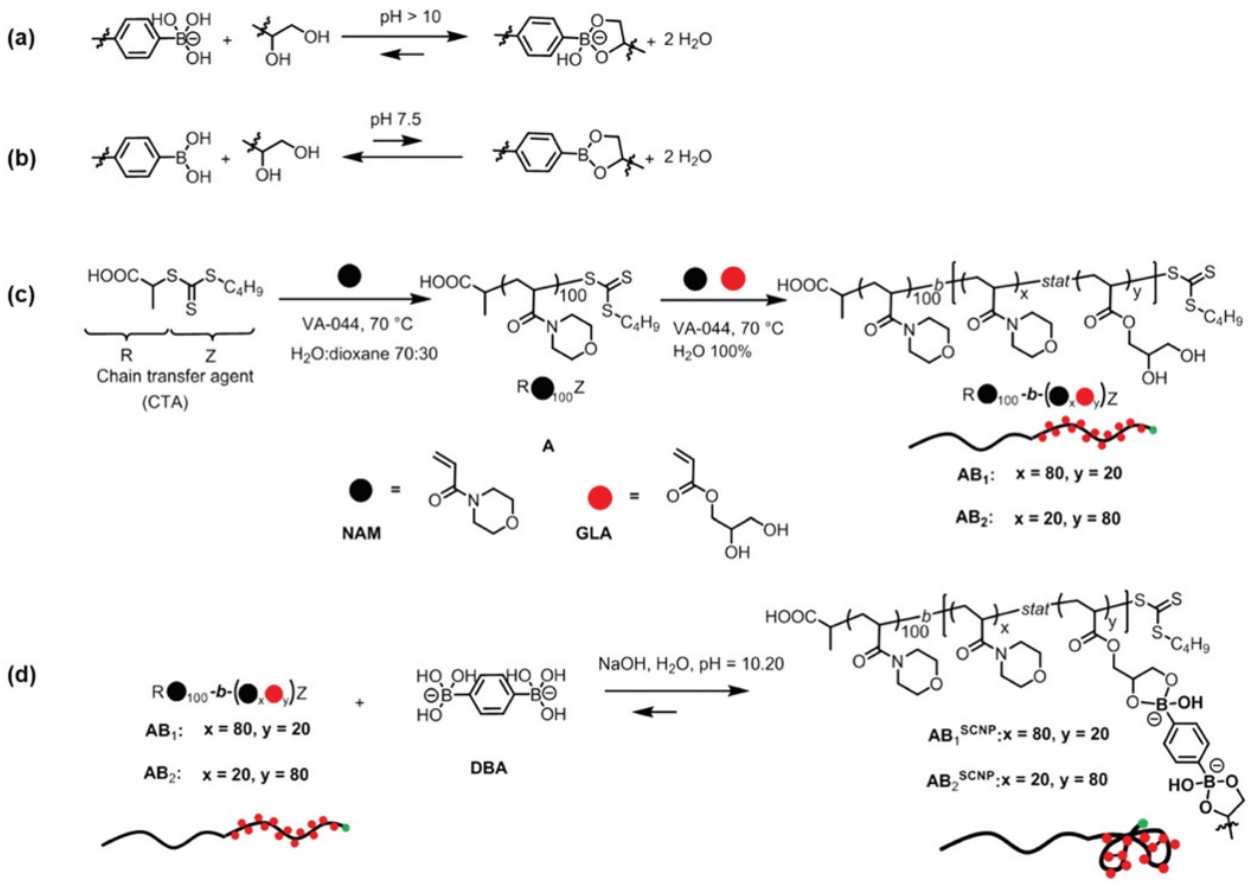

Scheme 5 Dynamic boronate cross-linking SCNPs. Reprinted with permission from ref 24. Copyright 2017 The Royal Society of Chemistry.

There are also other dynamic covalent chemistries applied in SCNPs synthesis. In 2017, Fulton and Turnbull reported dynamic covalent SCNPs cross-linked by hydrazone formation.[38] Because of the dynamic property of acylhydrazone, succinic dihydrazide was utilized as the cross-linker to substitute hydrazone on the polymer chain. The dynamic SCNPs can be treated with $NaCNBH_3$ to reduce the acylhydrazone to hydrazide to avoid reconfiguration. Besides, as the cross-linker, boronic acid can not only form dynamic covalent cross-linking bonds but also can change its hydrophilicity at different environmental pH (Scheme 5). The study was published by Perrier group in the same year.[39] The boronate ester linkage performed hydrophilic or hydrophobic in basic or neutral environments.

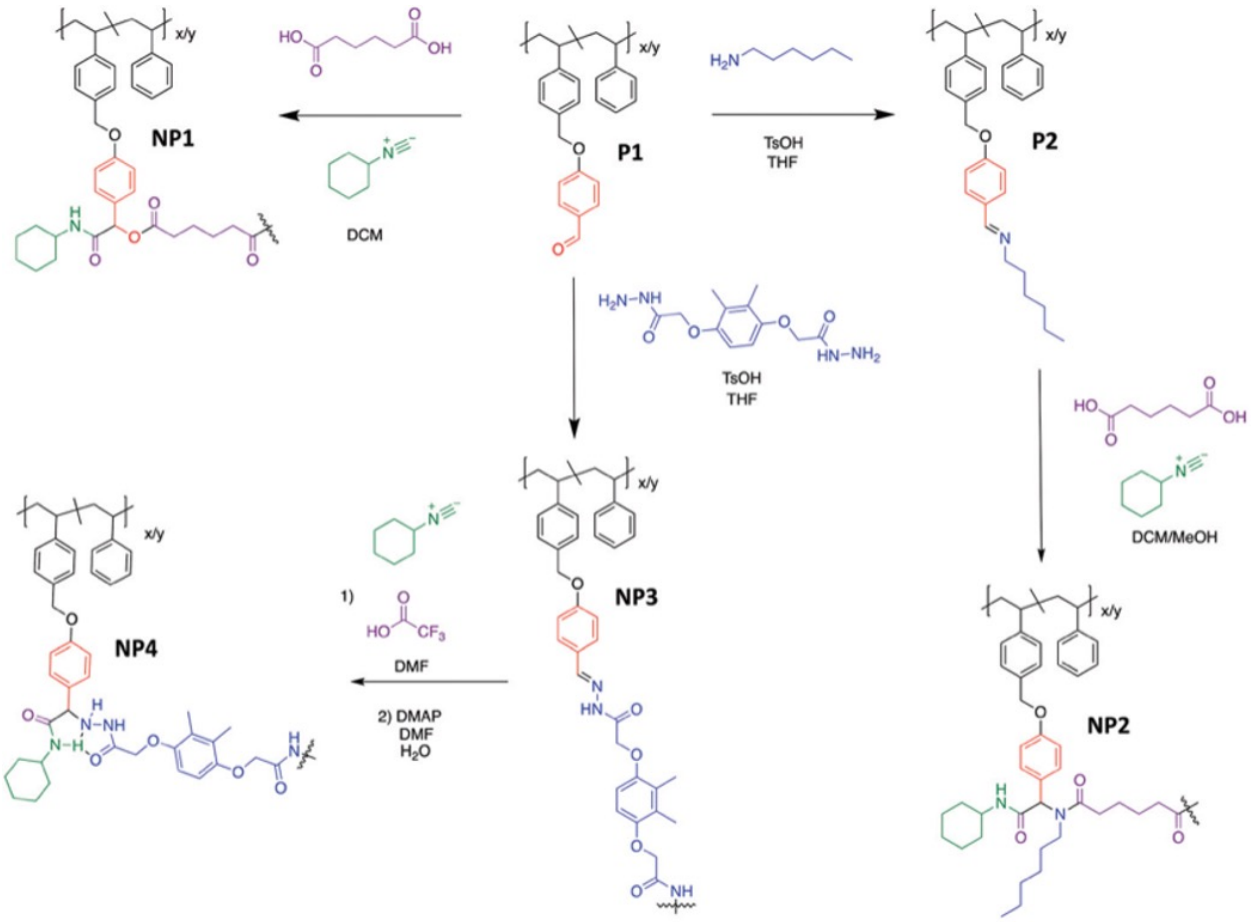

Scheme 6 Synthetic route of SCNPs cross-linked by multicomponent reactions. Reprinted with permission from ref 22. Copyright 2017 The Royal Society of Chemistry.

To achieve more complicated secondary structures and other novel properties, the interest in multicomponent reactions was raised in SCNPs synthesis. Isocyanide-based multicomponent reactions (IMCR), the Passerini reaction and the Ugi reaction, on polymer functionalization have been investigated in the last decade.[25] IMCRs were applied in SCNPs synthesis in 2017 for the first time by our group (Scheme 6).[22] Because the Passerini reaction was sensitive to concentration, $BF_3 \bullet OEt_2$ was added as a Lewis acid catalyst to improve the cross-linking efficiency. In 2021, Pomposo and co-workers introduced self-reporting SCNP synthesis by the Hantzsh reaction.[40] Interestingly, the SCNP shows fluorescence after cross-linking, while the pre-folded polymer

chain was not luminescent. additionally, the metal-ligand complex can act as the cross-linker for the SCNP. Demirelli used phthalonitrile on the polymer chain, extra phthalonitrile in solution, and cobalt salt to synthesize cobalt phthalocyanine as the crosslinker of SCNP.[41]

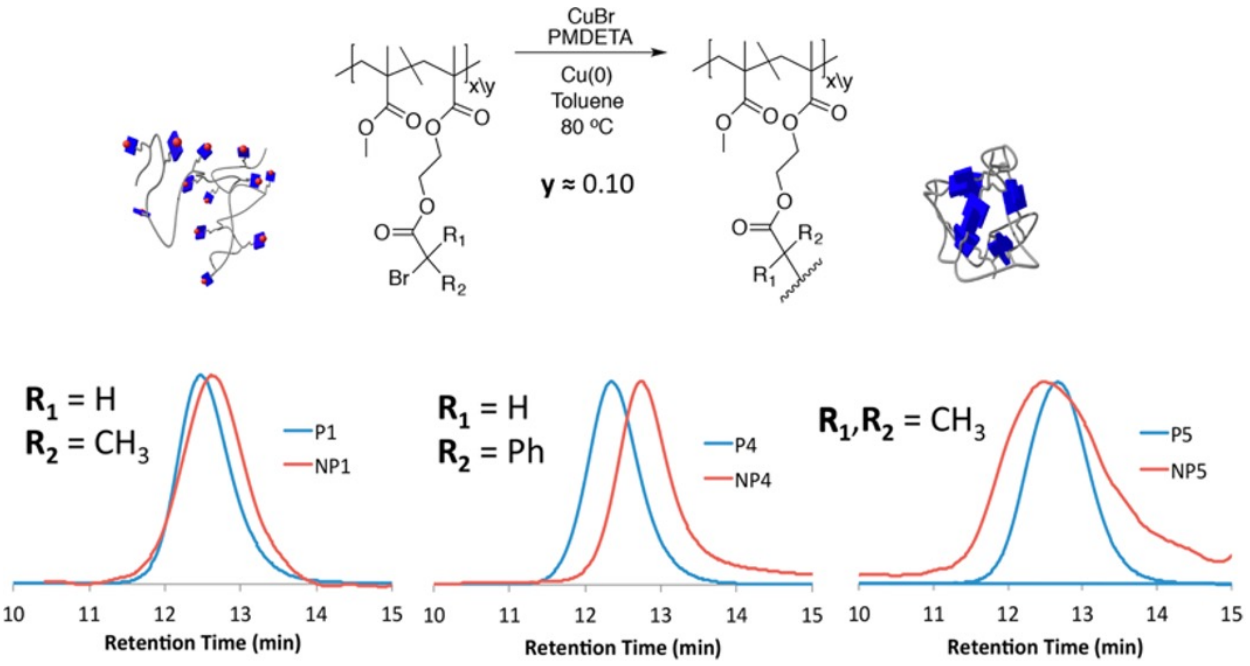

Figure 4 GPC traces of ATRC cross-linking SCNPs. Reprinted with permission from ref 42. Copyright 2017 American Chemical Society.

Radical chemistry is another abundant reaction library that provides cross-linking methodologies in SCNPs synthesis. There are two major types of radical reactions reported in recent publications about SCNPs, homo-coupling of radicals on pendant group and radical polymerization, reported in recent publications about SCNPs synthesis. Atom transfer radical coupling (ATRC) is a radical homo-coupling reaction catalyzed by copper. Our group employed this process in intramolecular cross-linking to achieve scalable SCNPs synthesis.[42] Similar to ATRP, a radical is produced by abstraction of halide. However, a second pathway to terminate a radical exists, called disproportionation (Scheme 7). From characterization results, disproportionation was the major competitive reaction. In some cases, a radical abstract a proton on the end of pendant group to

produce an alkene, which was supported by ^{1}H NMR. By comparing the SEC-MALS trace of polymers and SCNPs containing different ATRC-active monomers, the less disproportionation occurs, the larger and cleaner shift was seen (Figure 3). A polymer with no chance for disproportionation showed the best result on SEC-MALS trace. Besides, by utilizing a continuous addition method, the ATRC SCNPs can be produced up to 600-700 mg by one reaction. In 2018, the Pomposo group reported another application of homo-coupling of radicals in SCNPs synthesis.[43] Radicals were generated on commercial Poly(N-Vinyl Pyrrolidone) by the Fenton reaction. Then two radicals on the same chain reacted to form new carbon-carbon bonds as cross-linking bonds of SCNPs. For intra-chain radical polymerization, our group applied a similar AIBN initiated radical polymerization as a cross-linking chemistry in 2015,[44] 2016,[45] and 2019.[27] Because the AIBN initiated radical polymerization is extremely sensitive to oxygen, a freeze-pump-thaw technique was applied in most experiments. The carbon-carbon double bonds on the pendant groups can also be polymerized under oxygen or light while the monomers were polymerized by ROMP. So, in these cases, BHT is necessary to avoid the intermolecular cross-linking in ROMP polymer synthesis.

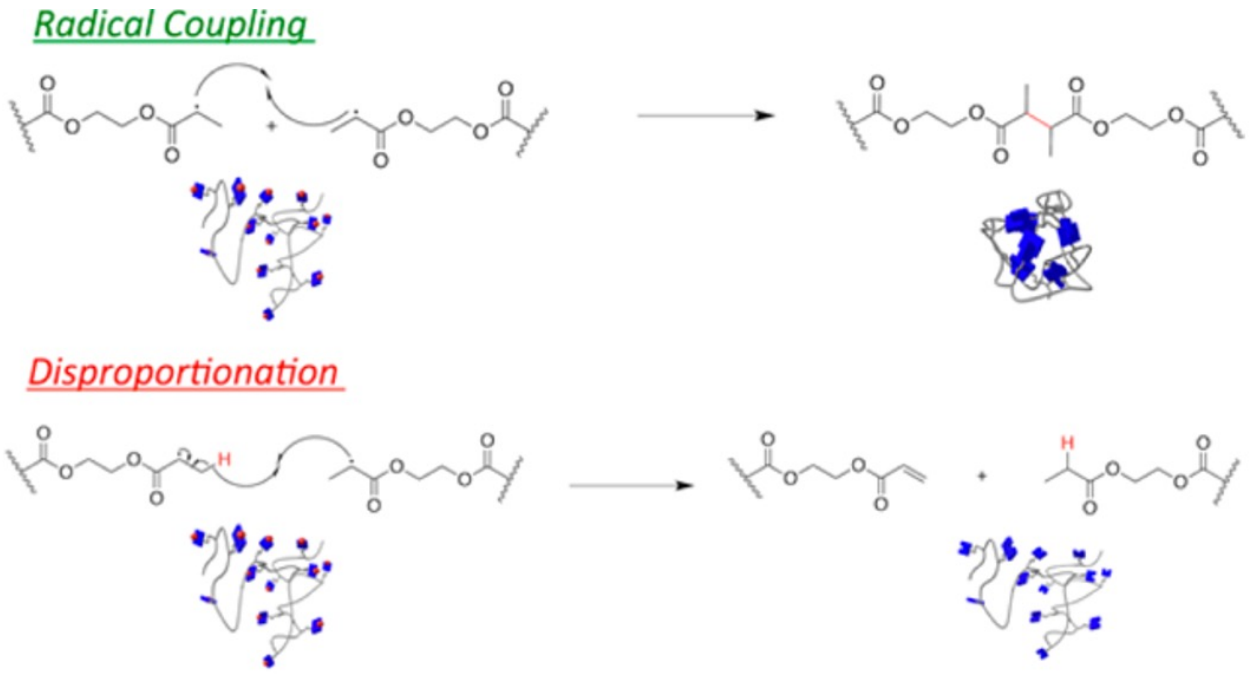

Scheme 7 Radical coupling and disproportionation. Reprinted with permission from ref 42. Copyright 2017 American Chemical Society.

In the past decades, transition metal catalyzed reactions played a critical role in synthetic chemistry. More and more transition metal catalyzed reactions have been proved to be capable in polymer intramolecular cross-linking. Besides ATRC, our group explored the application of Sonogashira coupling chemistry in SCNPs synthesis in 2016.[46] Trimethylsilyl protected alkyne methacrylate monomers were copolymerized with methyl methacrylate by RAFT. After deprotection by tetrabutylammonium fluoride, the carbon-carbon triple bond was reacted with 1,4-diiodobenzene under the catalysis of Cu(I) and Pd(0) to form SCNP. Olefin metathesis is another common reaction in polymer chemistry. Usually, it is utilized in polymer backbone syntheses, such as ROMP and acyclic diene metathesis polymerization (ADMET). However, Isono and Satoh proved olefin metathesis can be a robust tool in intramolecular cross-linking of various parent polymers polymerized by group transfer polymerization, anionic polymerization, and ring-opening

polymerization to synthesize SCNPs (Scheme 8).[47] As one of the most frequently used polymer functionalization reactions, copper-catalyzed azide alkyne cycloaddition reaction (CuAAC) was also applied in SCNPs synthesis by Dove, O'Relly,[5] and Maiz.[48]

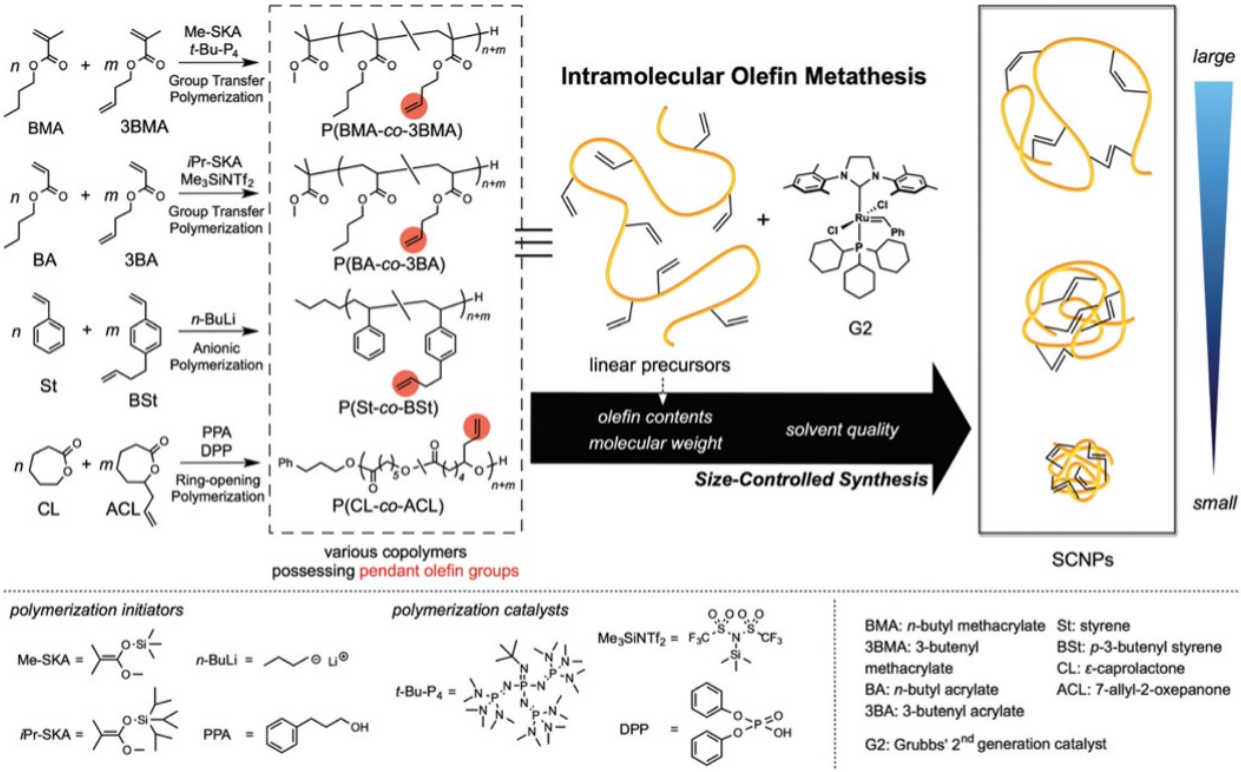

Scheme 8 Synthesis of parent polymer and intrachain cross-linking by olefin metathesis. Reprinted with permission from ref 47. Copyright 2016 The Royal Society of Chemistry.

Even though more and more new methodologies in organic chemistry were studied, some "old fashion", like nucleophilic substitution reactions, are still popular in SCNPs synthesis. SN2 reaction was employed in intramolecular cross-linking by Taton in 2017.[49] On polystyrene-based polymer chains, imidazole working as a nucleophile attacked benzylic carbon to form imidazolium salt cross-linker. Interestingly, the imidazolium salt can form N-heterocyclic carbene in situ, which showed catalytic activity in benzoin condensation. Aromatic nucleophilic substitution reactions

are another classic organic reaction applied in SCNPs synthesis. The reaction between thiol and fluorophenyl pendant group was utilized by Barner-Kowollik and Lederer to form linkage of SCNPs in 2020.[50] Due to the nature of pentafluorophenyl, the cross-linking process can be monitored by ^{19}F NMR and ^{1}H NMR conveniently. Besides, activated ester substitution also can be used in intramolecular cross-linking. Jackson and Thoniyot reported SCNPs synthesized by the reaction between activated succinimidyl ester and diamine in the same year.[51]

In the last decade, photochemistry has become to be one of the most popular chemistries in polymer intrachain cross-linking. Photochemistry is highly efficient and compatible with an array of reactions without generating undesirable side reactions. Most photochemistry utilized for SCNP formation are photoinduced cycloaddition reactions. The photoinduced [2+2] cycloaddition of coumarin has been proved to be an efficient tool in intramolecular cross-linking by Zhao[52, 53] and Sumerlin.[54] Similarly, the photoinduced [2+2] cycloaddition of styrylpyrene was studied as SCNPs cross-linking chemistry by Barner-Kowollik in 2018.[55] Rather than UV light, the reaction occurs under visible light or even ambient light, providing more possibilities for biological applications. Interestingly, the quantum yield of the intrachain photocycloaddition is dramatically higher than interchain cross-linking within the confined environment of the polymer chain (Figure 4). Consequently, the concentration of the solution in SCNP synthesis was promoted to 25 mg mL^{-1}. In 2020, Elacqua and co-workers employed styrlpyrene as both the SCNP cross-linker and the electron-relay catalyst for a stereospecific [2+2] cycloaddition.[56] Besides [2+2] cycloaddition, [4+4] cycloaddition is another common photoinduced cycloaddition reaction in photochemistry.

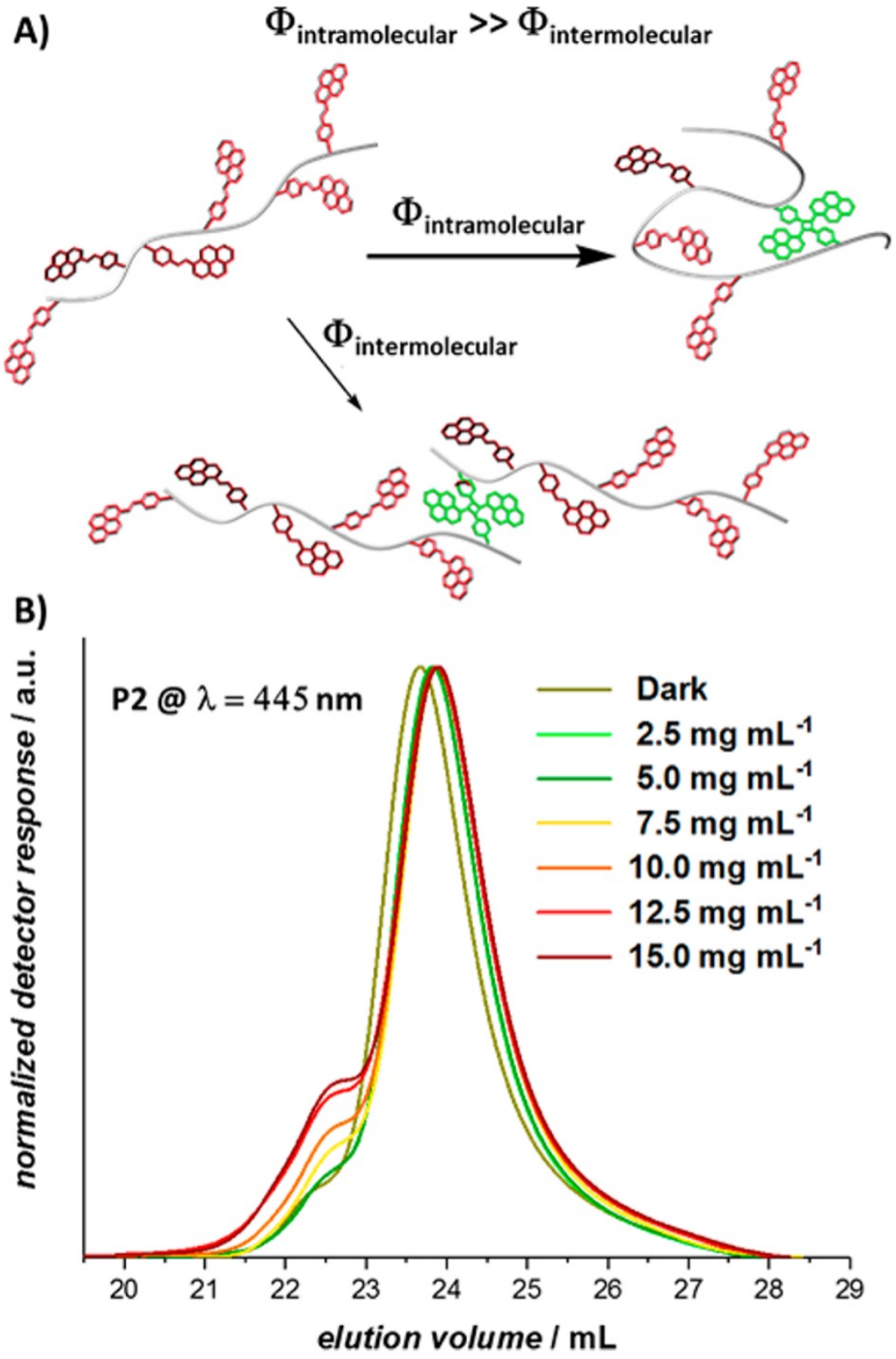

Figure 5 (A) The (B) Photoinduced single-chain collapse at different concentration. Reprinted with permission from ref 55. Copyright 2018 American Chemical Society.

The first application of a photoinduced [4+4] cycloaddition in SCNPs was reported by our group in 2014.[57] We studied [4+4] cycloaddition of anthracene under 350 nm UV light in intrachain cross-linking, which showed it is a competitive candidate in the library of SCNPs cross-linking chemistry. The cycloaddition reaction was applied by Simon in 2020 to fold comb polymers.[23] Besides, Barner-Kowollik and Diesendruck's recent study of flow chemistry for SCNPs synthesis utilized same reaction.[58]

The photo-induced [4+2] hetero Diels—Alder reaction is another photoinduced cycloaddition reaction applied in SCNPs synthesis. Pomposo and Barner-Kowollik employed the reaction to link the two ends of polymer to ring-shaped polymer.[59] α-Methylbenzaldehyde was activated by UV light to produce a dienophile that then reacts with carbon-sulfur double bonds to form new six-membered rings. The photoactive dienophile can also react with carbon-carbon double bonds. Recently, Barner-Kowollik and co-workers reported α-Methylbenzaldehyde and maleimide based photoinduced Diels-Alder reaction cross-linking SCNPs.[60] The SCNPs were degraded by the cleavage of phenyloxalate on the cross-linker through peroxyoxalate chemiluminescent reaction (Scheme 9). The phenyloxlate linkage was broken by H_2O_2 to produce 1,2-dioxetanedione, a high-energy intermediate. Then the high-energy intermediate transferred energy to pyrene on the polymer chain and degraded to CO_2. Finally, the pyrene on excited state released energy by the emission of light.

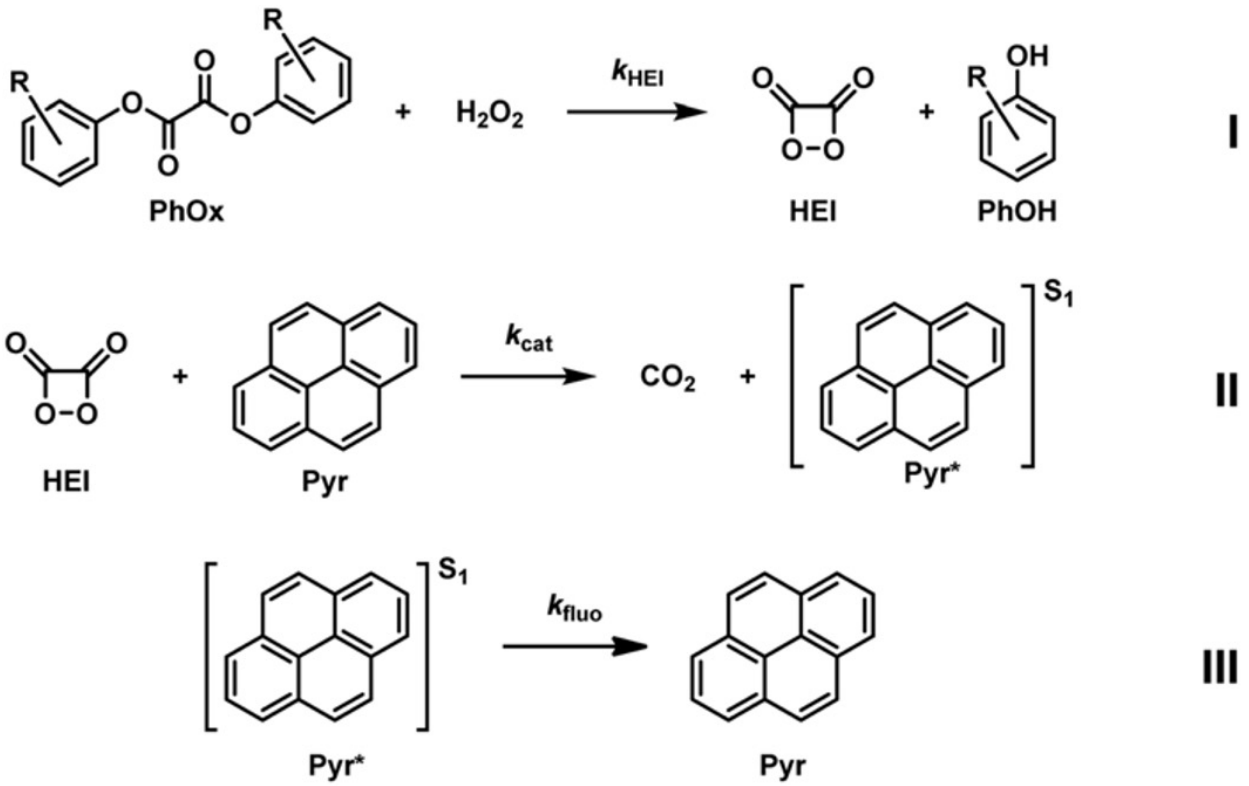

Scheme 9 Degradation of phenyloxalate. Reprinted with permission from ref 60. Copyright 2021 The Royal Society of Chemistry.

Unlike photoinduced pericyclic chemistry, other photochemistry applied in SCNPs synthesis consists of reactions induced by reactive intermediates formed under light, such as tetrazole-ene cycloaddition and photoinduced radical reactions. As the vital reactant in tetrazole-ene cycloaddition, tetrazoles can be activated by light and generate reactive intermediate nitril imine. Then the nitril imine can react with a range of structures, such as double bonds, carboxylic acid, and even itself. Moreover, the different linkage formed by tetrazole with different compounds shows different fluorescence (Scheme 10).[61-63]

Azide is another photosensitive group employed in intramolecular cross-linking. Under UV light, azide pendant groups undergo photodecomposition to form a reactive nitrene intermediate. Then, nitrene reacts with various functionalities to form new C-N bonds. For the synthesis of deuterated SCNPs, Pomposo and co-workers utilized a C-D insertion reaction by including nitrene produced from azide.[64] The polymer backbone was synthesized by $B(C_6F_5)_3$ initiated ring-opening polymerization of deuterated tetrahydrofuran and deuterated epichlorohydrin. Then chloride on the pendant group was substituted by azide and photodecompose to nitrene. Finally, deuterated SCNP was formed by nitrene C-D insertion in highly dilute solution.

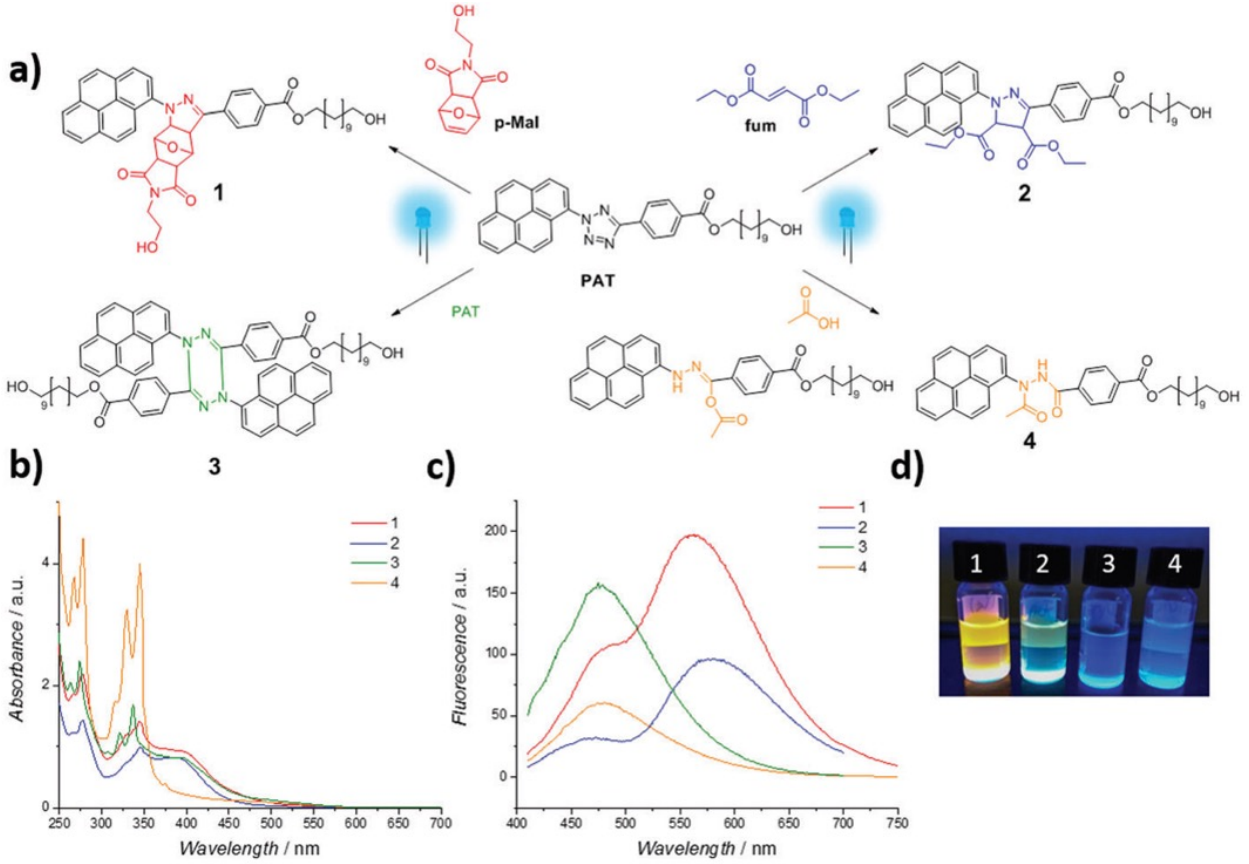

Scheme 10 (a) Different reaction options of tetrazole. (b) UV/Vis and (c) fluorescence spectra of the products. (d) Image of the fluorescent products. Reprinted with permission from ref 61. Copyright 2018 The Royal Society of Chemistry.

Besides photoinduced nitrene formation, photoinduced radical reactions were also applied in intramolecular cross-linking. In 2018, Blinco, Mutlu, and Barner-Kowollik explored the photoreaction between nitroxide and Irgacure 2959 as cross-linking chemistry for SCNPs.[65] Under UV light, radicals formed on both ends of Irgacure 2959 based cross-linker by C-C bonds cleavage. Then the polymer chains were folded by radical coupling (Scheme 11). Interestingly, the SCNPs showed luminescence that cannot be observed in both the unfolded parent polymer and the cross-linker, which means these SCNPs are self-reporting. Also, the nitroxide radical can be regenerated by mCPBA and react again. Similarly, the same group employed oxime ester as the precursor to form radical under visible light so that the polymer chain was folded by radical coupling in the next year.[66] As one of the most common photoinitiators, benzophenone was also utilized in a photochemical approach to SCNPs. The photoinduced homocoupling of ketyl radicals produced from pendant benzophenone groups on the polymer chain were employed as cross-linking chemistry by Temel.[67, 68]

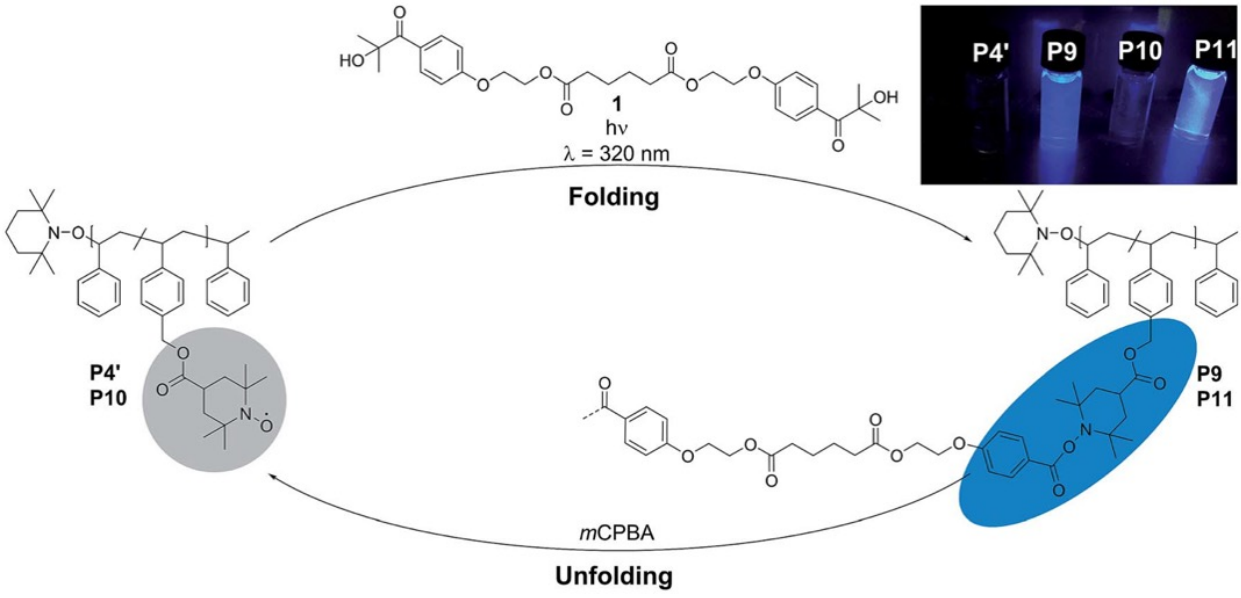

Scheme 11 Folding of parent polymer by photoreaction of TEMPO and Irgacure 2959 and unfolding by mCPBA. Reprinted with permission from ref 65. Copyright 2018 The Royal Society of Chemistry.

1.2.2 Non-covalent Chemistry

Research on SCNP formation through use of supramolecular chemistry has increased in the last several years. With interest shifting from synthesis to application, non-covalent chemistry has been a useful approach in intramolecular cross-linking. Non-covalent chemistry, such as hydrogen bonding, hydrophobic interactions, and metal coordination, offers various application advantages including reversible binding under different conditions and catalytic activity.

Hydrogen bonding is one of the most studied supramolecular interactions. With the development of protein mimicking SCNPs, hydrogen bonding has appeared more often in SCNPs cross-linking designing to construct secondary or even tertiary polymeric structures. In 2015, Barner-Kowollik and Meijer combined Hamilton wedge (HW) and cyanuric acid (CA) with benzene-1,3,5-tricarboxamide (BTA) to synthesize hydrogen bonding SCNPs with complex secondary structures by orthogonal self-assembly (Scheme 12).[6] The HW-CA system was reported by Barner-Kowollik in 2010,[69] one year before Palmans and Meijer published the first BTA system based SCNPs.[70] Unlike homodimer systems,[71] the HW-CA system forms hydrogen bonds specifically within an α,ω-donor/acceptor. While BTA was a successful attempt in SCNPs secondary construction. Proved by CD spectra, a helical conformation was formed by hydrogen bonding in appropriate solvent.[9, 70] In addition to the HW-CA system, Meijer and Palmans studied SCNPs cross-linked by other combinations, such as BTA and phosphine Ruthenium coordination,[7] BTA and Ureidopyrdinone (UPy),[8] as well as hydrogen bonding and π-stacking of chiral 3,3′-bis(acylamino)-2,2′-bipyridine-substituted benzene-1,3,5-tricarboxamide (BiPy-BTA).[10] The

HW-CA system was also compatible with other supramolecular cross-linking chemistry including the host-guest interaction of benzo-21-crown-7 and secondary ammonium salt.[72]

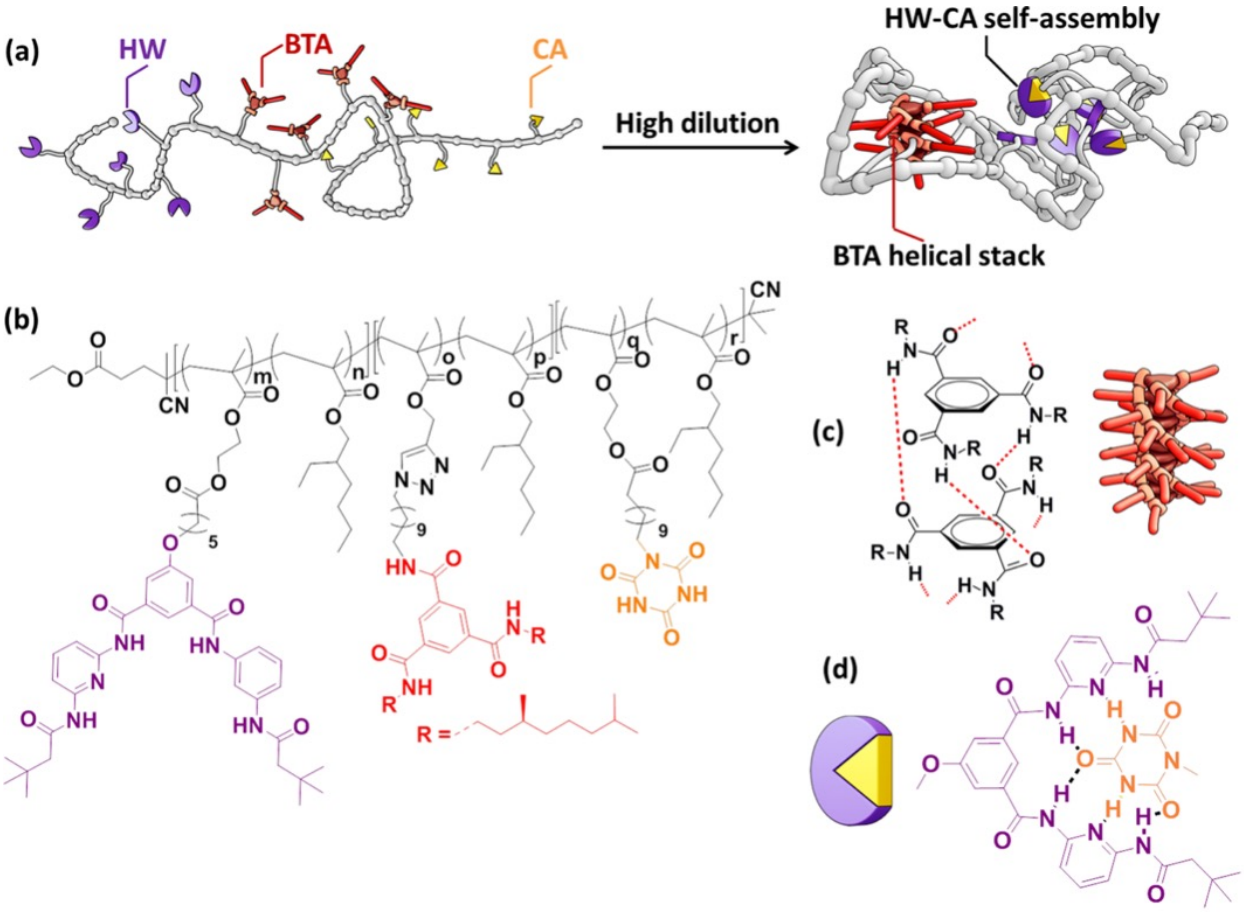

Scheme 12 (a) Folding process of HW-CA and BTA systems in highly dilute solution. (b) Structure of HW-CA BTA containing polymer. (C) Self-assembly of BTA. (D) Self-assembly of HW-CA. Reprinted with permission from ref 6. Copyright 2015 American Chemical Society.

Hydrophobic interactions are another essential supramolecular interaction employed in SCNPs synthesis. As a core factor of hydrophobic interaction, solvent promotes the folding and unfolding of amphiphilic polymer chains. By self-assembly in water, amphiphilic polymer chains form SCNPs with a hydrophobic core and hydrophilic pendant chains on the outer shell. In 2016, Terashima and Sawamoto reported three types of SCNPs folded by hydrophobic interaction (Scheme 13).[12-14] In these studies, poly (ethylene glycol) (PEG) was utilized as the hydrophilic

pendant chains, while three different hydrophobic pendent groups were selected to express various properties. When the hydrophobic pendant chains are alkyl groups, the amphiphilic polymer chain folds in water to form SCNPs with a hydrophobic core and unfolds in organic solvents, such as chloroform and DMF.[12] The PEG-based amphiphilic copolymers can also form SCNPs in DMF when the hydrophobic pendant chains are fluorous perfluoroalkyl groups. Interestingly, the fluorous polymer chains can form reverse unimer micelles with a hydrophilic core in 2H, 3H-perfluoropentane (2HPFP). Both fluorous SCNPs are unfolded in chloroform.[13] However, the folding behavior changed when hydrogen-bonding active groups appeared on hydrophobic pendant groups.[14] These hydrogen-bonding active PEG based co-polymer chains folded into SCNPs in water and chloroform and unfolded by adding methanol in water to change polarity or adding trifluoroacetic acid in chloroform besides changing solvent to DMF. Remarkably, the concentration of folding these SCNPs folded via hydrophobic interaction was relatively high in water even at 100mg/mL. However, the good performance of single-chain folding is only for random co-polymer, while multi-chain aggregation occurs on gradient and block co-polymers. These type of PEG based SCNPs were also studied by Boyer, Wong,[73] Pu,[74] Cheng,[75] Alegria[76] and Biagini[77]. The excellent solubility extends the biological applications of SCNPs, such as drug

delivery.[77]

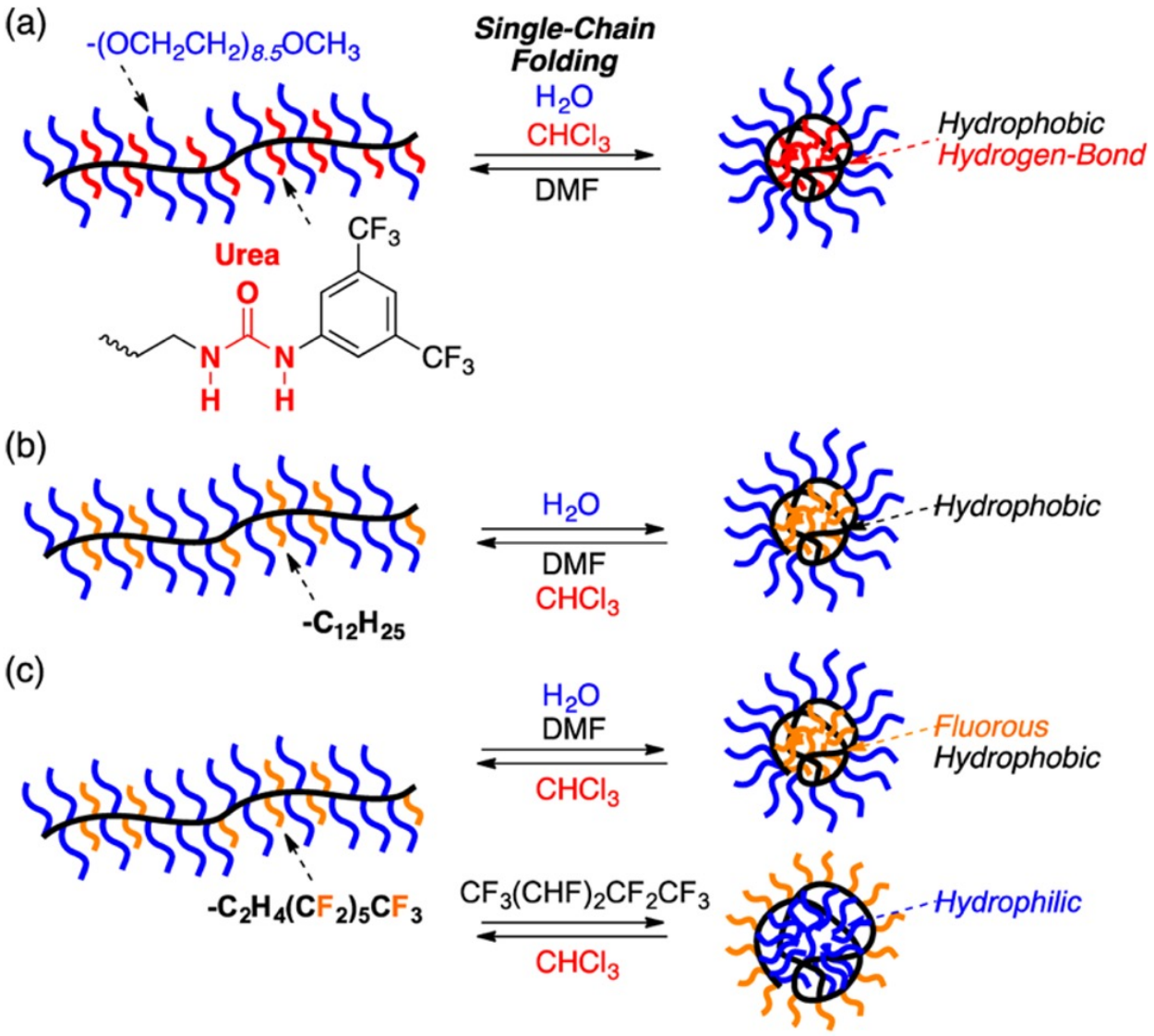

Scheme 13 Folding and unfolding of three different PEG based amphiphilic polymers in different solvent. Reprinted with permission from ref 13. Copyright 2016 American Chemical Society.

Lately, more studies on metal-coordination SCNPs have emerged. As one of the major applications of SCNPs, catalytic nanoreactors usually consist of polymer chains, ligands on pendant groups, and transition metals. Except for few cases that ligands work as cross-linkers of SCNPs,[26] most of these metal-core SCNPs are cross-linked by ligand-metal coordination (Figure 5). As a vital part

of coordination, various transition metal ions were employed in metal-core SCNPs synthesis, including Cu(II),[16, 78-81] Fe(II),[82-84] Pd(II),[15, 19, 83] Ni(II),[85] Rh(I),[17] Pt(II),[18, 20] and Eu(III).[20] The metal source for coordination is usually metal salts, such as $CuSO_4$ and $Pd(OAc)_2$. In some special cases, precursor complexes were employed. For instance, $Pt(COD)Cl_2$ was utilized as a Pt source for syntheses of Platinum-Phosphine SCNPs by Barner-Kowollik and Roesky.[18, 20] Additionally, ligand selection is another vital part for coordination. Suitable ligands were selected and installed by ligand-containing monomer synthesis or post-polymerization functionalization. Since the interactions between the ligand and a copper catalyst might affect ATRP, most of the polymer backbone of SCNPs with ligand-containing monomers was synthesized by RAFT polymerization or NMP. In addition, metal-free polymerization reactions avoid the unexpected coordination between metal and ligand. Aside from SCNPs containing one type of metal, heterobimetallic SCNPs were explored by Lamcoff[86] and Barner-Kowollik.[20] Especially in Barner-Kowollik's study in 2020, the realization of heterobimetallic SCNP was achieved by specific coordination between ligand and metal. In most of these cases, metal-core SCNPs were designed to mimic metalloenzymes because of similar size, reversible folding mechanism, and cavity for reaction.[87] Hence, water soluble SCNPs have been the major metal-core SCNPs recently for catalysis in aqueous media. To provide water solubility, water soluble pendant chains often appeared in polymer syntheses, such as PEG[78] and imidazolium group.[16]

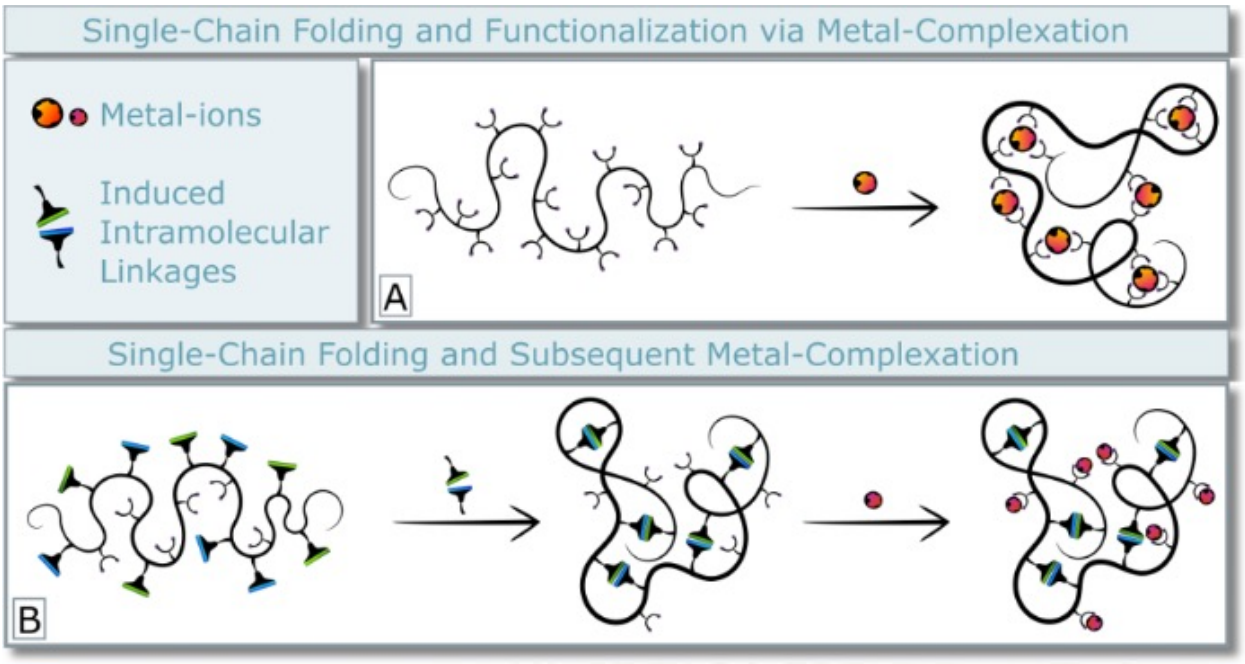

Figure 6 (A) SCNP cross-linked via metal-complexation. (B) Metal-complexation with folded SCNP. Reprinted with permission from ref 87. Copyright 2018 American Chemical Society.

The controlled folding and unfolding of polymer coils have always been a difficult challenge in SCNPs studies. Besides dynamic covalent chemistry and reversible photochemistry, there are some novel solutions via supramolecular chemistry explored in the last several years. In cases of SCNPs folded by hydrophobic interactions, the folding and unfolding processes can change based on the solvent used.[12-14] Moreover, varying the temperature and pH of a solution, or even by applying a mechanical force has induced reversible folding of SCNPs cross-linked by hydrogen bonding.[8, 14] Host-guest interactions provided new paths for controlling the folding and unfolding of polymer coils. In 2016, Pu and co-workers reported the SCNPs cross-linked by host-guest interaction between β-cyclodextrin and ferrocene (Scheme 14).[88] The inclusion ability of β-cyclodextrin for neutral ferrocene is stronger than charged ferrocene, which can be controlled by external voltage stimuli. Therefore, the folding and unfolding of the SCNPs can be controlled by

external voltage stimuli reversibly. However, the host-guest interaction can also cause the unfolding of SCNPs. In 2018, the same group reported hydrophobic interaction folding SCNPs were unfolded by host-guest interaction triggered by cyclodextrin.[74] Besides, the host-guest interaction between benzo-21-crown-7 and secondary ammonium salts was employed and work with HW-CA hydrogen bonding system to form SCNPs, which can be unfolded by addition of KPF_6.[72]

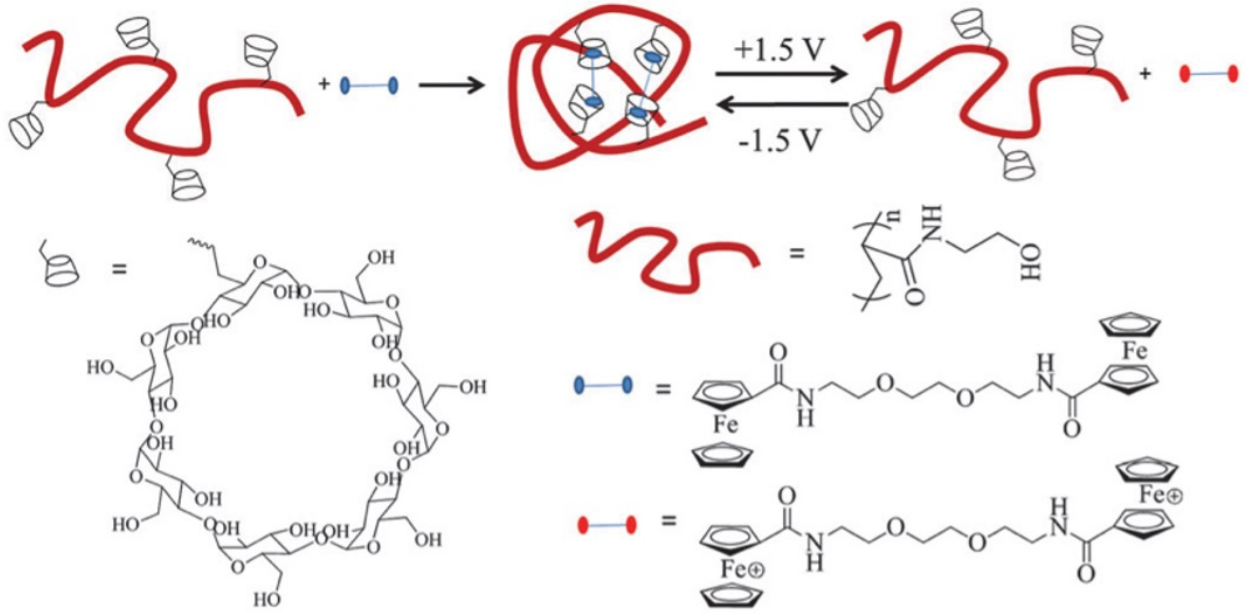

Scheme 14 Formation and voltage responsiveness of SCNP via host-guest interaction. Reprinted with permission from ref 88. Copyright 2016 The Royal Society of Chemistry.

1.3 Summary and outlook

In the past years, the interests in the synthesis and application of SCNPs have attracted more attention in polymer science. The diversity in synthetic methodology of intramolecular cross-linking was extended to be more abundant due to many recent and novel scientific contributions. Compared to studies before 2015, more publications have focused on reversible folded SCNPs to achieve more complex architectures and better application performance. Consequently, dynamic covalent chemistry and photochemistry were studied in more cases. As reversible processes, supramolecular interactions were also developed in numerous studies. Especially various transition metals were employed in syntheses of SCNPs via metal coordination to perform catalytic activity for enzyme mimicking. Besides, the combination of orthogonal interactions or reactions allows the construction of more complex secondary structures or even tertiary structures. However, except in some special cases, the syntheses of SCNPs were still limited in highly dilute solution, which is an inevitable barrier in potential applications. In the next several years, we expect to see more SCNPs syntheses relating clever designing, advanced synthetic methodology, and experimental technique. And there is still a long way to study SCNP in designing, synthesis, characterization, and application.

Chapter 2. Metalloenzyme mimicking *via* metal containing single-chain nanoparticles

2.1 Introduction

One of major applications of SCNP is protein mimicking because of its sophisticated secondary or even tertiary microstructure and uniform size[4, 89]. In the last decades, how to construct regular secondary microstructure became a major challenge in the field[2]. Many groups started studying how to utilize new cross-linking chemistry characterization technique to construct and characterize secondary structure, such as BTA cross-linking SCNP with helical structure characterized by circular dichroism spectroscopy[9, 11, 70]. Additionally, more and more SCNPs with novel topologies were reported, such as tadpole-shaped SCNP[90], dumbbell-shaped SCNP[91], and Janus SCNP[92].

As a large group of protein, enzyme plays an important role in every cell of biological world. To study the catalytic mechanism of enzyme more deeply and explore even more robust macromolecular catalyst, enzyme mimicking attracts more and more attention from not only chemist but also engineer. Water-soluble transition metal containing SCNP has been considered to be an ideal choice for this due to macromolecular environment, catalytic activity of metal, and water solubility. This class of SCNP typically consist of normal polymer backbone synthesized through controlled radical polymerization, transition metal cations coordinated with ligands on pendent groups, and water-soluble pendent groups.

Various transition metals have been employed in SCNP catalysis in aqueous system, such as Cu for cooper catalyzed alkyne azide cycloaddition "click" reaction[16, 80] and hydroxylation reaction[79],

Pd for Suzuki reaction[19], and Ru for photoreduction of azide into amine[26]. In many cases, similar with real enzyme, metal-SCNP complex catalysts show higher catalytic performance than metal salts and metal ligand complexes[16, 19, 79]. As amphiphilic polymers, water-soluble SCNPs' behavior in aqueous system was considered to relate hydrophobic effect[12-14]. In this hypothesis, the local concentration of organic reactant inside of SCNP should be much higher than overall average solution[80], because the enthalpy of whole system is more favored[91]. Consequently, these SCNPs can work as nanoreactors in aqueous solution[11]. Following this hypothesis, it will enhance the catalysis that to keep the catalytic centers, transition metals, inside of the SCNPs. Therefore, hydrophobic ligands that can form strong coordination bonds are desired to prevent releasing transition metals into solution.

N-heterocyclic carbene (NHC) is a series of cyclic diaminocarbene, which can form Fischer type complexes with transition metals[93]. After studied in decades, numerous NHC-metal complexes have been synthesized and characterized[94]. Compared to traditional phosphine ligands, NHC ligands are also good σ donor but poor π acceptor[95]. From many reported cases, NHC ligands largely enhance the catalytic activity of transition metals, such as ruthenium in olefin metathesis[96] and palladium in coupling reactions[97]. For instance, in the kinetics study of olefin metathesis reaction catalyzed by Grubbs' 2nd generation catalyst, the NHC ligand makes the process that the phosphine-dissociated complex bind with olefin much more favored than bind with phosphine ligand again[98]. Consequently, the reaction rate of whole reaction is improved dramatically. Additionally, the bond dissociation energy of NHC-metal complex is relatively higher than most of ligand-metal complex that is catalytic active[99]. Because there are various published synthetic routes for NHC ligands containing numerous methodologies, it is possible to synthesize some

derivatives by using different reactants[93]. Besides, many positions on the ligand are accessible to functionalize. Therefore, NHC ligands would be a reasonable choice for SCNP-metal complex.

2.2 Results and Discussion

2.2.1 Parent polymer design

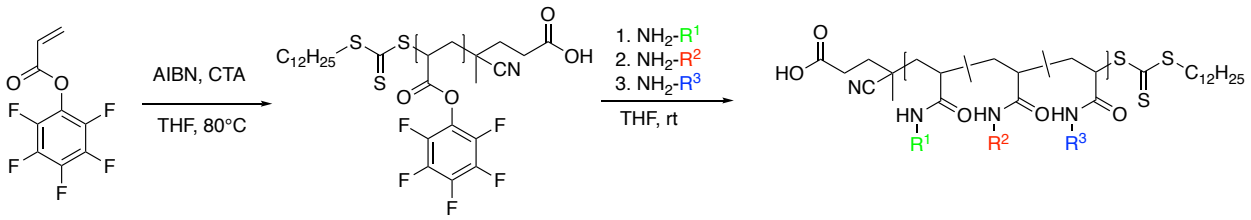

Scheme 15 Synthesis of PPFPA and substitution by primary amine

Based on our knowledge, a less basic anion can be a better leaving group. Consequently, a series of activated esters, such as pentafluorophenyl ester and N-hydroxysuccinimide ester, was utilized in not only organic synthesis but also polymer functionalization. The conjugated base of pentafluorophenyl oxide anion, pentafluorophenol, is one of the most acidic phenols, which was reflected in its low pKa (5.5). In polymer functionalization, poly (pentafluorophenyl acrylate) (PPFPA) can react with primary amine under ambient temperature without oxygen and water sensitivity[11, 100]. Moreover, by adding different ratio of amines, different random copolymers can be synthesized, which is especially useful when there are incompatible structures for polymerization reactions on pendent groups (Scheme 15)[11]. Additionally, the whole process of polymer functionalization can be monitored through ^{19}F NMR by calculating the ratio of integration after each reaction between parent polymer and amine additives[9].

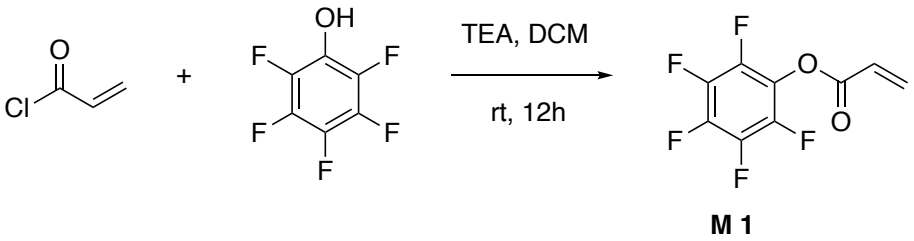

M 1

Scheme 16 Synthesis of M1

The monomer pentafluorophenyl acrylate (**M1**) was synthesized by reaction between acryloyl chloride and pentafluorophenol. Steglich reaction was also tried in M1 synthesis, but there was no expected product produced. We suggested that N,N-dimethylaminopyridine (DMAP), as a strong nucleophile, might attack the fluorobenzene ring and lose its catalytic activity. After acquired enough quantity of monomer, poly (pentafluorophenyl acrylate) (**PP1**) was synthesized by reversible addition fragmentation transfer polymerization (RAFT). As a controlled radical polymerization, RAFT was utilized to synthesize polymer in low polydispersity (PDI)[24]. In other words, polymer chains with similar length can be produced by RAFT, which is vital to form single-chain nanoparticles with uniform size[1]. However, the molecular weight and polydispersity of **PP1** were not acquired from size-exclusion chromatography (SEC) because of the insufficient solubility of **PP1** in dimethylformamide (DMF).

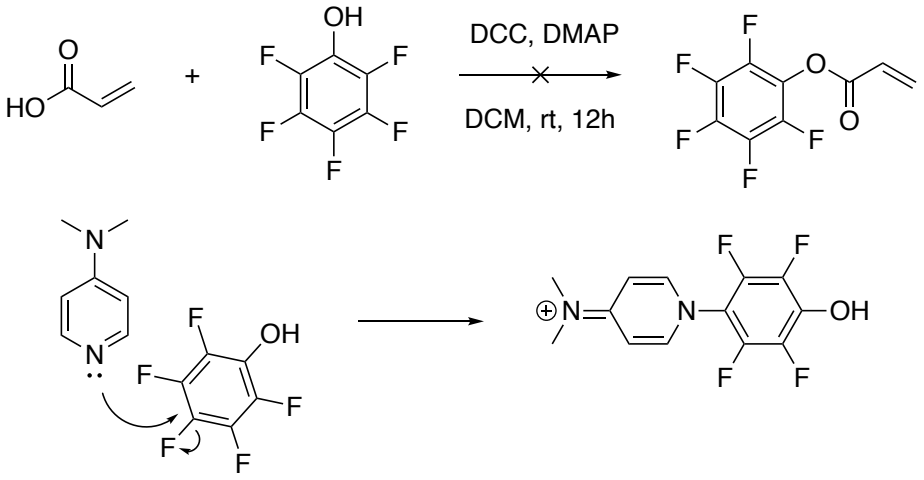

Scheme 17 Proposed reaction between pentafluorophenol and DMAP

2.2.2 Ligand design and synthesis

As the component to link transition metal and polymer chain, ligand is one of the most important parts of the project. To prove the SCNP aqueous catalysis hypothesis, a ligand with high coordination dissociation energy was desired. Additionally, promotion of catalytic activity is also desired in ligand selection. Got inspired by transition metal complex catalytic chemistry, N-heterocyclic carbene ligands (NHC) were selected to be the ligands in SCNP catalysis. As a strong σ donor and weak π acceptor, NHC ligand can form strong coordination bond with various transition metals and improve the catalytic activity dramatically, which suit the requirements of ligands designing appropriately. Based on reported data from publications, compared with metal salts NHC-metal complexes perform much higher efficiency in a variety of reactions, such as Suzuki reaction and olefin metathesis. And in many mechanism studies, the NHC-metal bonds won't break in catalytic cycles[101], which means it is highly possible that the NHC functionalized SCNP won't release transition metal into the aqueous solution. By constructing amine groups, the NHC ligand can also work as cross-linker to form SCNP.

We applied the strategy of ring closing of diimine to form imidazolium salt and finally produce the NHC ligand by deprotonation[93]. The diimine can be produced by the imination reaction between ketone and aniline. Because two amine end group need to be constructed to react with parent polymer chain, two reactive groups are necessary on the ketone. Consequently, 4, 4'-dibromobenzil (**L2.1**) was selected as the starting material, since the aryl bromide groups are reactive in Suzuki reaction, which is one of the most common methodologies to form new C-C bonds in synthetic chemistry (Scheme 18). Additionally, Boc protection was utilized to protect amine end from imination.

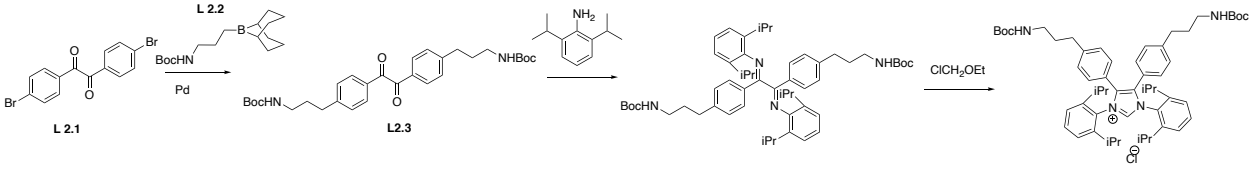

Scheme 18 Proposed synthetic route of L2.6

The imination reaction was tried in different conditons, including classic acetic acid catalyzed imination, magnesium sulfate dehydration, titanium tetrachloride dehydration, and trimethylaluminum imination. Only trimethylaluminum imination showed good yield of diimine (86%). To react with bromo group on 4, 4'-dibromobenzil, borane structure was constructed by the reaction between C-C double bonds and 9-borabicyclo(3.3.1)nonane (9-BBN). The borane product was used in next step Suzuki reaction without purification. To make the Suzuki reaction more efficient, palladium tetrakistriphenylphosphine [$Pd(PPh_3)_4$] was used as catalyst in the reaction. Besides borane, aryl bromide, and palladium catalyst, base is another important factor to

make the reaction occur. By our knowledge, a stronger base can make the reaction more efficient. However, benzil and its derivatives undergoes benzilic acid rearrangement under strong basic conditions[102]. Based on this mechanism, no expected product was observed in the entry using sodium hydroxide. Because the first step fundamental mechanism of benzilic acid rearrangement is that base anion nucleophilic attack carbonyl, more bulky base potassium tert-butoxide (t-BuOK) was added as the base in the next entry and the expected product still was not observed, which indicates that the basicity shows larger influence than the steric hinder. Following this hypothesis, the weaker base, potassium carbonate, was utilized and made the reaction occur and shows 70% yield in 12 hours and 90% yield in 24 hours.

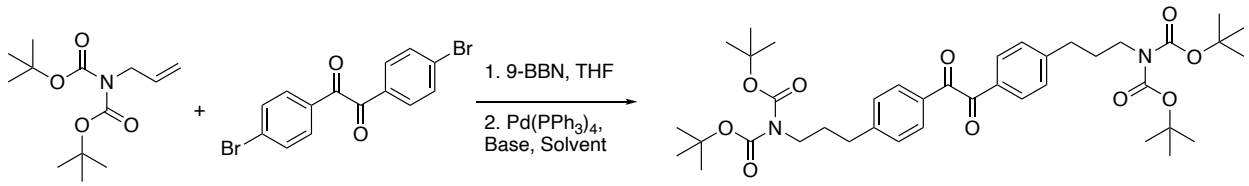

Scheme 19 Suzuki reaction for condition optimization

Table 1 Condition optimization of Suzuki reaction

Entry	Base	Solvent	Temperature	Time	Yield
1	NaOH	THF:H_2O 5:1	reflux	12	-
2	NaOH	THF:H_2O 5:1	r.t.	12	-
3	t-BuOK	THF	reflux	12	-
4	t-BuOK	THF	r.t.	12	-
5	K_2CO_3	THF:H_2O 5:1	r.t.	24	90%
6	K_2CO_3	THF:H_2O 5:1	r.t	12	70%

Although the imination and Suzuki reaction had been optimized to good yields, the order of reactions became a problem in the process of synthesis. We planned to do the imination after the Suzuki reaction in the original synthetic route. As shown in scheme, no expected imine was produced in the reaction. Because the appearance of the product was similar with rubber, we proposed that the product would be a polyimine formed by the amine ends and carbonyl groups (Scheme 20). Interestingly, trimethylaluminum is a reagent that can be Lewis acid and Brønsted base simultaneously[103]. As mentioned before, boc protecting group, which can be removed by addition of strong Brønsted acid, was installed to prevent the amine ends reacting with carbonyl during the imination process. However, boc protecting group was not compatible with strong Lewis acid neither based on the failed imination experiment. Consequently, we decided to change the order of reactions. The imination reaction was moved to be the first step to avoid the deprotection of boc group. Following this order, the amine-end diimine was produced.

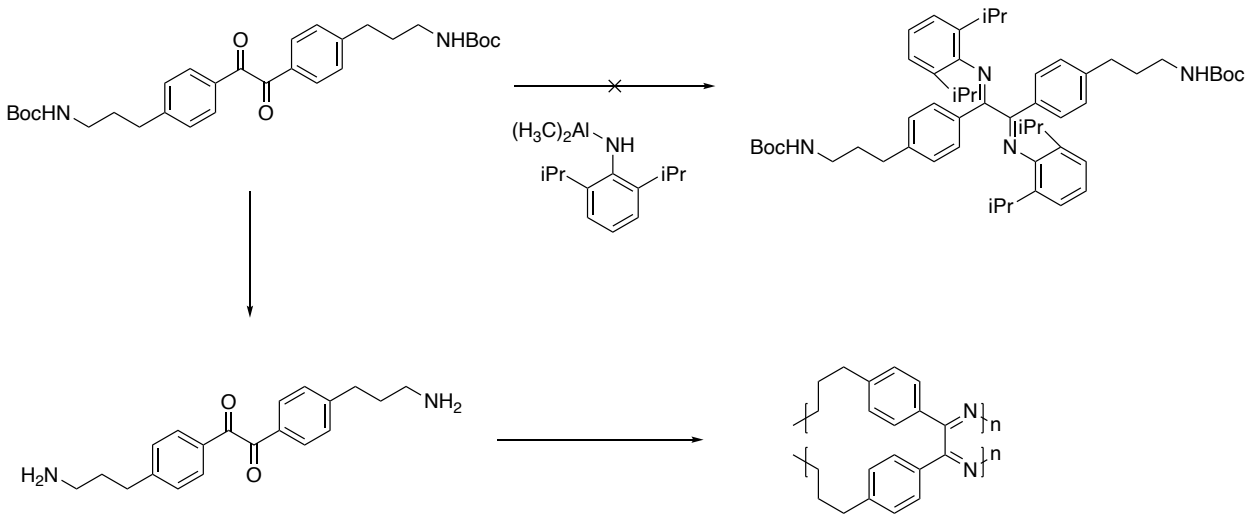

Scheme 10 Proposed polymerization of aminobenzil

The last step of synthesis of precursor of double amine-end NHC ligand is the ring-closing reaction of diimine to form imidazolium salt. The common methodology of formation of imidazolium salt by ring-closing was the reaction between chloromethyl ethyl ether and diimine, which was proved that couldn't work in this case because of the steric hinder.

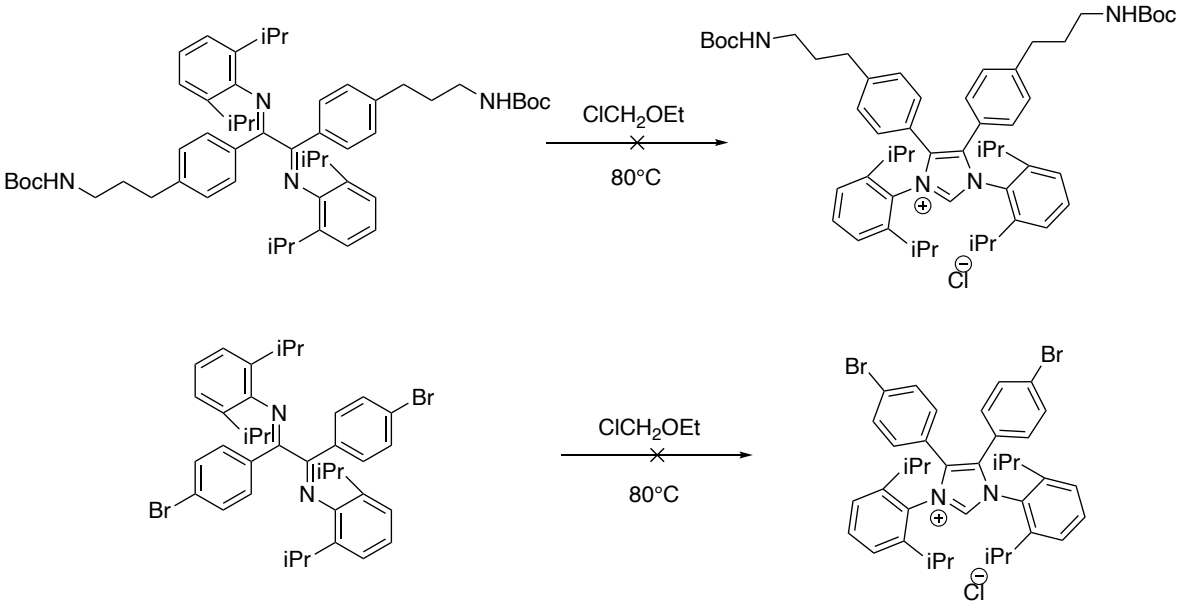

Scheme 11 The bulk diimine cannot be ring-closed by normal ring-cloing reagent

For bulky diimines, chloromethyl pivalate was proved to be better ring-closing reagent in some published cases[104, 105]. And it showed good performance in the ring-closing of the synthesis. From ^{1}H NMR data, the obvious difference was the peak with chemical shift of 9.7ppm, which was considered to be significant evidence of the formation of imidazolium salt.

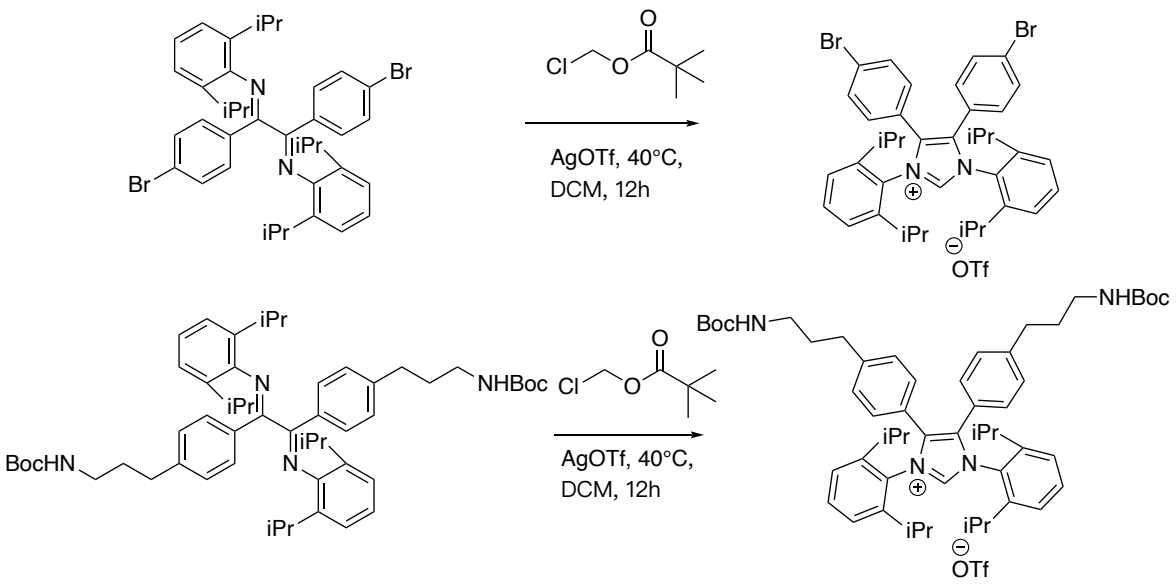

Scheme 12 Ring-closing reaction to form imidazolium salt

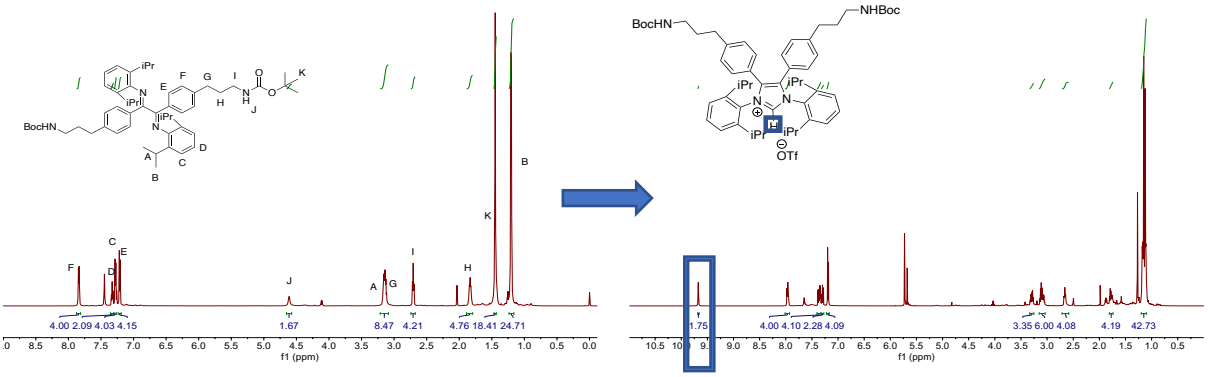

Figure 7 Comparison of ^{1}H NMR before and after ring-closing

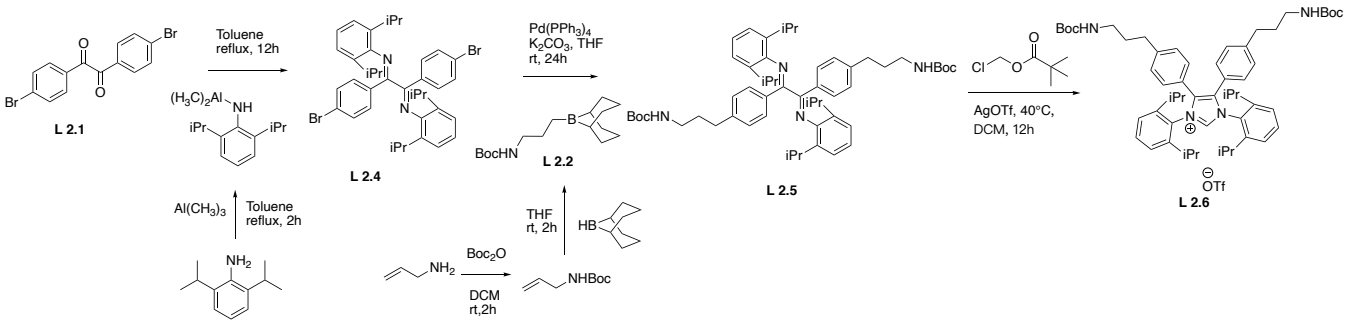

Scheme 13 Finally version of synthetic route of L2.6

2.2.3 Polymer functionalization and single-chain nanoparticle formation

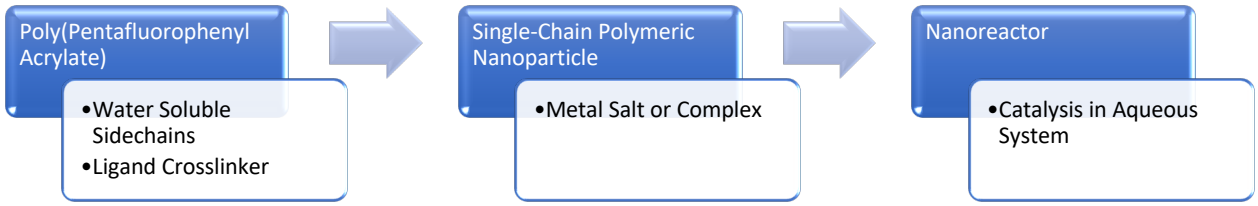

Figure 8 Synthetic strategy of SCNP catalyst

As mentioned in polymer design portion, poly (pentafluorophenyl acrylate) was selected to be the parent polymer of the project because of convenience of functionalization. To provide the water solubility, Jeffamine (Mn~600), a type of amine-end poly propylene glycol (PPG), was selected to be majority of pendent group. Additionally, the 100% Jeffamine substituted PPFPA was synthesized to calculate the original molecular weight of parent polymer. Three Jeffamine substituted polymers with different ratio were synthesized by the reaction between PPFPA and Jeffamine in tetrahydrofuran at ambient temperature. The ratio of Jeffamine was monitored by ^{19}F NMR. These polymers were characterized by SEC to get number average molecular weight Mn, weight average molecular weight Mw, and polydispersity index PDI.

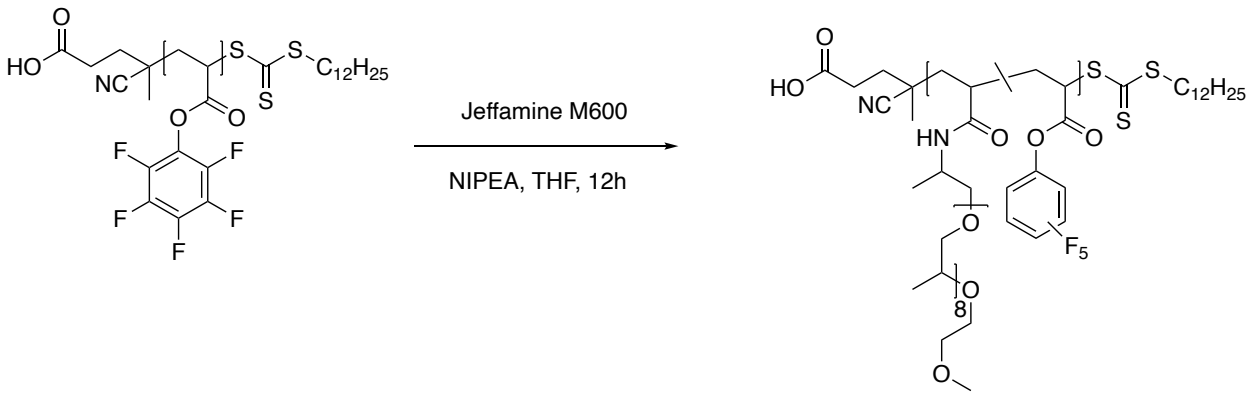

Scheme 14 PPFPA functionalized by Jeffamine

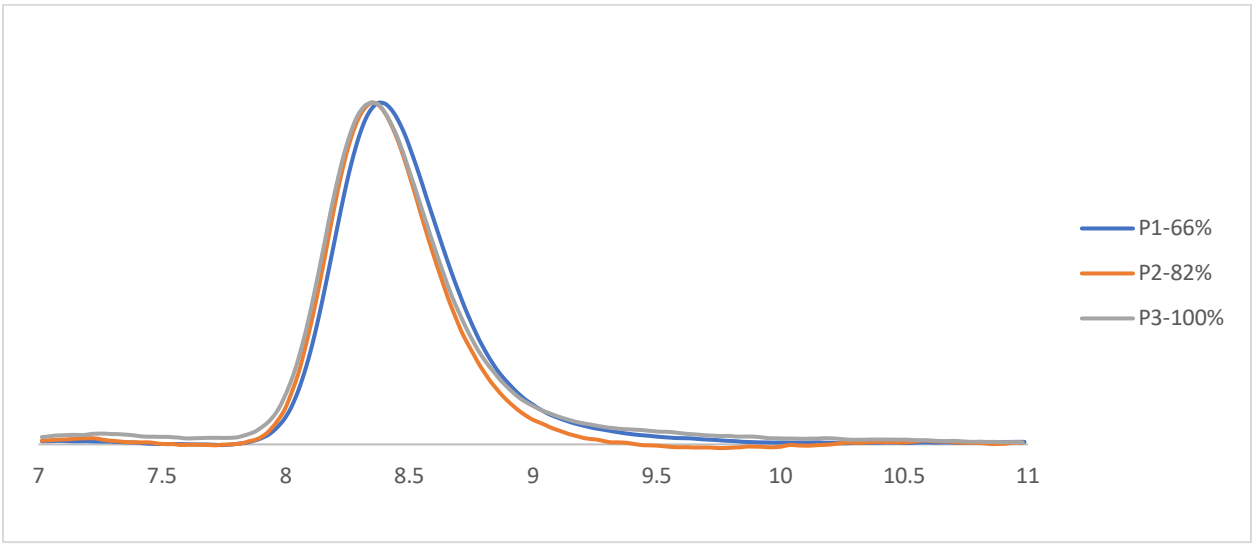

Figure 9 SEC trace of Jeffamine substituted PPFPA P1, P2, and P3

Table 2 Molecular weight and polydispersity of P1, P2, and P3

Polymers	Mn	Mw	PDI
P1 (Jeffamine 66%)	37kDa	54kDa	1.442
P2 (Jeffamine 82%)	40kDa	58kDa	1.452
P3 (Jeffamine 100%)	42kDa	59kDa	1.411

The even increasing Mn and Mw as well as the similar PDI are strong evidence of substitution reaction occurring. Running at 1mg/mL, the Jeffamine substituted parent polymers were reacted with excess ligand cross-linker, which was deprotected by trifluoracetic acid (TFA). Based on ^{19}F NMR result, the reaction was finished when there was no polymer peak. Compared to parent polymer, SCNP usually has a longer retention time in SEC, because the dynamic size of polymer became smaller when it gets intramolecular cross-linked. However, the SCNP cross-linked by ligand cross-linker showed a shorter retention time rather than longer retention time in SEC. The reason we proposed is that the molecular weight of SCNP is actually higher than the molecular weight of parent polymer caused by the higher molar mass of ligand cross-linker. Besides, because the addition of ligand cross-linker was largely excess, it is possible that part of ligand cross-linker reacted with polymer only on one side of amine end, which caused the molecular weight of functionalized polymer increased with low cross-linking degree.

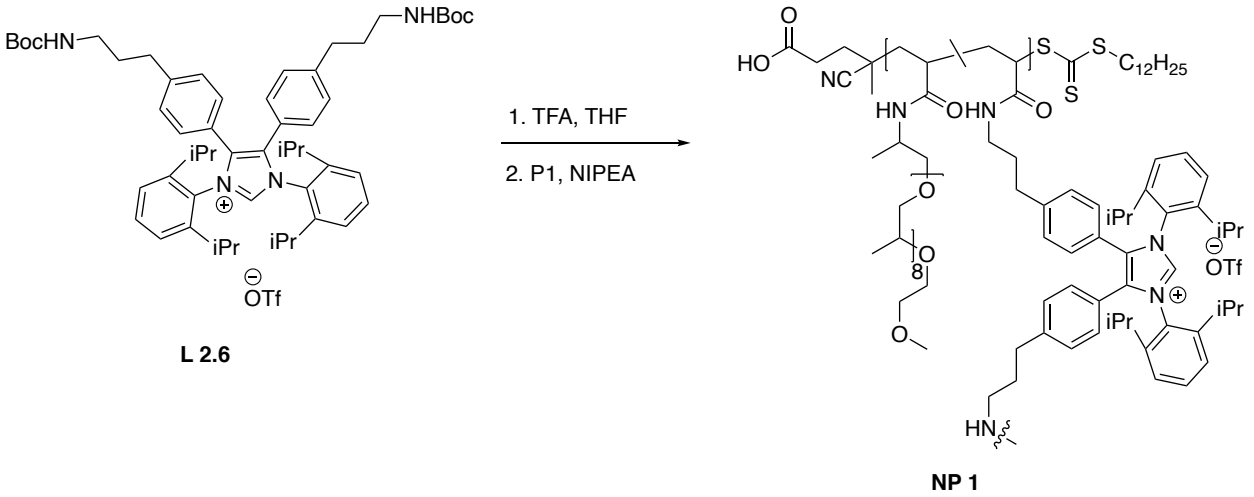

Scheme 15 P1 cross-linked by ligand cross-linker to form SCNP NP1

Even though various transition metals have been selected to bind with SCNPs to form robust SCNP catalysts, the ruthenium coordinated SCNP for olefin metathesis is still novel. The most common methodology for NHC enhanced Grubbs' catalyst is the reaction between Grubbs' 1st generation catalyst and NHC ligand produced by deprotonation of imidazolium salt. The successful produce of NHC ruthenium complex can be proved by ^{31}P NMR[106]. Because Grubbs' 1st generation catalyst is symmetrical, there is only one signal of phosphorus from two phosphine ligands. However, there should be two peaks, free phosphine ligand and NHC ruthenium complex, in ^{31}P NMR of ligand substitution reaction solution before purification. Following this direction, the ligand functionalized SCNP was treated t-BuOK to generate free NHC ligand. Then, Grubbs' 1st generation catalyst solution was added. Unfortunately, two expected peaks didn't appear on ^{31}P NMR. The only peak in the spectra was recognized to tricyclohexylphosphine oxide, which means the Grubbs' 1st generation catalyst was consumed but no NHC ruthenium complex formed. In the next entry, the base was changed to a stronger base, potassium bis(trimethylsilyl)amide (KHMDS). However, the ^{31}P NMR result sill didn't show the expected peaks. The explanation we suggested is that the NHC ligand utilized in this project was too bulky and the reaction between polymer ligand and metal complex is still complicated and need further study. Additionally, other transition metal, such as palladium and copper, will be tried in the future to produce robust SCNP catalysts in aqueous system.

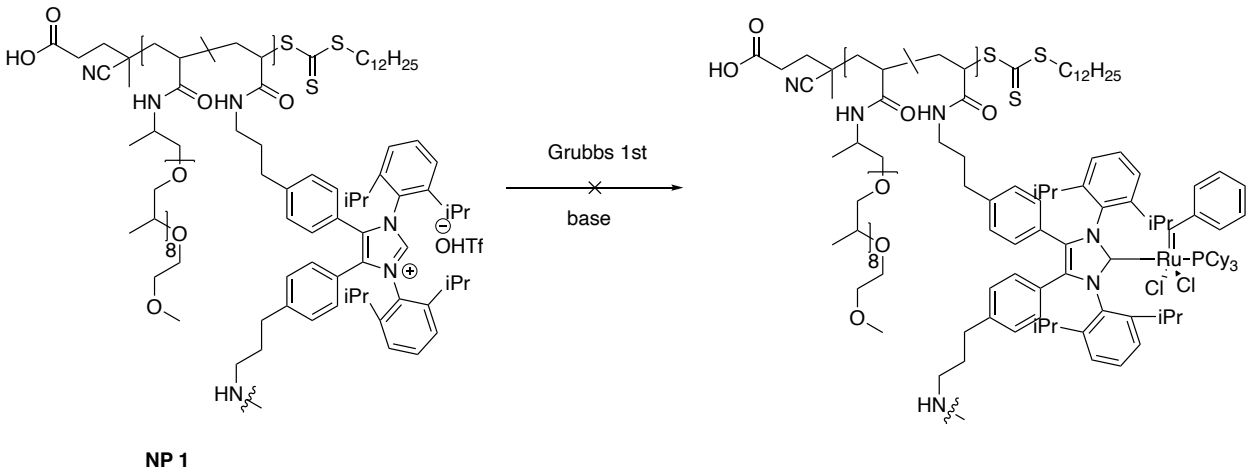

Scheme 16 Unsuccessful ruthenium coordination on NP1

The water solubility experiments of Jeffamine functionalized parent polymer and SCNP were done under different concentrations and temperatures. Although the Jeffamine with Mn of 600 used in the project was shown a moderate solubility in water, it didn't provide water solubility as pendent group based on the water solubility experiments. From P1 (66 % Jeffamine) to P3 (100% Jeffamine), no clear and transparent solution was formed even in the concentration lower than 1mg/mL. We proposed that there were not enough water molecules that can form hydrogen bonding with oxygen atoms on Jeffamine pendent groups, which are much more concentrated, even at low polymer concentration, than free Jeffamine solution. Moreover, as we knew, poly ethylene glycol (PEG) is more hydrophilic than PPG. The water solubility can be improved by changing the proportion of PPG in the Jeffamine.

2.3 Conclusions

We have shown the synthesis of ligand functionalized SCNP synthesized through PPFPA functionalization strategy. We polymerized pentafluorophenyl acrylate through RAFT to get low-dispersity PPFPA parent polymer. The double amine-end NHC ligand was synthesized through various reactions, including trimethylaluminum imination, Suzuki reaction, and imidazolium salt formation by ring closing. The process of substitution was monitored by ^{19}F NMR, and the functionalized polymers were characterized by SEC after purification. Based on ^{31}P NMR, the production of NHC ruthenium complex was not achieved. New coordination methodologies and different transition metals need to be done in the future.

2.4 Experimental

2.4.1 Materials

Reagents were obtained from the indicated commercial suppliers and used without further purification unless otherwise stated: 2,4-diisopropylaniline (TCI), Di-Tert-Butyl Pyrocarbonate (boc anhydride, Chem-Inpex), 4,4'-dibromobenzil (TCI), trimethylaluminum (Sigma-Aldrich), allylamine (Alfa Aeser), 9-BBN monomer (Fisher Scientific), Tetrakis(Triphenylphosphine)Palladium(0) (Sigma-Aldrich), chloromethyl pivalate (Sigma-Aldrich), Silver Trifluoromethanesulfonate (Sigma-Aldrich), pentafluorophenol (Oakwood Products, Inc), acryloyl chloride (Sigma-Aldrich), 4-cyano-4-(((dodexylthio)carbonthioyl)thio)pentanoic acid (CTA, Boron Molecular), Grubbs catalyst 1st generation (Sigma-Aldrich), Grubbs catalyst 2nd generation (Sigma-Aldrich), hexanes (Fisher Scientific), ethyl acetate (Fisher Scientific), 2,2'-azobis(2-methylpropionitrile) (AIBN, Sigma-Scientific, recrystallized from methanol), silica gel (230 – 400 mesh, SiliCycle), N,N'-dimethylformamide (HPLC grade, Fisher Scientific), dimethyl sulfoxide-d6 (Cambridge Isotope Laboratories), chloroform-d (CDCl3, Cambridge Isotope Laboratories). Dry dichloromethane (DCM) was obtained from refluxing with calcium hydride. Dry toluene and tetrahydrofuran (THF) were obtained from refluxing with sodium in presence of benzophenone as indicator.

2.4.2 Instrumentation

^{1}H, ^{13}C, ^{19}F and ^{31}P NMR spectra were acquired with a Varian Unity INOVA 500 MHz or Varian Mercury 400 MHz spectrometer. Chemical shifts (δ) were reported in parts per million (ppm) relative to tetramethylsilane (TMS). Solvent (CDCl3) contained 0.03% v/v TMS as an internal

reference. Peak abbreviations are used as follows: s = singlet, d = doublet, t = triplet, q = quartet, m = multiplet, br = broad).

SEC was performed on a Tosoh EcoSEC dual detection (RI and UV) SEC system coupled to an external Wyatt Technologies miniDAWN Treos multiangle light scattering (MALS). Samples were run in DMF at 50 °C at a flow rate of 0.45 mL/min. The column set contained one Tosoh SuperH-L column, one Tosoh SuperH2500 column and a Tosoh SuperH4000 column. All polymer solutions characterized by SEC were 1.0 mg/mL in DMF, stirred magnetically for at least 10 hours and filtered through 0.45 μm PTFE syringe filters before analysis.

2.4.3 Experimental procedures

2.4.3.1 Synthesis of pentafluorophenyl acrylate (M1)

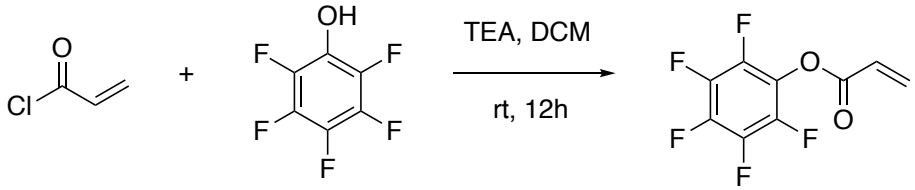

M 1

In a 50mL round bottom flask, pentafluorphenol (1.84g, 10mmol, 1eq) triethylamine (1.67 mL, 1.21g, 12mmol, 1.2 eq) were dissolved in 25mL dry DCM under argon. The mixture was cooled over an ice bath and acryloyl chloride (0.97mL, 1.09g, 12mmol, 1.2eq) was added dropwise. The reaction was allowed to stir 12 hours and then quenched with saturated sodium bicarbonate solution. Organic layer was washed with saturated sodium bicarbonate solution (50 mL × 2) and Brine (50 mL × 2) and dried with sodium sulfate. Crude product purified by column chromatography to afford colorless liquid (1.43g, 60%). ^{1}H NMR (500 MHz, $CDCl_3$, δ, ppm): 6.45 (s, 1H), 5.90 (s, 1H), 2.09 (s, 3H); ^{13}C NMR (500 MHz, $CDCl_3$, δ, ppm): 165.95, 142.79, 140.71,

138.90, 137.43, 133.71, 129.52, 20.07; ^{19}F NMR (500 MHz, $CDCl_3$, δ, ppm): -152.87, -158.29, -162.62.

2.4.3.2 Synthesis of poly (pentafluorophenyl acrylate) (PP1)

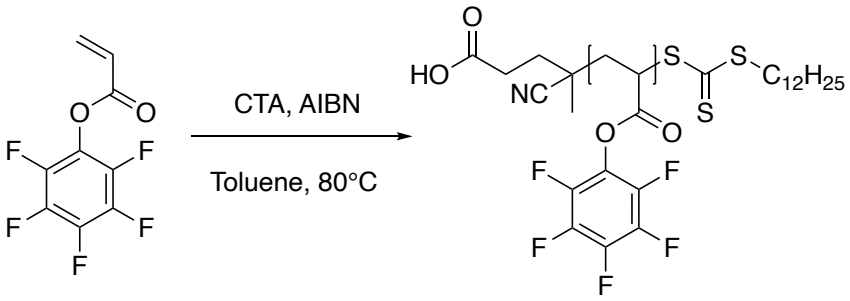

Pentafluorophenyl acrylate (2.38g), CTA (38.9mg) and AIBN (1.64mg) were dissolved in 5mL dry toluene in a 10mL Schlenk flask and sparged with argon over an ice bath for 30 min. The mixture was heated to 80 °C and stirred for 24 hours. Monomer conversion was calculated from ^{19}F NMR of the mixture. Product was precipitated from cold methanol and collected by vacuum filtration.

2.4.3.3 Synthesis of N-bocallylamine

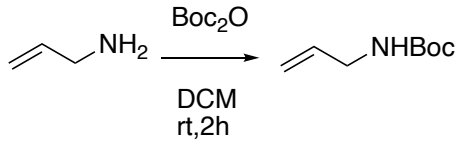

Boc anhydride (12.0g, 55mmol, 1.1eq) was added in a dry DCM solution of allylamine (3.76mL, 2.86g, 50mmol, 1eq) under ice bath. The mixture was allowed to stir for 2 hours and then was concentrated under reduced pressure. The crude product was dried under vacuum without purification to afford colorless solid (7.85g, 99%). ^{1}H NMR (500 MHz, $CDCl_3$, δ, ppm): 5.18 (d,

2H), 5.10 (d, 2H), 4.63 (s,1H), 3.75 (s, 2H), 1.45 (s, 9H); ^{13}C NMR (500 MHz, $CDCl_3$, δ, ppm): 155.79, 134.95, 115.67, 85.15, 28.39, 27.42.

2.4.3.4 Synthesis of L2.4[103]

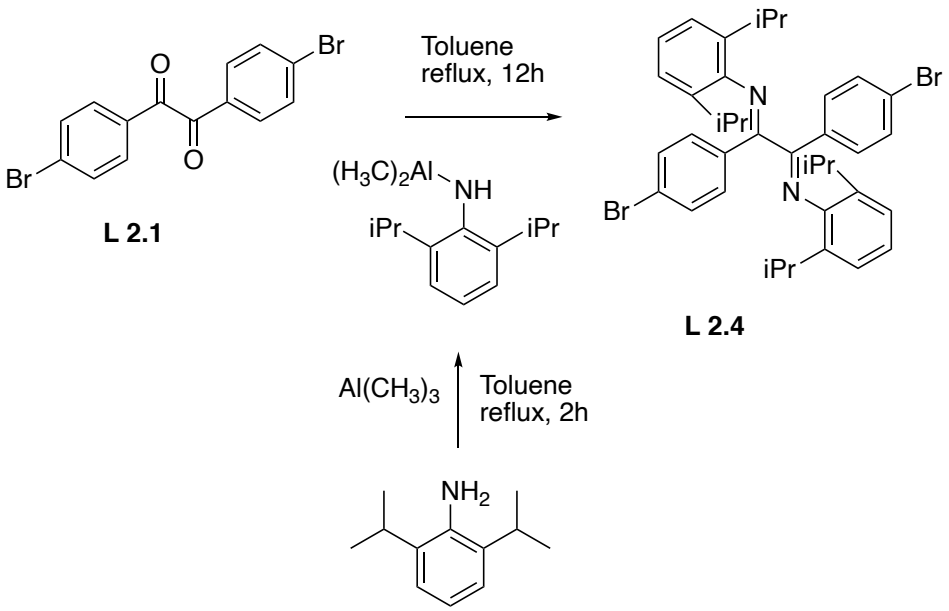

2,6-diisopropylaniline (2.26mL, 2.13g, 12mmol, 2.4 eq) in dry toluene solution was injected into a 500mL 3-neck round bottom flask under argon, 6mL 2.0M trimethylaluminum in toluene solution was added dropwise at ambient temperature. Then the mixture was heated to reflux for 2hours. After the reaction was cooled at ambient temperature, 4,4'-dibromobenzil (1.84g, 5mmol, 1 eq) was added and the mixture was allowed to stir at reflux temperature for 12hours before quenched by adding 5% aqueous sodium hydroxide solution under ice bath. The aqueous layer was extracted with ethyl acetate twice. The combined organic layer was dried with sodium sulfate. After removing solvent by rotary evaporator, the crude product was purified by column chromatography to afford white solid (4.88g, 71.3%). ^{1}H NMR (500 MHz, $CDCl_3$, δ, ppm): 7.80 (d, 4H), 7.64 (d, 4H), 7.33 (m,2H), 7.23 (d, 4H), 3.10 (m, 4H), 1.21 (d, 24H); ^{13}C NMR (500 MHz, $CDCl_3$, δ, ppm): 155.79, 134.95, 115.67, 85.15, 28.39, 27.42.

2.4.3.5 Synthesis of L2.2

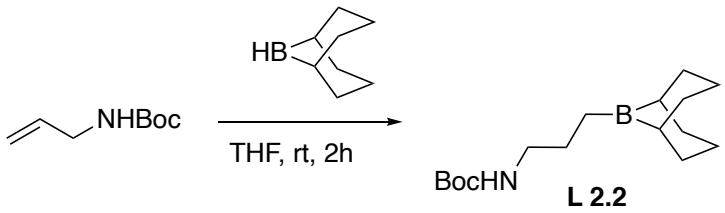

L 2.2

N-bocallylamine (0.157g, 1mmol, 1 eq) was dissolved in dry THF under argon at ambient temperature. 2mL 0.5M 9-BBN in THF solution was added dropwise. The mixture was allowed to stir for 2hours and used without purification.

2.4.3.6 Synthesis of L2.5[107]

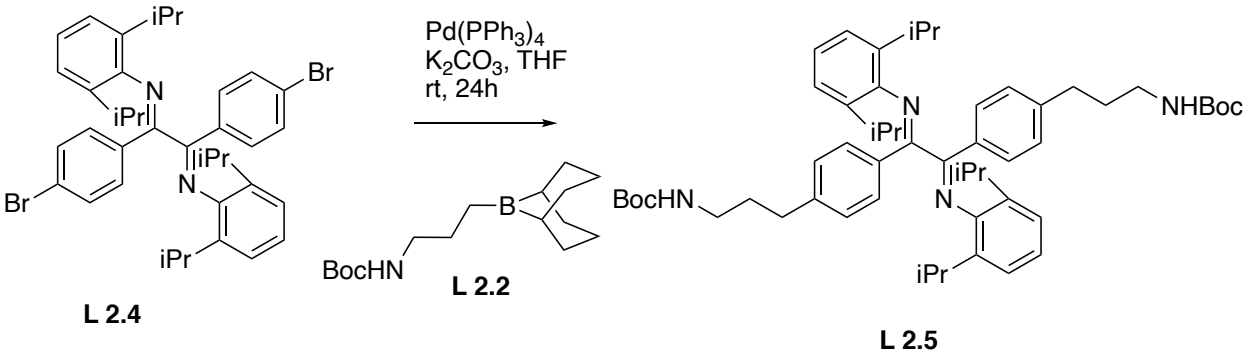

L 2.4 **L 2.2** **L 2.5**

L2.4 (0.275g, 0.4mmol, 0.4 eq), $Pd(PPh_3)_4$ (0.0347g, 0.03mmol, 0.03 eq), and potassium carbonate (0.415g, 3mmol, 3 eq) were dissolved by 100mL THF:H_2O 5:1 solution in an addition funnel. The solution was added into the reaction solution of L2.2 under argon and allowed to stir 24hours before added ethanolamine. Then water and ethyl acetate were added. Organic layer was washed by water × 2 and brine. Solvent was removed by rotary evaporator after dried with sodium sulfate. The crude product was purified by column chromatography (0.301g, 90%). ^{1}H NMR (500 MHz, $CDCl_3$, δ, ppm): 7.78 (d, 4H), 7.35 (m, 2H), 7.26 (d,4H), 7.21 (d, 4H), 4.60 (s, 2H), 3.11 (m, 8H), 2.68 (t, 4H), 1.86 (q, 4H), 1.45 (s, 18H), 1.21 (d, 24H).

2.4.3.7 Synthesis of L2.6[104]

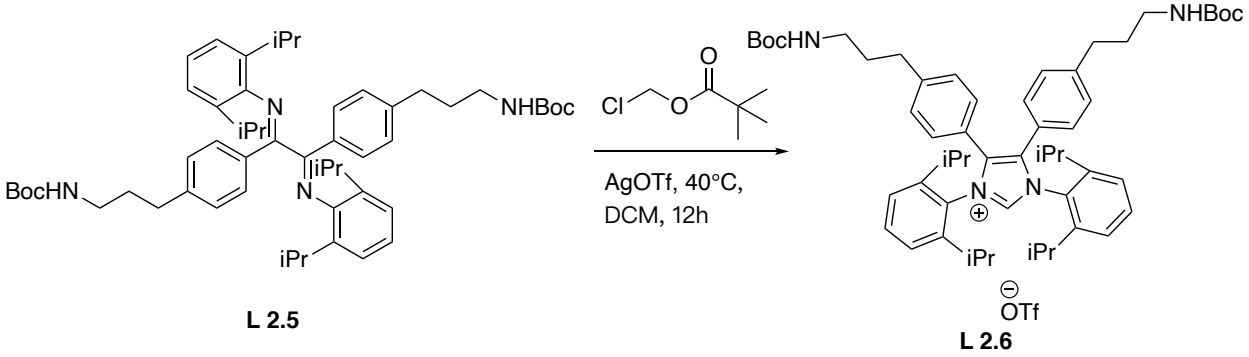

Chloromethyl pivalate (0.045g, 0.3mmol, 1.5 eq) and AgOTf (0.077g, 0.3mmol, 1.5 eq) was added into DCM solution of L2.5 (0.169 g, 0.2mmol, 1 eq) in a 5mL Schlenk flask under argon. The mixture was heated to 40°C for 12hours. After removing solvent by rotary evaporator, the crude product was purified by column chromatography to afford brown liquid (0.186g, 93%). ^{1}H NMR (500 MHz, DMSO-d_6, δ, ppm): 9.89 (s, 1H), 7.98 (d, 4H), 7.43 (m, 2H), 7.38 (d, 4H), 7.28 (d, 4H), 3.20 (m, 8H), 2.87 (m, 4H), 2.17(m, 4H), 1.18 (m, 42H).

2.4.3.8 Synthesis of Jeffamine substituted PPFPA (P1-P3)

To a dry THF solution of PPFPA, NIPEA and dry THF solution of Jeffamine (Mn~600) was added at ambient temperature. The reaction was monitored by ^{19}F NMR and shut off when the target degree of substitution was reached. The mixture was concentrated to 10mL and then dialyzed against THF:H_2O 1:1, against ethanol:H_2O 1:1, and against H_2O. The solvent of the final mixture was removed by lyophilizer.

2.4.3.9 Synthesis of NP1

To a dry THF solution of 60mg L2.6, 30 mg TFA was added and allowed to stir 30minutes. Then 80mg NIPEA was added. The mixture was added dropwise into 120mL dry THF solution of 65mg P1. The reaction was monitored by ^{19}F NMR and shut off when the target degree of substitution was reached. The mixture was concentrated to 10mL and then dialyzed against THF:H_2O 1:1, against ethanol:H_2O 1:1, and against H_2O. The solvent of the final mixture was removed by lyophilizer.

Chapter 3. Inverse temperature dependent olefin metathesis catalyzed by thermosensitive ruthenium-containing polymer

3.1 Introduction

One of most interesting property of enzyme is its optimal temperature. Usually, the efficiency of catalysts increases with temperature, so does enzyme when the temperature lower than optimal temperature. However, the catalytic efficiency of enzyme decreases dramatically when the temperature is higher than optimal temperature. The process called denaturation is even irreversible. To mimic enzyme more completely, how to control the efficiency of SCNP catalyst by temperature became a goal. Although there are already some ruthenium complex catalysis of olefin metathesis in aqueous system reported[108], inverse temperature controlling is still novel in the field.

As mentioned in chapter 2, we aimed to catalyze organic reactions in aqueous system by transition metal containing SCNP. However, the Jeffamine pendent group didn't improve the solubility of SCNP in water remarkably. When we were reselecting water-soluble pendent groups, a series of poly N-alkylacrylamide attracted our attention by their interesting property of solubility in water. By our knowledge, as a key structure in protein, amide structure can form hydrogen bonding as not only donor but also acceptor, which help it get dissolved in water. However, the alkyl group on poly N-alkylacrylamide are hydrophobic, which is a negative influence for water-solubility of polymer[109]. The balance is controlled by the temperature of solution, because the strength of hydrogen bonding decreases in higher temperature. Consequently, different poly N-

alkylacrylamide has different temperature of cloud point, also known as lower critical solution temperature (LCST), in aqueous solution[110]. When the temperature of solution is higher than LCST, the solubility of the polymer decreases dramatically, which remind us of the optimal temperature of enzyme[111]. Additionally, poly N-alkylacrylamide can be synthesized by PPFPA functionalization. Therefore, we decided to utilize poly N-alkylacrylamide as polymer backbone to continued studying the enzyme mimicking by SCNP.

3.2 Results and Discussion

3.2.1 Ligand synthesis

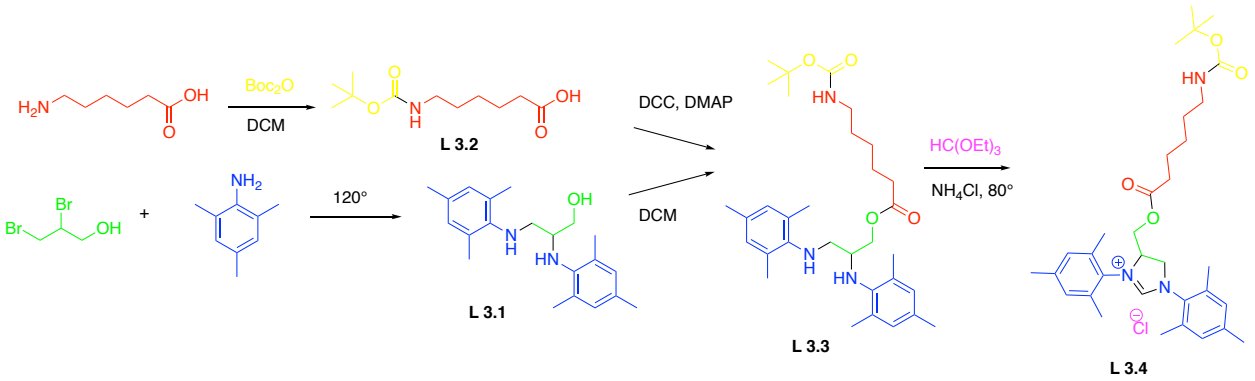

Scheme 17 Synthetic route of L3.4

To produce NHC ruthenium catalyst successfully, ligand was redesigned. Because the substitution of tricyclohexylphosphine ligand to NHC ligand has been applied extensively in synthesis of derivatives of Grubbs' 2nd generation catalyst, major part of ligand was kept. To link the NHC ligand to polymer, amine end linker was added on tetrahydroimidazole ring. Following retrosynthesis strategy, the ligand compound was divided into six parts. Similar with chapter 2, boc protecting group was constructed to prevent amine group reacting in latter steps. Different with previous ligand synthesis, diamine was synthesized to form dihydroimidazolium salt ring. Following claasic SN2 mechanism, 2,4,6-trimethylaniline was reacted with 2,3-dibromopropanol to produce diamine **L3.1**[112]. To get higher yield, 2,4,6-trimethylaniline worked as solvent in the reaction. The diamine **L3.1** was esterified with boc-aminocaproic acid **L3.2** by Steglich reaction. The final ring closing reaction occurred between diamine **L3.3** and triethyl orthoformate. ^{1}H NMR

was still a major characterization of product from every steps. The peak with chemical shift 9.5ppm indicates the successful ring closing reaction.

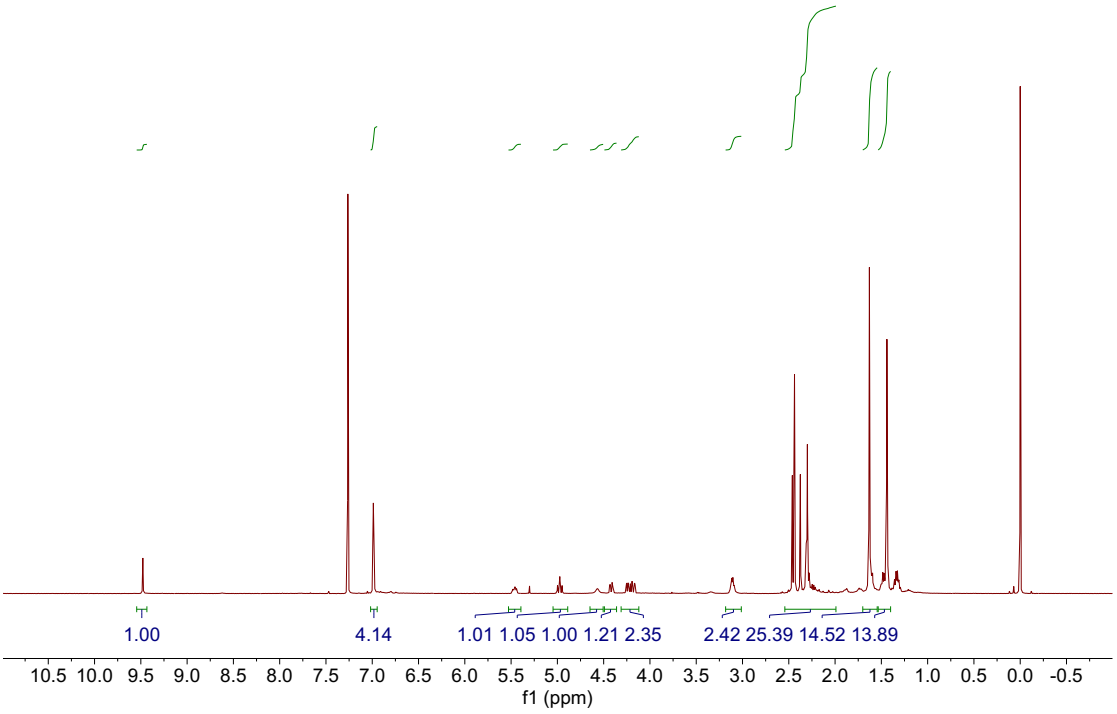

Figure 10 1H NMR of L3.4

The ligand was tested in coordination reaction as soon as acquired from the last step of synthesis. After treated with t-BuOK, the deprotonated imidazolium salt was reacted with Grubbs' 1st generation catalyst in dry toluene. The result mixture of complex C1 was characterized by ^{31}P NMR and ^{1}H NMR. There was obvious shift in ^{31}P NMR from 35ppm to 28ppm, which is close to the chemical shift of the phosphorus peak in Grubbs' 2nd generation catalyst. Additionally, the peak of proton on C=Ru bond in ^{1}H NMR is another key evidence of NHC-Ru complex formation. Compared to ^{1}H NMR of Grubbs' 1st generation catalyst, the peak of the proton of the product from the reaction was closer to Grubbs' 2nd generation. Although we didn't find a suitable method

of purification for the product of coordination reaction, these two comparisons in NMR are significant evidence for the formation of NHC-Ru complex.

3.2.2 Polymer functionalization and single-chain nanoparticles formation

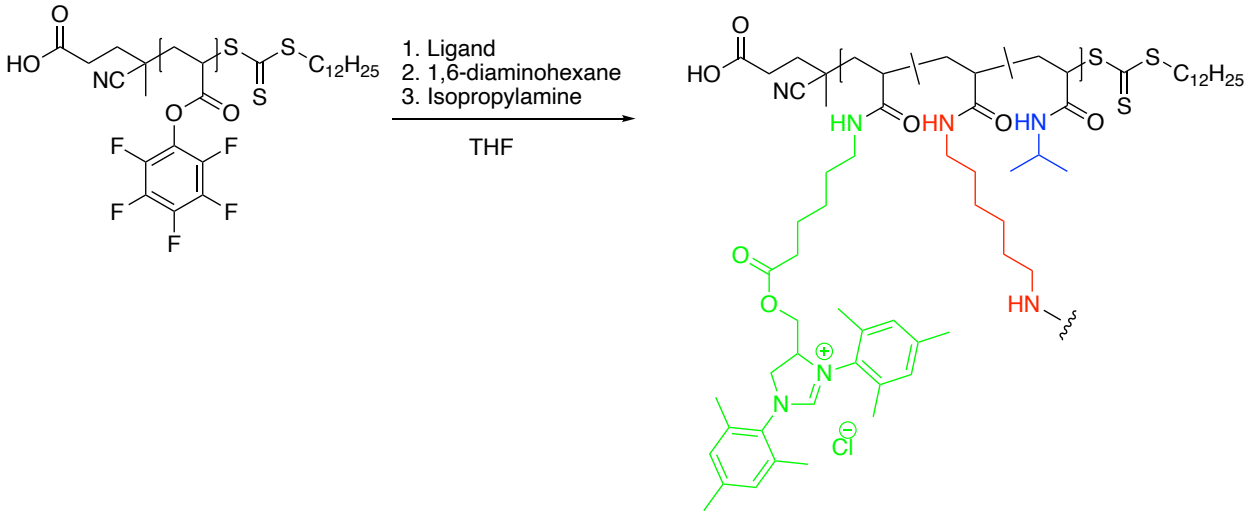

Scheme 18 Synthetic strategy of functionalization of PPFPA to form SCNP

We utilized the same PPFPA from chapter 2 as parent polymer, since every pendent functional group designed in this project still can be installed conveniently by the substitution reaction. By addition of isopropylamine, it is easily to construct PNIPAM structure on the polymer. Because there is only one amine on the new ligand, a cross-linker become necessary for polymer folding. 1,6-diaminohexane was selected to be cross-linker to make the core of SCNP more hydrophobic. In the functionalization experiment, deprotected amine-end ligand, cross-linker, and isopropylamine were added into dilute PPFPA solution followed the order. The process of the experiment was monitored by ^{19}F NMR. After purified by dialysis, the two SCNPs with different ratio of pendent groups were characterized by SEC. Compared to 100% PNIPAM substituted from

PP1 (P4), the clear right shift of trace was not observed from SEC output data neither in multiangle light scattering detector nor in reflective index detector. And the trace was not as smooth as standard trace. We proposed two explanations. Firstly, because PNIPAM is a typical polar polymer that can form hydrogen bonding with DMF, the interaction between PNIPAM and the mobile phase DMF might affect the retention time. Secondly, there might be some impurities of small molecules in the simple. In other words, the dialysis process might not purify the polymer completely.

Table 3 Ratio of pendent groups determined by ^{19}F NMR

SCNPs	Ligand	Crosslinker	NIPAM
NP2	21	51	28
NP3	12	17	71

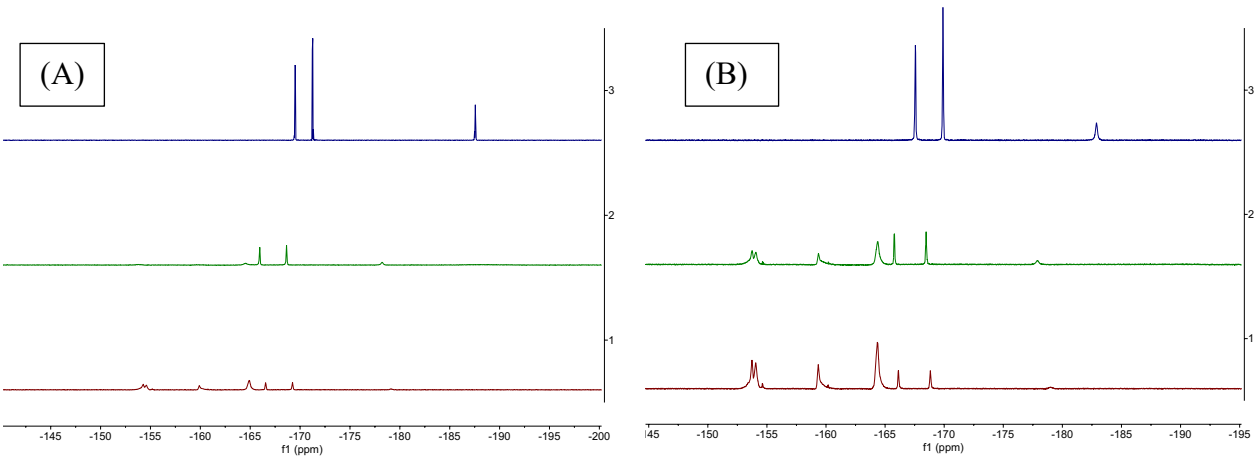

Figure 11 Functionalization of PPFPA to form (A) NP2 and (B) NP3 monitored by ^{19}F NMR

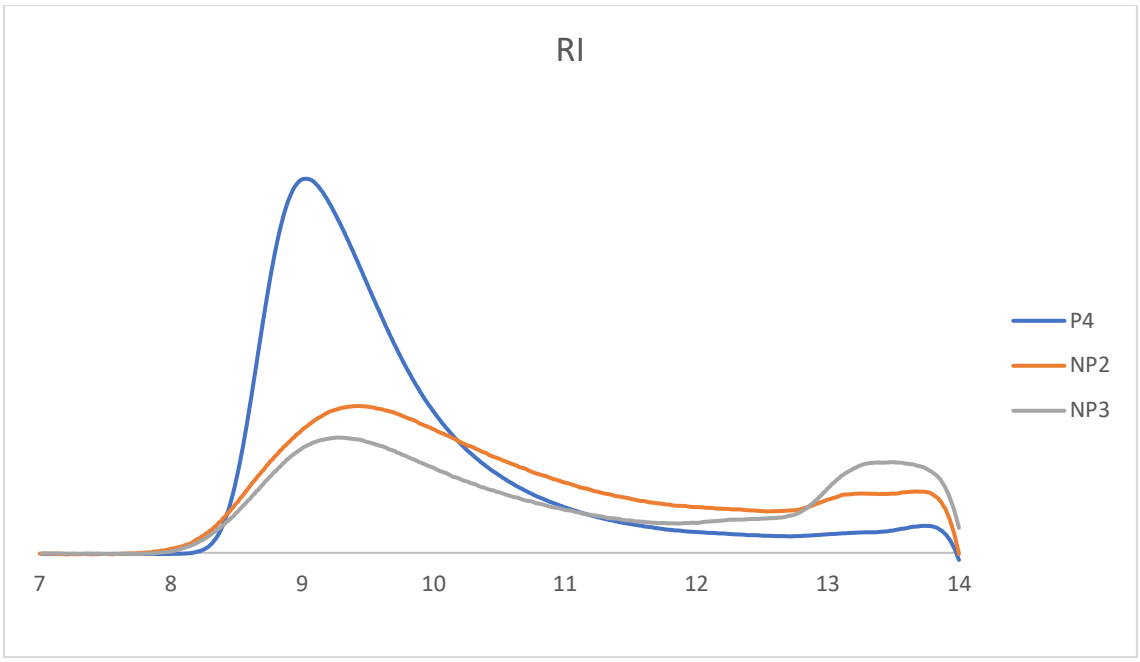

Figure 12 Comparison of SEC trace of P4, NP2, and NP3 from RI detector

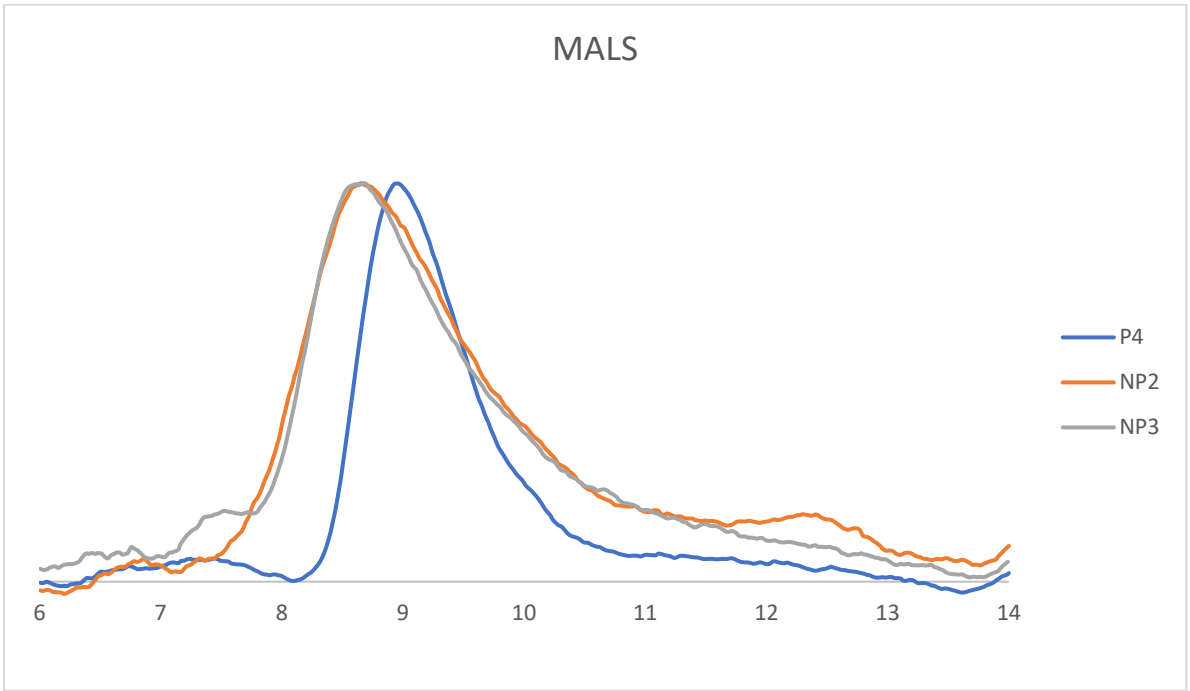

Figure 13 Comparison of SEC trace of P4, NP2, and NP3 from MALS detector

To test the thermo sensitivity of PNIPAM, P4 was characterized by dynamic light scattering (DLS). The particle size increased dramatically from 10nm to 1000nm when the temperature was higher than 30°C in the heating process. And the process was proved to be reversible after cooling process.

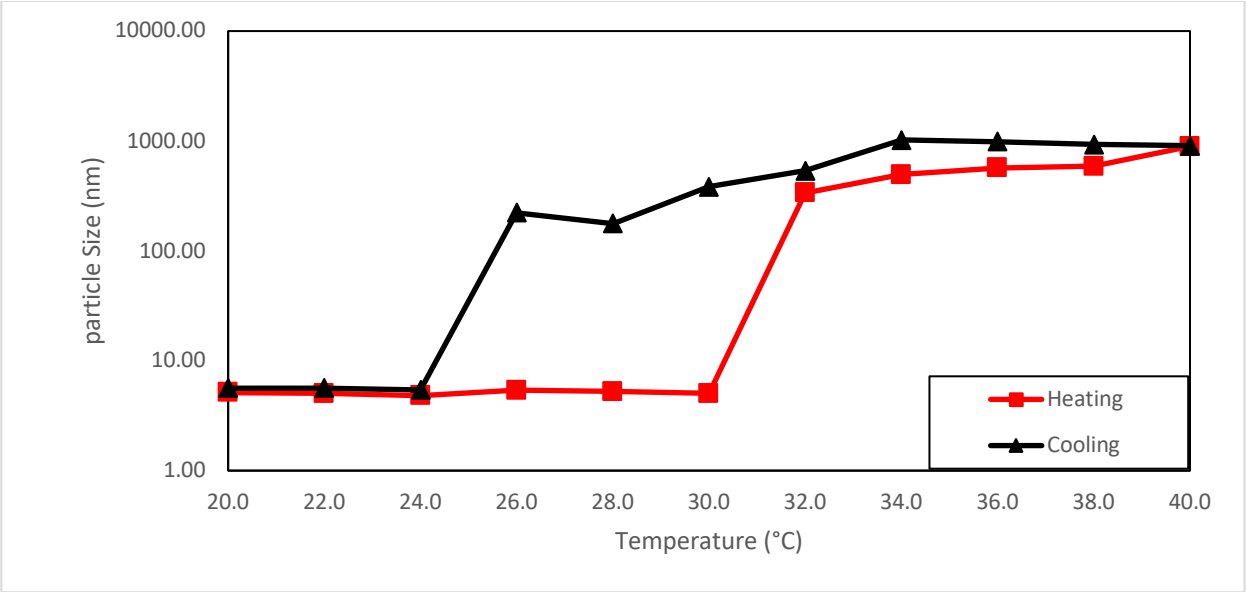

Figure 14 DLS result of P4

3.2.3 Metal coordination

The coordination reaction was tried to produce SCNP-Ru complex (Scheme 29). The ligand functionalized SCNP was treated t-BuOK in anhydrous THF to form active NHC ligand by deprotonation of dihydroimidazolium salt. Then the solution of Grubbs' 1st catalyst was added. However, the expected peaks in ^{1}H NMR and ^{31}P NMR that were clear in small molecular

coordination experiment didn't appear. KHMDS was also tried as the base of reaction. No expected product was observed.

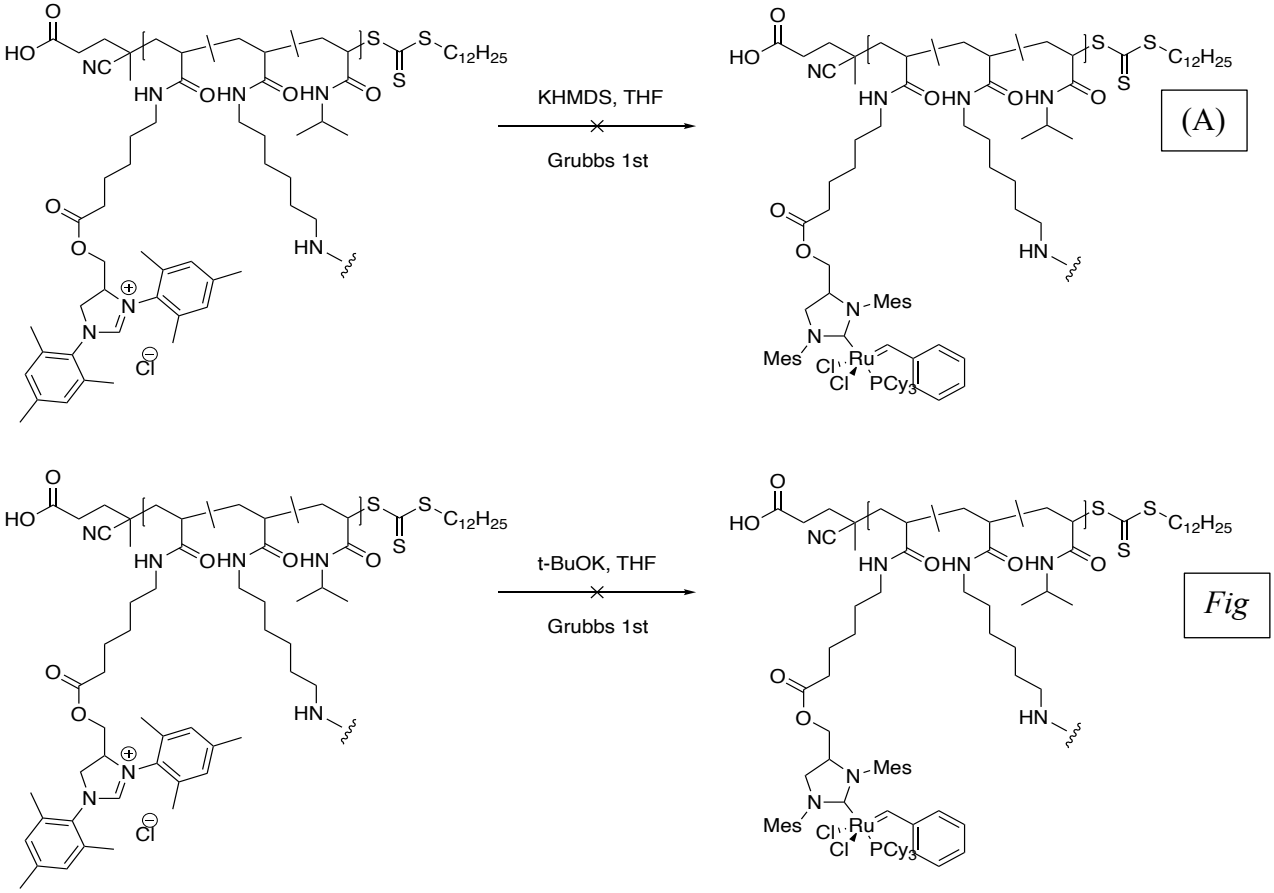

Scheme 19 Ruthenium coordination of NP3 with (A) KHMDS and (B) t-BuOK

Then, we tried to achieve the goal of coordination by employing transmetalation strategy, which is another common methodology for organometallic synthesis. Silver has been applied in NHC transitional metal complex synthesis by transmetalation widely in the last decades. Following published procedure, silver oxide, which can work as not only silver(I) source but also base, was selected react with the SCNP (Scheme 30). Unfortunately, the coordination of silver still didn't work for macromolecular scenario.

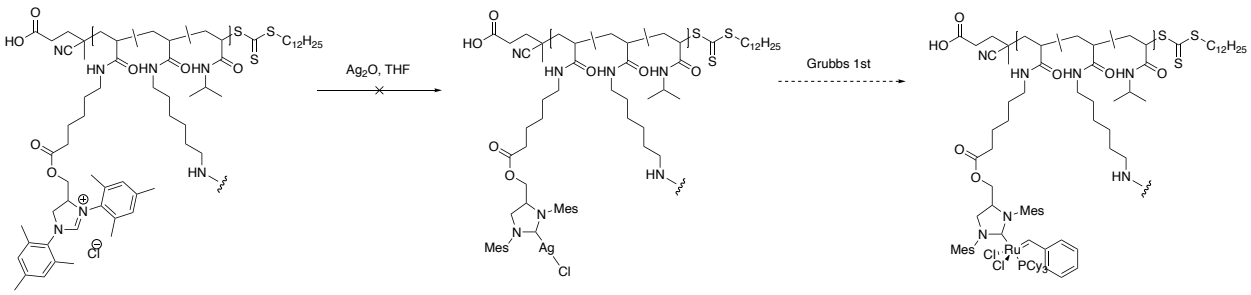

Scheme 20 Transmetalation strategy for ruthenium SCNP coordination

3.3 Conclusion

We utilized PPFPA functionalization strategy to synthesize thermosensitive PNIAM based ligand containing SCNP. In the redesigning of ligand, we tried to keep most structures of NHC ligand in Grubbs' 2nd catalyst so that the coordination reaction can be run at similar condition. The only difference was addition of amine end to install on polymer. The coordination process was proved to work in small molecular scenario from ^{1}H NMR and ^{31}P NMR results. Then we synthesize the SCNP by adding deprotected ligand, cross-linker, and isopropylamine. The reversible thermosensitivity of PNIPAM was tested by DLS. The goal of production of SCNP-Ru complex was not achieved by neither ligand substitution nor transmetalation.

3.4 Experimental

3.4.1 Materials

Reagents were obtained from the indicated commercial suppliers and used without further purification unless otherwise stated: 2,4,6-trimethylaniline (Sigma-Aldrich), 6-aminocaproic acid (Sigma-Aldrich), di-tert-butyl pyrocarbonate (boc anhydride, Chem-Inpex), triethyl orthoformate (Acros), isopropylamine (Alfa Aeser), 1,6-diaminohexane (Acros), N,N'-dicyclohexylcarbodiimide (Sigma-Aldrich), 4-dimethylamino pyridine (Oakwood Products, Inc), Grubbs catalyst 1st generation (Sigma-Aldrich), Grubbs catalyst 2nd generation (Sigma-Aldrich), hexanes (Fisher Scientific), ethyl acetate (Fisher Scientific), 2,2'-azobis(2-methylpropionitrile) (AIBN, Sigma-Scientific, recrystallized from methanol), silica gel (230 – 400 mesh, SiliCycle), N,N'-dimethylformamide (HPLC grade, Fisher Scientific), dimethyl sulfoxide-d6 (Cambridge Isotope Laboratories), chloroform-d (CDCl3, Cambridge Isotope Laboratories). Dry dichloromethane (DCM) was obtained from refluxing with calcium hydride. Dry toluene and tetrahydrofuran (THF) were obtained from refluxing with sodium.

3.4.2 Instrumentation

^{1}H, ^{13}C, ^{19}F and ^{31}P NMR spectra were acquired with a Varian Unity INOVA 500 MHz or Varian Mercury 400 MHz spectrometer. Chemical shifts (δ) were reported in parts per million (ppm) relative to tetramethylsilane (TMS). Solvent (CDCl3) contained 0.03% v/v TMS as an internal

reference. Peak abbreviations are used as follows: s = singlet, d = doublet, t = triplet, q = quartet, m = multiplet, br = broad).

SEC was performed on a Tosoh EcoSEC dual detection (RI and UV) SEC system coupled to an external Wyatt Technologies miniDAWN Treos multiangle light scattering (MALS). Samples were run in DMF at 50 °C at a flow rate of 0.45 mL/min. The column set contained one Tosoh SuperH-L column, one Tosoh SuperH2500 column and a Tosoh SuperH4000 column. All polymer solutions characterized by SEC were 1.0 mg/mL in DMF, stirred magnetically for at least 10 hours and filtered through 0.45 μm PTFE syringe filters before analysis.

3.4.3 Experimental procedures

3.4.3.1 Synthesis of L3.1[112]

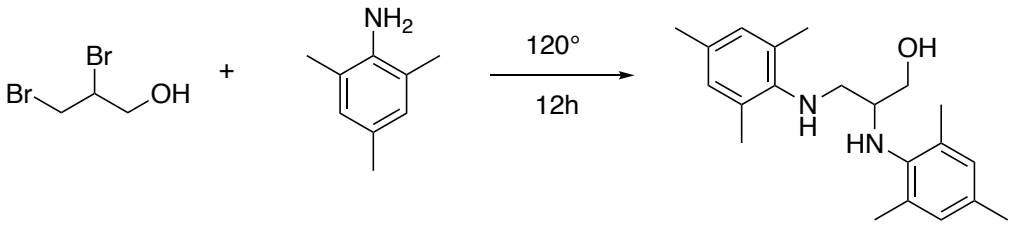

2,3-dibromopropanol (2.05mL, 4.35g, 20mmol, 1 eq) was mixed with 2,4,6-trimethylaniline (8.42mL, 8.11g, 60mmol, 3 eq), and the reaction was stirred for 12hours at 120°C. The solidified product was dissolved in bilayer of 300mL DCM and 300mL 15% NaOH aqueous solution. The organic layer was dried with sodium sulfate and evaporate by rotary evaporator. The crude product was purified by column chromatography to afford a beige solid (5.69g, 87.2%). ^{1}H NMR (500 MHz, $CDCl_3$, δ, ppm): 6.82 (s, 2H), 6.80 (s, 2H), 3.94 (dd, 1H), 3.84 (dd, 1H), 3.38 (m, 1H), 3.22 (dd, 1H), 2.97 (dd, 1H), 2.28 (s, 6H), 2.22 (d, 6H), 2.16 (s, 6H); ^{13}C NMR (500 MHz, $CDCl_3$, δ,

ppm): 142.55, 141.85, 132.55, 130.95, 130.63, 129.85, 129.60, 128.82, 66.09, 60.44, 56.95, 52.33, 21.08, 20.50, 18.95, 17.82, 14.23.

3.4.3.2 Synthesis of L3.2

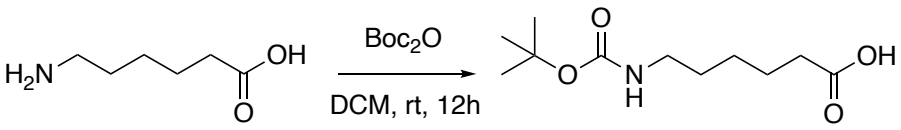

Boc anhydride (2.62g, 12mmol, 1.2eq) was added in a dry DCM solution of aminocaproic acid (1.35g, 10mmol, 1eq) under ice bath. The mixture was allowed to stir for 12 hours and then was concentrated under reduced pressure. The crude product was dried under vacuum without purification to afford colorless solid (2.22g, 96%). ^{1}H NMR (500 MHz, $CDCl_3$, δ, ppm): 4.55 (s, 1H), 3.11 (m, 2H), 2.35 (t, 2H), 1.65 (m, 2H), 1.50 (m, 2H), 1.44 (s, 9H), 1.38 (m, 2H); ^{13}C NMR (500 MHz, $CDCl_3$, δ, ppm): 207.13, 178.42, 33.78, 30.94, 29.73, 28.43, 27.43, 26.22, 24.34.

3.4.3.3 Synthesis of L3.3

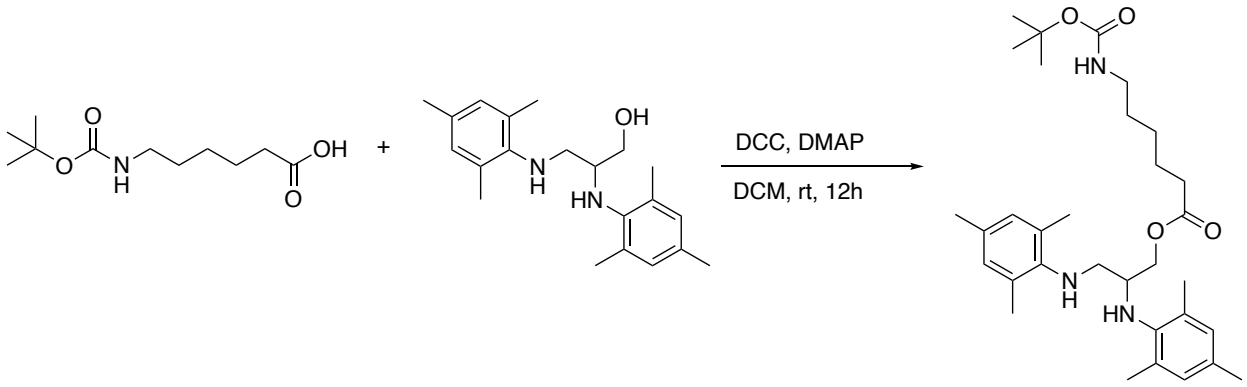

In a round bottom flask, L3.1 (3.97g, 12mmol, 1.2 eq), L3.2 (2.31g, 10mmol, 1 eq), and DMAP (0.12g, 1mmol, 0.1eq) were dissolved in DCM. Then N,N'-dicyclohexylcarbodiimide (3.09g, 15mmol, 1.5 eq) was added into the mixture. The mixture turned turbid immediately and was

allowed to stir 12hours. After removing solvent by rotary evaporator, the crude product was purified by column chromatography to afford colorless solid (4.48g, 83%). ^{1}H NMR (500 MHz, $CDCl_3$, δ, ppm): 6.80 (s, 4H), 4.51 (m, 1H), 4.26 (dd, 1H), 4.13 (q, 1H), 4.04 (dd, 1H), 3.63 (m, 1H), 3.53(s, 1H), 3.18 (m, 2H), 2.22 (m, 18H), 1.73 (m, 2H), 1.59 (m, 4H), 1.44 (s, 9H), 1.32 (m, 2H).

3.4.3.4 Synthesis of L3.4[113]

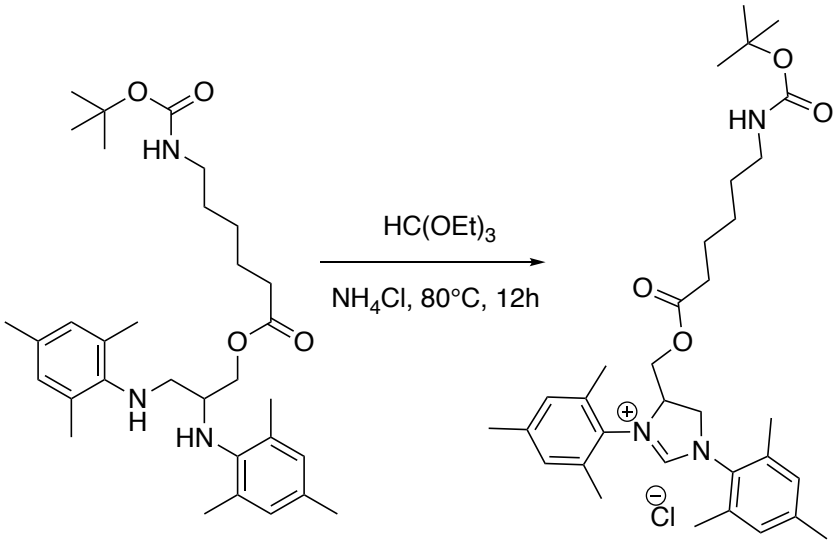

In a 5mL Schlenk flask, L3.3 (0.27g, 0.5mmol, 1 eq) and ammonium chloride (0.03g, 0.55mmol, 1.1eq) were added into triethyl orthoformate (0.22g, 1.5mmol, 3 eq) under argon. The mixture was heated at 110°C for 12hours before cooled down. After removing solvent by rotary evaporator, the crude product was purified by column chromatography to afford brown solid (0.27g, 92%). ^{1}H NMR (500 MHz, $CDCl_3$, δ, ppm): 9.53 (s, 1H), 6.97 (s, 4H), 5.48 (m, 1H), 4.97 (t, 1H), 4.58 (s, 1H), 4.42 (dd, 1H), 4.24 (m, 1H), 4.17 (dd, 1H), 3.10 (m, 2H), 2.45 (m, 9H), 2.30 (m, 9H), 1.61 (m, 2H), 1.45 (m, 13H), 1.32 (m, 2H).

3.4.3.5 Synthesis of C1[96]

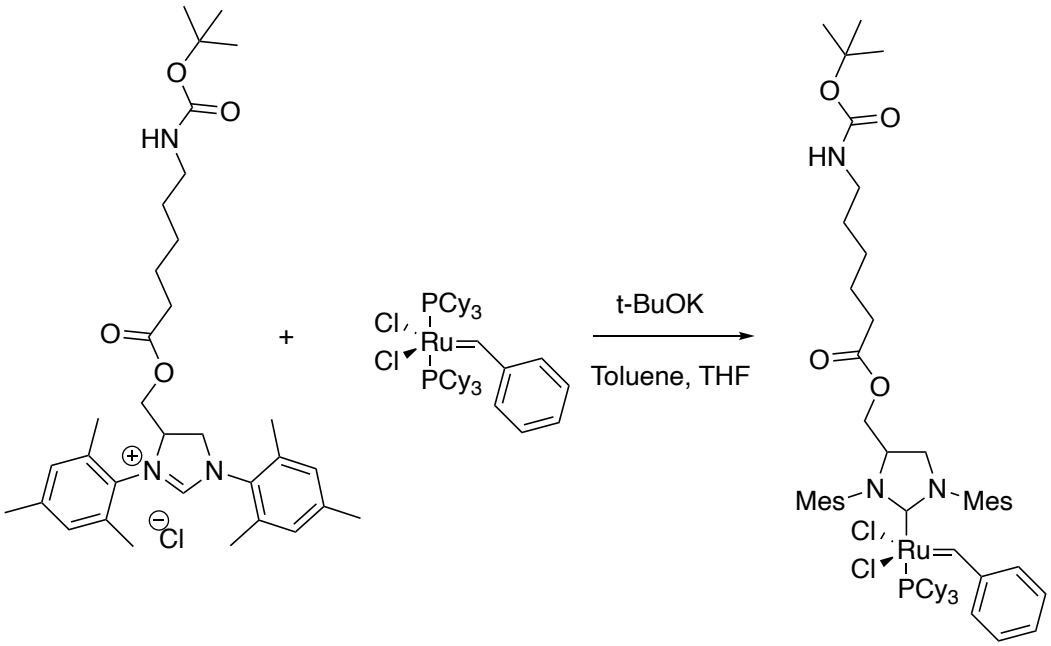

In a 5mL Schlenk flask, t-BuOK (16.8mg, 0.15mmol, 1.5 eq) was added into a dry toluene solution of L3.4. The mixture was allowed to stir at ambient temperature for 2hours. Then a dry THF solution of Grubbs' 1st generation catalyst (82.3 mg, 0.1mmol, 1 eq) was added into the mixture and heated at 80°C for 8hours. The result mixture was characterized by NMR without purification.

3.4.3.6 Synthesis of NP2 and NP3

To a dry THF solution of L3.4, TFA was added and allowed to stir 30minutes. Then NIPEA was added. The mixture was added dropwise into 100mL dry THF solution of 100mg PP1 and stirred for 2hours. Then 1,6-diaminohexane was added and stirred for 2hours. Finally, excess isopropylamine was added and stirred for 8hours. The reaction was monitored by ^{19}F NMR and shut off when the target degree of substitution was reached. The mixture was concentrated to 10mL and then dialyzed against THF:H_2O 1:1, against ethanol:H_2O 1:1, and against H_2O. The solvent of the final mixture was removed by lyophilizer.

3.4.3.7 Synthesis of P4

To a 100 mL dry THF solution of 100 mg PP1, 200mg isopropylamine was added and allowed to stir 8hours. The reaction was monitored by ^{19}F NMR and shut off when the target degree of substitution was reached. The mixture was concentrated to 10mL and then dialyzed against THF:H_2O 1:1, against ethanol:H_2O 1:1, and against H_2O. The solvent of the final mixture was removed by lyophilizer.

REFERENCE

1. Lyon, C. K.; Prasher, A.; Hanlon, A. M.; Tuten, B. T.; Tooley, C. A.; Frank, P. G.; Berda, E. B., A brief user's guide to single-chain nanoparticles. *Polymer Chemistry* **2015,** *6* (2), 181-197.

2. Hanlon, A. M.; Lyon, C. K.; Berda, E. B., What Is Next in Single-Chain Nanoparticles? *Macromolecules* **2016,** *49* (1), 2-14.

3. Mavila, S.; Eivgi, O.; Berkovich, I.; Lemcoff, N. G., Intramolecular Cross-Linking Methodologies for the Synthesis of Polymer Nanoparticles. *Chemical Reviews* **2016,** *116* (3), 878-961.

4. Chen, R.; Berda, E. B., 100th Anniversary of Macromolecular Science Viewpoint: Re-examining Single-Chain Nanoparticles. *ACS Macro Letters* **2020,** *9* (12), 1836-1843.

5. Williams, R. J.; Pitto-Barry, A.; Kirby, N.; Dove, A. P.; O'Reilly, R. K., Cyclic Graft Copolymer Unimolecular Micelles: Effects of Cyclization on Particle Morphology and Thermoresponsive Behavior. *Macromolecules* **2016,** *49* (7), 2802-2813.

6. Altintas, O.; Artar, M.; ter Huurne, G.; Voets, I. K.; Palmans, A. R. A.; Barner-Kowollik, C.; Meijer, E. W., Design and Synthesis of Triblock Copolymers for Creating Complex Secondary Structures by Orthogonal Self-Assembly. *Macromolecules* **2015,** *48* (24), 8921-8932.

7. Artar, M.; Souren, E. R. J.; Terashima, T.; Meijer, E. W.; Palmans, A. R. A., Single Chain Polymeric Nanoparticles as Selective Hydrophobic Reaction Spaces in Water. *ACS Macro Letters* **2015,** *4* (10), 1099-1103.

8. Hosono, N.; Kushner, A. M.; Chung, J.; Palmans, A. R. A.; Guan, Z.; Meijer, E. W., Forced Unfolding of Single-Chain Polymeric Nanoparticles. *Journal of the American Chemical Society* **2015,** *137* (21), 6880-6888.

9. Liu, Y.; Pauloehrl, T.; Presolski, S. I.; Albertazzi, L.; Palmans, A. R. A.; Meijer, E. W., Modular Synthetic Platform for the Construction of Functional Single-Chain Polymeric Nanoparticles: From Aqueous Catalysis to Photosensitization. *Journal of the American Chemical Society* **2015,** *137* (40), 13096-13105.

10. ter Huurne, G. M.; Gillissen, M. A. J.; Palmans, A. R. A.; Voets, I. K.; Meijer, E. W., The Coil-to-Globule Transition of Single-Chain Polymeric Nanoparticles with a Chiral Internal Secondary Structure. *Macromolecules* **2015,** *48* (12), 3949-3956.

11. Liu, Y.; Pujals, S.; Stals, P. J. M.; Paulöhrl, T.; Presolski, S. I.; Meijer, E. W.; Albertazzi, L.; Palmans, A. R. A., Catalytically Active Single-Chain Polymeric Nanoparticles: Exploring Their Functions in Complex Biological Media. *Journal of the American Chemical Society* **2018,** *140* (9), 3423-3433.

12. Hirai, Y.; Terashima, T.; Takenaka, M.; Sawamoto, M., Precision Self-Assembly of Amphiphilic Random Copolymers into Uniform and Self-Sorting Nanocompartments in Water. *Macromolecules* **2016,** *49* (14), 5084-5091.

13. Koda, Y.; Terashima, T.; Sawamoto, M., Multimode Self-Folding Polymers via Reversible and Thermoresponsive Self-Assembly of Amphiphilic/Fluorous Random Copolymers. *Macromolecules* **2016,** *49* (12), 4534-4543.

14. Matsumoto, K.; Terashima, T.; Sugita, T.; Takenaka, M.; Sawamoto, M., Amphiphilic Random Copolymers with Hydrophobic/Hydrogen-Bonding Urea Pendants: Self-Folding Polymers in Aqueous and Organic Media. *Macromolecules* **2016,** *49* (20), 7917-7927.

15. Willenbacher, J.; Altintas, O.; Trouillet, V.; Knöfel, N.; Monteiro, M. J.; Roesky, P. W.; Barner-Kowollik, C., Pd-complex driven formation of single-chain nanoparticles. *Polymer Chemistry* **2015,** *6* (24), 4358-4365.

16. Bai, Y.; Feng, X.; Xing, H.; Xu, Y.; Kim, B. K.; Baig, N.; Zhou, T.; Gewirth, A. A.; Lu, Y.; Oldfield, E.; Zimmerman, S. C., A Highly Efficient Single-Chain Metal–Organic Nanoparticle Catalyst for Alkyne–Azide "Click" Reactions in Water and in Cells. *Journal of the American Chemical Society* **2016,** *138* (35), 11077-11080.

17. Berkovich, I.; Mavila, S.; Iliashevsky, O.; Kozuch, S.; Lemcoff, N. G., Single-chain polybutadiene organometallic nanoparticles: an experimental and theoretical study. *Chemical Science* **2016,** *7* (3), 1773-1778.

18. Knöfel, N. D.; Rothfuss, H.; Willenbacher, J.; Barner-Kowollik, C.; Roesky, P. W., Platinum(II)-Crosslinked Single-Chain Nanoparticles: An Approach towards Recyclable Homogeneous Catalysts. *Angewandte Chemie International Edition* **2017,** *56* (18), 4950-4954.

19. Lambert, R.; Wirotius, A.-L.; Garmendia, S.; Berto, P.; Vignolle, J.; Taton, D., Pd(ii)–NHC coordination-driven formation of water-soluble catalytically active single chain nanoparticles. *Polymer Chemistry* **2018,** *9* (23), 3199-3204.

20. Knöfel, N. D.; Rothfuss, H.; Tzvetkova, P.; Kulendran, B.; Barner-Kowollik, C.; Roesky, P. W., Heterobimetallic Eu(iii)/Pt(ii) single-chain nanoparticles: a path to enlighten catalytic reactions. *Chemical Science* **2020,** *11* (38), 10331-10336.

21. Wen, W.; Chen, A., Influence of single chain nanoparticle stabilizers on polymerization induced hierarchical self-assembly. *Polymer Chemistry* **2021,** *12* (18), 2743-2751.

22. Cole, J. P.; Lessard, J. J.; Rodriguez, K. J.; Hanlon, A. M.; Reville, E. K.; Mancinelli, J. P.; Berda, E. B., Single-chain nanoparticles containing sequence-defined segments: using primary structure control to promote secondary and tertiary structures in synthetic protein mimics. *Polymer Chemistry* **2017,** *8* (38), 5829-5835.

23. Liu, C. H.; Dugas, L. D.; Bowman, J. I.; Chidanguro, T.; Storey, R. F.; Simon, Y. C., Forcing single-chain nanoparticle collapse through hydrophobic solvent interactions in comb copolymers. *Polymer Chemistry* **2020,** *11* (2), 292-297.

24. Perrier, S., 50th Anniversary Perspective: RAFT Polymerization—A User Guide. *Macromolecules* **2017,** *50* (19), 7433-7447.

25. Blasco, E.; Sims, M. B.; Goldmann, A. S.; Sumerlin, B. S.; Barner-Kowollik, C., 50th Anniversary Perspective: Polymer Functionalization. *Macromolecules* **2017,** *50* (14), 5215-5252.

26. Chen, J.; Li, K.; Shon, J. S. L.; Zimmerman, S. C., Single-Chain Nanoparticle Delivers a Partner Enzyme for Concurrent and Tandem Catalysis in Cells. *Journal of the American Chemical Society* **2020,** *142* (10), 4565-4569.

27. Chen, R.; Benware, S. J.; Cawthern, S. D.; Cole, J. P.; Lessard, J. J.; Crawford-Eng, I. M.; Saxena, R.; Berda, E. B., Assessing structure/property relationships and synthetic protocols in the fabrication of poly(oxanorbornene imide) single-chain nanoparticles. *European Polymer Journal* **2019,** *112*, 206-213.

28. Tuten, B. T.; Chao, D.; Lyon, C. K.; Berda, E. B., Single-chain polymer nanoparticles via reversible disulfide bridges. *Polymer Chemistry* **2012,** *3* (11), 3068-3071.

29. Harth, E.; Horn, B. V.; Lee, V. Y.; Germack, D. S.; Gonzales, C. P.; Miller, R. D.; Hawker, C. J., A Facile Approach to Architecturally Defined Nanoparticles via Intramolecular Chain Collapse. *Journal of the American Chemical Society* **2002,** *124* (29), 8653-8660.

30. González-Burgos, M.; Asenjo-Sanz, I.; Pomposo, J. A.; Radulescu, A.; Ivanova, O.; Pasini, S.; Arbe, A.; Colmenero, J., Structure and Dynamics of Irreversible Single-Chain Nanoparticles in Dilute Solution. A Neutron Scattering Investigation. *Macromolecules* **2020,** *53* (18), 8068-8082.

31. Kröger, A. P. P.; Boonen, R. J. E. A.; Paulusse, J. M. J., Well-defined single-chain polymer nanoparticles via thiol-Michael addition. *Polymer* **2017,** *120*, 119-128.

32. Kröger, A. P. P.; Komil, M. I.; Hamelmann, N. M.; Juan, A.; Stenzel, M. H.; Paulusse, J. M. J., Glucose Single-Chain Polymer Nanoparticles for Cellular Targeting. *ACS Macro Letters* **2019,** *8* (1), 95-101.

33. Kröger, A. P. P.; Paats, J.-W. D.; Boonen, R. J. E. A.; Hamelmann, N. M.; Paulusse, J. M. J., Pentafluorophenyl-based single-chain polymer nanoparticles as a versatile platform towards protein mimicry. *Polymer Chemistry* **2020,** *11* (37), 6056-6065.

34. Zhang, J.; Gody, G.; Hartlieb, M.; Catrouillet, S.; Moffat, J.; Perrier, S., Synthesis of Sequence-Controlled Multiblock Single Chain Nanoparticles by a Stepwise Folding–Chain Extension–Folding Process. *Macromolecules* **2016,** *49* (23), 8933-8942.

35. Wang, F.; Diesendruck, C. E., Advantages and limitations of diisocyanates in intramolecular collapse. *Polymer Chemistry* **2017,** *8* (24), 3712-3720.

36. Hanlon, A. M.; Martin, I.; Bright, E. R.; Chouinard, J.; Rodriguez, K. J.; Patenotte, G. E.; Berda, E. B., Exploring structural effects in single-chain "folding" mediated by intramolecular thermal Diels–Alder chemistry. *Polymer Chemistry* **2017,** *8* (34), 5120-5128.

37. Wedler-Jasinski, N.; Lueckerath, T.; Mutlu, H.; Goldmann, A. S.; Walther, A.; Stenzel, M. H.; Barner-Kowollik, C., Dynamic covalent single chain nanoparticles based on hetero Diels–Alder chemistry. *Chemical Communications* **2017,** *53* (1), 157-160.

38. Mahon, C. S.; McGurk, C. J.; Watson, S. M. D.; Fascione, M. A.; Sakonsinsiri, C.; Turnbull, W. B.; Fulton, D. A., Molecular Recognition-Mediated Transformation of Single-Chain Polymer Nanoparticles into Crosslinked Polymer Films. *Angewandte Chemie International Edition* **2017,** *56* (42), 12913-12918.

39. Zhang, J.; Tanaka, J.; Gurnani, P.; Wilson, P.; Hartlieb, M.; Perrier, S., Self-assembly and disassembly of stimuli responsive tadpole-like single chain nanoparticles using a switchable hydrophilic/hydrophobic boronic acid cross-linker. *Polymer Chemistry* **2017,** *8* (28), 4079-4087.

40. De-La-Cuesta, J.; Verde-Sesto, E.; Arbe, A.; Pomposo, J. A., Self-Reporting of Folding and Aggregation by Orthogonal Hantzsch Luminophores Within a Single Polymer Chain. *Angewandte Chemie International Edition* **2021,** *60* (7), 3534-3539.

41. Biryan, F.; Tuncer, H.; Demirelli, K., Electrical, thermal behaviors and synthesis of intramolecular cobalt phthalocyanine with single-chain polymer structure. *Polymer Bulletin* **2020,** *77* (5), 2461-2484.

42. Hanlon, A. M.; Chen, R.; Rodriguez, K. J.; Willis, C.; Dickinson, J. G.; Cashman, M.; Berda, E. B., Scalable Synthesis of Single-Chain Nanoparticles under Mild Conditions. *Macromolecules* **2017,** *50* (7), 2996-3003.

43. González-Burgos, M.; González, E.; Pomposo, J. A., Excellent Stability in Water of Single-Chain Nanoparticles against Chain Scission by Sonication. *Macromolecular Rapid Communications* **2018,** *39* (6), 1700675.

44. Cole, J. P.; Lessard, J. J.; Lyon, C. K.; Tuten, B. T.; Berda, E. B., Intra-chain radical chemistry as a route to poly(norbornene imide) single-chain nanoparticles: structural considerations and the role of adventitious oxygen. *Polymer Chemistry* **2015,** *6* (31), 5555-5559.

45. Lyon, C. K.; Hill, E. O.; Berda, E. B., Zipping Polymers into Nanoparticles via Intrachain Alternating Radical Copolymerization. *Macromolecular Chemistry and Physics* **2016,** *217* (3), 501-508.

46. Prasher, A.; Loynd, C. M.; Tuten, B. T.; Frank, P. G.; Chao, D.; Berda, E. B., Efficient fabrication of polymer nanoparticles via sonogashira cross-linking of linear polymers in dilute solution. *Journal of Polymer Science Part A: Polymer Chemistry* **2016,** *54* (1), 209-217.

47. Watanabe, K.; Tanaka, R.; Takada, K.; Kim, M.-J.; Lee, J.-S.; Tajima, K.; Isono, T.; Satoh, T., Intramolecular olefin metathesis as a robust tool to synthesize single-chain nanoparticles in a size-controlled manner. *Polymer Chemistry* **2016,** *7* (29), 4782-4792.

48. Maiz, J.; Verde-Sesto, E.; Asenjo-Sanz, I.; Fouquet, P.; Porcar, L.; Pomposo, J. A.; de Molina, P. M.; Arbe, A.; Colmenero, J., Collective Motions and Mechanical Response of a Bulk of Single-Chain Nano-Particles Synthesized by Click-Chemistry. *Polymers* **2021,** *13* (1), 50.

49. Lambert, R.; Wirotius, A.-L.; Taton, D., Intramolecular Quaternization as Folding Strategy for the Synthesis of Catalytically Active Imidazolium-Based Single Chain Nanoparticles. *ACS Macro Letters* **2017,** *6* (5), 489-494.

50. Engelke, J.; Tuten, B. T.; Schweins, R.; Komber, H.; Barner, L.; Plüschke, L.; Barner-Kowollik, C.; Lederer, A., An in-depth analysis approach enabling precision single chain nanoparticle design. *Polymer Chemistry* **2020,** *11* (41), 6559-6578.

51. Jackson, A. W.; Chennamaneni, L. R.; Mothe, S. R.; Thoniyot, P., A general strategy for degradable single-chain nanoparticles via cross-linker mediated chain collapse of radical copolymers. *Chemical Communications* **2020,** *56* (68), 9838-9841.

52. Fan, W.; Tong, X.; Li, G.; Zhao, Y., Photoresponsive liquid crystalline polymer single-chain nanoparticles. *Polymer Chemistry* **2017,** *8* (22), 3523-3529.

53. Fan, W.; Tong, X.; Farnia, F.; Yu, B.; Zhao, Y., CO2-Responsive Polymer Single-Chain Nanoparticles and Self-Assembly for Gas-Tunable Nanoreactors. *Chemistry of Materials* **2017,** *29* (13), 5693-5701.

54. Scheutz, G. M.; Elgoyhen, J.; Bentz, K. C.; Xia, Y.; Sun, H.; Zhao, J.; Savin, D. A.; Sumerlin, B. S., Mediating covalent crosslinking of single-chain nanoparticles through solvophobicity in organic solvents. *Polymer Chemistry* **2021**.

55. Frisch, H.; Menzel, J. P.; Bloesser, F. R.; Marschner, D. E.; Mundsinger, K.; Barner-Kowollik, C., Photochemistry in Confined Environments for Single-Chain Nanoparticle Design. *Journal of the American Chemical Society* **2018,** *140* (30), 9551-9557.

56. Piane, J. J.; Chamberlain, L. E.; Huss, S.; Alameda, L. T.; Hoover, A. C.; Elacqua, E., Organic Photoredox-Catalyzed Cycloadditions Under Single-Chain Polymer Confinement. *ACS Catalysis* **2020,** *10* (22), 13251-13256.

57. Frank, P. G.; Tuten, B. T.; Prasher, A.; Chao, D.; Berda, E. B., Intra-Chain Photodimerization of Pendant Anthracene Units as an Efficient Route to Single-Chain Nanoparticle Fabrication. *Macromolecular Rapid Communications* **2014,** *35* (2), 249-253.

58. Galant, O.; Donmez, H. B.; Barner-Kowollik, C.; Diesendruck, C. E., Flow Photochemistry for Single-Chain Polymer Nanoparticle Synthesis. *Angewandte Chemie International Edition* **2021,** *60* (4), 2042-2046.

59. Rubio-Cervilla, J.; Frisch, H.; Barner-Kowollik, C.; Pomposo, J. A., Synthesis of Single-Ring Nanoparticles Mimicking Natural Cyclotides by a Stepwise Folding-Activation-Collapse Process. *Macromolecular Rapid Communications* **2019,** *40* (1), 1800491.

60. Bloesser, F. R.; Walden, S. L.; Irshadeen, I. M.; Chambers, L. C.; Barner-Kowollik, C., Chemiluminescent self-reported unfolding of single-chain nanoparticles. *Chemical Communications* **2021,** *57* (42), 5203-5206.

61. Heiler, C.; Bastian, S.; Lederhose, P.; Blinco, J. P.; Blasco, E.; Barner-Kowollik, C., Folding polymer chains with visible light. *Chemical Communications* **2018,** *54* (28), 3476-3479.

62. Heiler, C.; Offenloch, J. T.; Blasco, E.; Barner-Kowollik, C., Photochemically Induced Folding of Single Chain Polymer Nanoparticles in Water. *ACS Macro Letters* **2017,** *6* (1), 56-61.

63. Offenloch, J. T.; Willenbacher, J.; Tzvetkova, P.; Heiler, C.; Mutlu, H.; Barner-Kowollik, C., Degradable fluorescent single-chain nanoparticles based on metathesis polymers. *Chemical Communications* **2017,** *53* (4), 775-778.

64. Rubio-Cervilla, J.; Malo de Molina, P.; Robles-Hernández, B.; Arbe, A.; Moreno, A. J.; Alegría, A.; Colmenero, J.; Pomposo, J. A., Facile Access to Completely Deuterated Single-Chain Nanoparticles Enabled by Intramolecular Azide Photodecomposition. *Macromolecular Rapid Communications* **2019,** *40* (9), 1900046.

65. Fischer, T. S.; Spann, S.; An, Q.; Luy, B.; Tsotsalas, M.; Blinco, J. P.; Mutlu, H.; Barner-Kowollik, C., Self-reporting and refoldable profluorescent single-chain nanoparticles. *Chemical Science* **2018,** *9* (20), 4696-4702.

66. Offenloch, J. T.; Blasco, E.; Bastian, S.; Barner-Kowollik, C.; Mutlu, H., Self-reporting visible light-induced polymer chain collapse. *Polymer Chemistry* **2019,** *10* (33), 4513-4518.

67. Dashan, I.; Balta, D. K.; Temel, B. A.; Temel, G., Preparation of single chain nanoparticles via photoinduced radical coupling process. *European Polymer Journal* **2019,** *113*, 183-191.

68. Dashan, I.; Balta, D. K.; Temel, B. A.; Temel, G., Preparation of Single Chain Nanoparticles via Photoinduced Double Collapse Process. *Macromolecular Chemistry and Physics* **2019,** *220* (10), 1900116.

69. Altintas, O.; Gerstel, P.; Dingenouts, N.; Barner-Kowollik, C., Single chain self-assembly: preparation of α,ω-donor–acceptor chains via living radical polymerization and orthogonal conjugation. *Chemical Communications* **2010,** *46* (34), 6291-6293.

70. Mes, T.; van der Weegen, R.; Palmans, A. R. A.; Meijer, E. W., Single-Chain Polymeric Nanoparticles by Stepwise Folding. *Angewandte Chemie International Edition* **2011,** *50* (22), 5085-5089.

71. Cheng, C.-C.; Chang, F.-C.; Yen, H.-C.; Lee, D.-J.; Chiu, C.-W.; Xin, Z., Supramolecular Assembly Mediates the Formation of Single-Chain Polymeric Nanoparticles. *ACS Macro Letters* **2015,** *4* (10), 1184-1188.

72. Fischer, T. S.; Schulze-Sünninghausen, D.; Luy, B.; Altintas, O.; Barner-Kowollik, C., Stepwise Unfolding of Single-Chain Nanoparticles by Chemically Triggered Gates. *Angewandte Chemie International Edition* **2016,** *55* (37), 11276-11280.

73. Nguyen, T.-K.; Lam, S. J.; Ho, K. K. K.; Kumar, N.; Qiao, G. G.; Egan, S.; Boyer, C.; Wong, E. H. H., Rational Design of Single-Chain Polymeric Nanoparticles That Kill Planktonic and Biofilm Bacteria. *ACS Infectious Diseases* **2017,** *3* (3), 237-248.

74. Wang, F.; Pu, H.; Ding, Y.; Lin, R.; Pan, H.; Chang, Z.; Jin, M., Single-chain folding of amphiphilic copolymers in water via intramolecular hydrophobic interaction and unfolding triggered by cyclodextrin. *Polymer* **2018,** *141*, 86-92.

75. Huang, S.-Y.; Cheng, C.-C., Spontaneous Self-Assembly of Single-Chain Amphiphilic Polymeric Nanoparticles in Water. *Nanomaterials* **2020,** *10* (10), 2006.

76. Robles-Hernández, B.; González, E.; Pomposo, J. A.; Colmenero, J.; Alegría, Á., Water dynamics and self-assembly of single-chain nanoparticles in concentrated solutions. *Soft Matter* **2020,** *16* (42), 9738-9745.

77. Shehata, S.; Serpell, C. J.; Biagini, S. C. G., Architecture-controlled release of ibuprofen from polymeric nanoparticles. *Materials Today Communications* **2020,** *25*, 101562.

78. Sanchez-Sanchez, A.; Arbe, A.; Kohlbrecher, J.; Colmenero, J.; Pomposo, J. A., Efficient Synthesis of Single-Chain Globules Mimicking the Morphology and Polymerase Activity of Metalloenzymes. *Macromolecular Rapid Communications* **2015,** *36* (17), 1592-1597.

79. Thanneeru, S.; Duay, S. S.; Jin, L.; Fu, Y.; Angeles-Boza, A. M.; He, J., Single Chain Polymeric Nanoparticles to Promote Selective Hydroxylation Reactions of Phenol Catalyzed by Copper. *ACS Macro Letters* **2017,** *6* (7), 652-656.

80. Chen, J.; Wang, J.; Bai, Y.; Li, K.; Garcia, E. S.; Ferguson, A. L.; Zimmerman, S. C., Enzyme-like Click Catalysis by a Copper-Containing Single-Chain Nanoparticle. *Journal of the American Chemical Society* **2018,** *140* (42), 13695-13702.

81. Zhu, Z.; Xu, N.; Yu, Q.; Guo, L.; Cao, H.; Lu, X.; Cai, Y., Construction and Self-Assembly of Single-Chain Polymer Nanoparticles via Coordination Association and Electrostatic Repulsion in Water. *Macromolecular Rapid Communications* **2015,** *36* (16), 1521-1527.

82. De-La-Cuesta, J.; Asenjo-Sanz, I.; Latorre-Sánchez, A.; González, E.; Martínez-Tong, D. E.; Pomposo, J. A., Enzyme-mimetic synthesis of PEDOT from self-folded iron-containing single-chain nanoparticles. *European Polymer Journal* **2018,** *109*, 447-452.

83. Rothfuss, H.; Knöfel, N. D.; Tzvetkova, P.; Michenfelder, N. C.; Baraban, S.; Unterreiner, A.-N.; Roesky, P. W.; Barner-Kowollik, C., Phenanthroline—A Versatile Ligand for Advanced Functional Polymeric Materials. *Chemistry – A European Journal* **2018,** *24* (66), 17475-17486.

84. Wang, F.; Pu, H.; Jin, M.; Wan, D., Supramolecular Nanoparticles via Single-Chain Folding Driven by Ferrous Ions. *Macromolecular Rapid Communications* **2016,** *37* (4), 330-336.

85. Reith, M. A.; Kardas, S.; Mertens, C.; Fossépré, M.; Surin, M.; Steinkoenig, J.; Du Prez, F. E., Using nickel to fold discrete synthetic macromolecules into single-chain nanoparticles. *Polymer Chemistry* **2021**.

86. Mavila, S.; Rozenberg, I.; Lemcoff, N. G., A general approach to mono- and bimetallic organometallic nanoparticles. *Chemical Science* **2014,** *5* (11), 4196-4203.

87. Rothfuss, H.; Knöfel, N. D.; Roesky, P. W.; Barner-Kowollik, C., Single-Chain Nanoparticles as Catalytic Nanoreactors. *Journal of the American Chemical Society* **2018,** *140* (18), 5875-5881.

88. Wang, F.; Pu, H.; Che, X., Voltage-responsive single-chain polymer nanoparticles via host–guest interaction. *Chemical Communications* **2016,** *52* (17), 3516-3519.

89. Cole, J. P.; Hanlon, A. M.; Rodriguez, K. J.; Berda, E. B., Protein-like structure and activity in synthetic polymers. *Journal of Polymer Science Part A: Polymer Chemistry* **2017,** *55* (2), 191-206.

90. Thanneeru, S.; Li, W.; He, J., Controllable Self-Assembly of Amphiphilic Tadpole-Shaped Polymer Single-Chain Nanoparticles Prepared through Intrachain Photo-cross-linking. *Langmuir* **2019,** *35* (7), 2619-2629.

91. Cui, Z.; Huang, L.; Ding, Y.; Zhu, X.; Lu, X.; Cai, Y., Compartmentalization and Unidirectional Cross-Domain Molecule Shuttling of Organometallic Single-Chain Nanoparticles. *ACS Macro Letters* **2018,** *7* (5), 572-575.

92. Wang, J.; Chen, X.; Lang, F.; Yang, L.; Qiu, D.; Yang, Z., Large scale synthesis of single-chain/colloid Janus nanoparticles with tunable composition. *Chemical Communications* **2020,** *56* (27), 3875-3878.

93. de Frémont, P.; Marion, N.; Nolan, S. P., Carbenes: Synthesis, properties, and organometallic chemistry. *Coordination Chemistry Reviews* **2009,** *253* (7), 862-892.

94. Diez-Gonzalez, S.; Marion, N.; Nolan, S. P., N-heterocyclic carbenes in late transition metal catalysis. *Chemical Reviews* **2009,** *109* (8), 3612-3676.

95. Kantchev, E. A. B.; O'Brien, C. J.; Organ, M. G., Palladium complexes of N-heterocyclic carbenes as catalysts for cross-coupling reactions—A synthetic chemist's perspective. *Angewandte Chemie International Edition* **2007,** *46* (16), 2768-2813.

96. Scholl, M.; Ding, S.; Lee, C. W.; Grubbs, R. H., Synthesis and Activity of a New Generation of Ruthenium-Based Olefin Metathesis Catalysts Coordinated with 1,3-Dimesityl-4,5-dihydroimidazol-2-ylidene Ligands. *Organic Letters* **1999,** *1* (6), 953-956.

97. Marion, N.; Nolan, S. P., Well-defined N-heterocyclic carbenes− palladium (II) precatalysts for cross-coupling reactions. *Accounts of chemical research* **2008,** *41* (11), 1440-1449.

98. Sanford, M. S.; Love, J. A.; Grubbs, R. H., Mechanism and Activity of Ruthenium Olefin Metathesis Catalysts. *Journal of the American Chemical Society* **2001,** *123* (27), 6543-6554.

99. Jacobsen, H.; Correa, A.; Poater, A.; Costabile, C.; Cavallo, L., Understanding the M(NHC) (NHC=N-heterocyclic carbene) bond. *Coordination Chemistry Reviews* **2009,** *253* (5), 687-703.

100. Eberhardt, M.; Mruk, R.; Zentel, R.; Théato, P., Synthesis of pentafluorophenyl (meth) acrylate polymers: New precursor polymers for the synthesis of multifunctional materials. *European Polymer Journal* **2005,** *41* (7), 1569-1575.

101. Valente, C.; Calimsiz, S.; Hoi, K. H.; Mallik, D.; Sayah, M.; Organ, M. G., The development of bulky palladium NHC complexes for the most-challenging cross-coupling reactions. *Angewandte Chemie International Edition* **2012,** *51* (14), 3314-3332.

102. Yamabe, S.; Tsuchida, N.; Yamazaki, S., A FMO-Controlled Reaction Path in the Benzil−Benzilic Acid Rearrangement. *The Journal of Organic Chemistry* **2006,** *71* (5), 1777-1783.

103. Gordon, J. C.; Shukla, P.; Cowley, A. H.; Jones, J. N.; Keogh, D. W.; Scott, B. L., Dialkyl aluminium amides: new reagents for the conversion of C [double bond, length as m-dash] O into C [double bond, length as m-dash] NR functionalities. *Chemical communications* **2002,** (22), 2710-2711.

104. Altenhoff, G.; Goddard, R.; Lehmann, C. W.; Glorius, F., Sterically demanding, bioxazoline-derived N-heterocyclic carbene ligands with restricted flexibility for catalysis. *Journal of the American Chemical Society* **2004,** *126* (46), 15195-15201.

105. Glorius, F.; Altenhoff, G.; Goddard, R.; Lehmann, C., Oxazolines as chiral building blocks for imidazolium salts and N-heterocyclic carbene ligands. *Chemical Communications* **2002,** (22), 2704-2705.

106. Hunter, A. D.; Williams, T. R.; Zarzyczny, B. M.; Bottesch, H. W.; Dolan, S. A.; McDowell, K. A.; Thomas, D. N.; Mahler, C. H., Correlations among 31P NMR Coordination Chemical Shifts, Ru–P Bond Distances, and Enthalpies of Reaction in Cp′Ru(PR3)2Cl Complexes (Cp′ = η5-C5H5, η5-C5Me5; PR3 = PMe3, PPhMe2, PPh2Me, PPh3, PEt3, PnBu3). *Organometallics* **2016,** *35* (16), 2701-2706.

107. Ishiyama, T.; Miyaura, N.; Suzuki, A., Palladium (0)-Catalyzed Reaction of 9-Alkyl-9-Borabicyclo [3.3. 1] Nonane with 1-Bromo-1-Phenylthioethene: 4-(3-Cyclohexenyl)-2-Phenylthio-1-Butene. *Organic Syntheses* **1993,** *71*, 89-96.

108. Burtscher, D.; Grela, K., Aqueous olefin metathesis. *Angewandte Chemie International Edition* **2009,** *48* (3), 442-454.

109. Halperin, A.; Kröger, M.; Winnik, F. M., Poly (N-isopropylacrylamide) phase diagrams: fifty years of research. *Angewandte Chemie International Edition* **2015,** *54* (51), 15342-15367.

110. Doberenz, F.; Zeng, K.; Willems, C.; Zhang, K.; Groth, T., Thermoresponsive polymers and their biomedical application in tissue engineering–a review. *Journal of Materials Chemistry B* **2020,** *8* (4), 607-628.

111. Lutz, J.-F.; Akdemir, Ö.; Hoth, A., Point by Point Comparison of Two Thermosensitive Polymers Exhibiting a Similar LCST: Is the Age of Poly(NIPAM) Over? *Journal of the American Chemical Society* **2006,** *128* (40), 13046-13047.

112. Gallagher, N. M.; Zhukhovitskiy, A. V.; Nguyen, H. V. T.; Johnson, J. A., Main-Chain Zwitterionic Supramolecular Polymers Derived from N-Heterocyclic Carbene–Carbodiimide (NHC–CDI) Adducts. *Macromolecules* **2018,** *51* (8), 3006-3016.

113. Hong, S. H.; Grubbs, R. H., Highly active water-soluble olefin metathesis catalyst. *Journal of the American Chemical Society* **2006,** *128* (11), 3508-3509.

APPENDIX

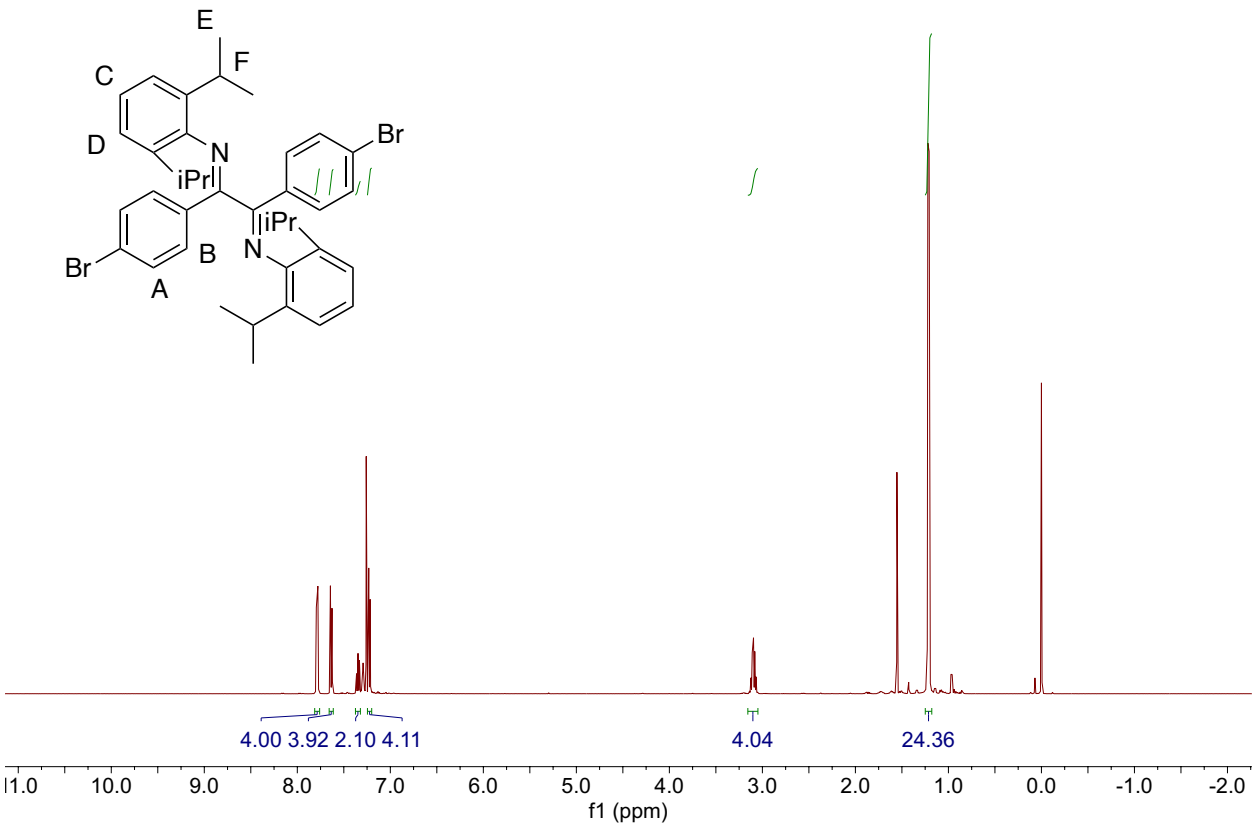

Figure A1 ^{1}H NMR of L2.4

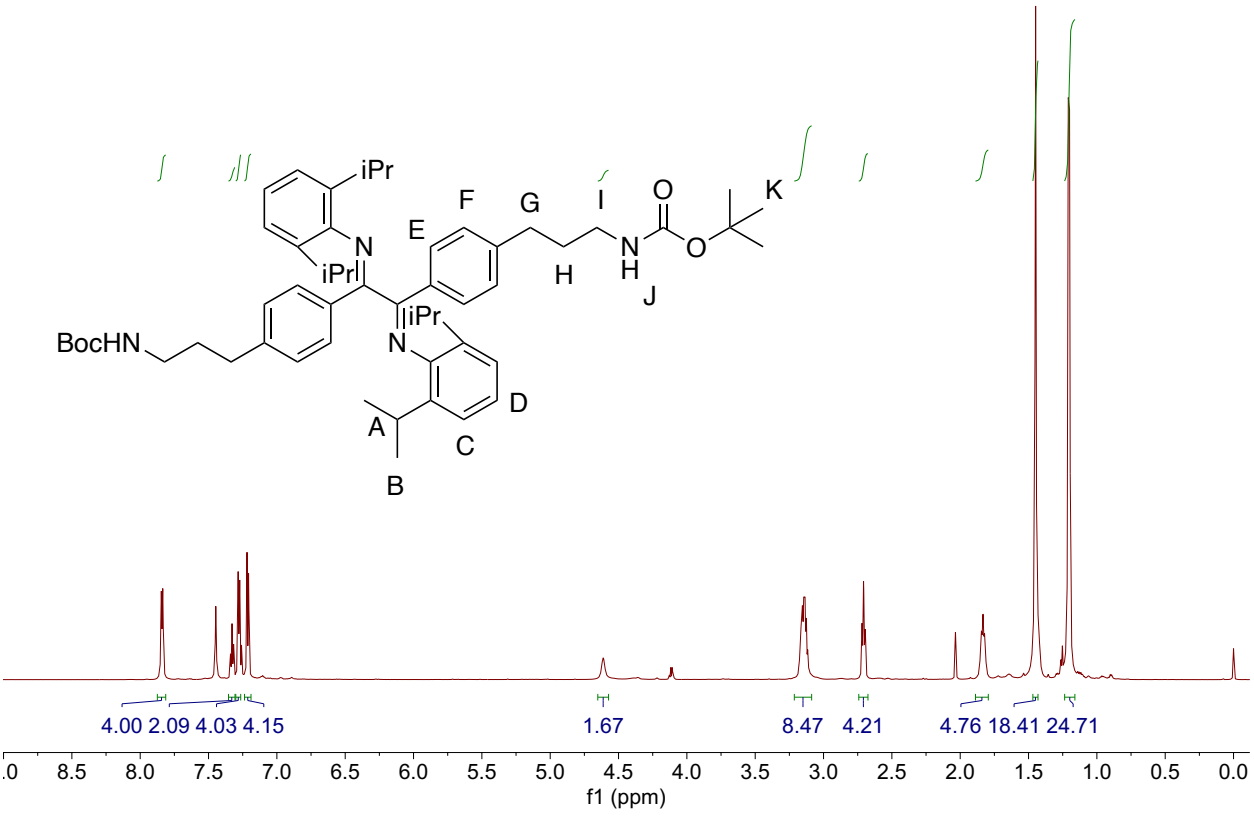

Figure A2 ^{1}H NMR of L2.5

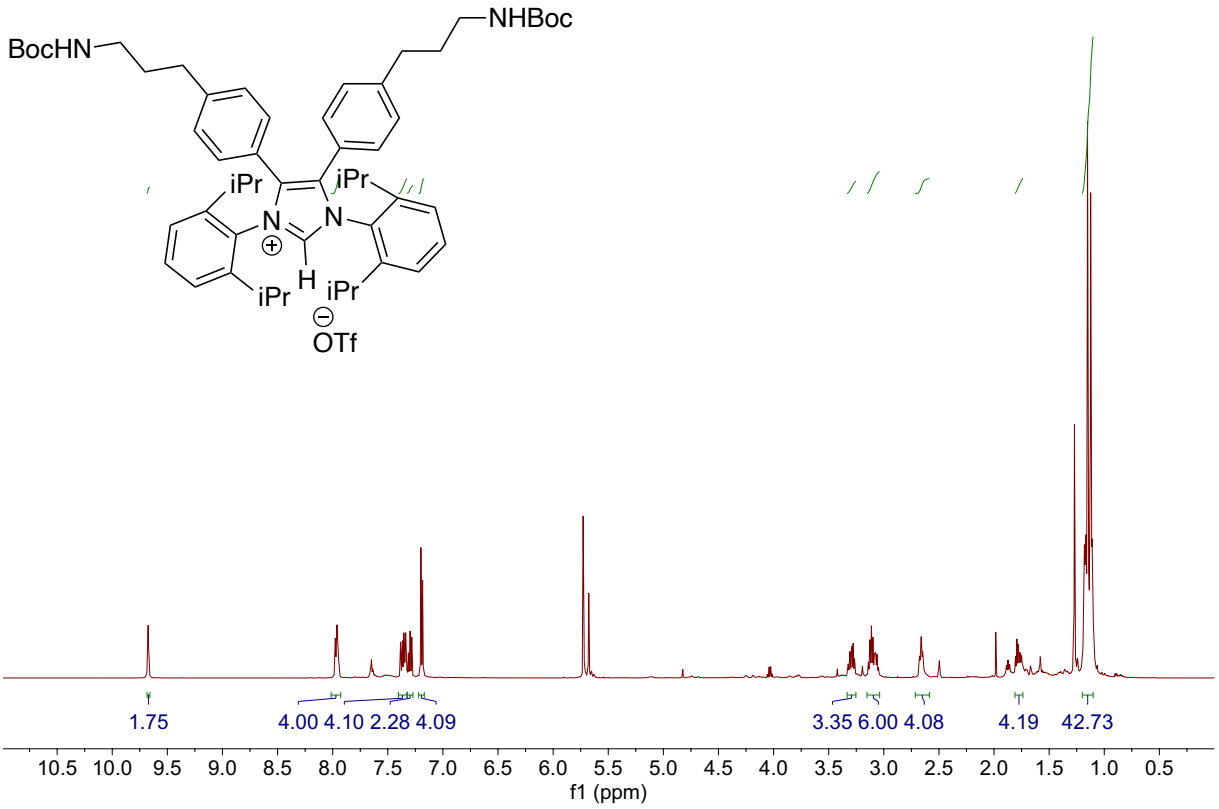

Figure A3 ^{1}H NMR of L2.6

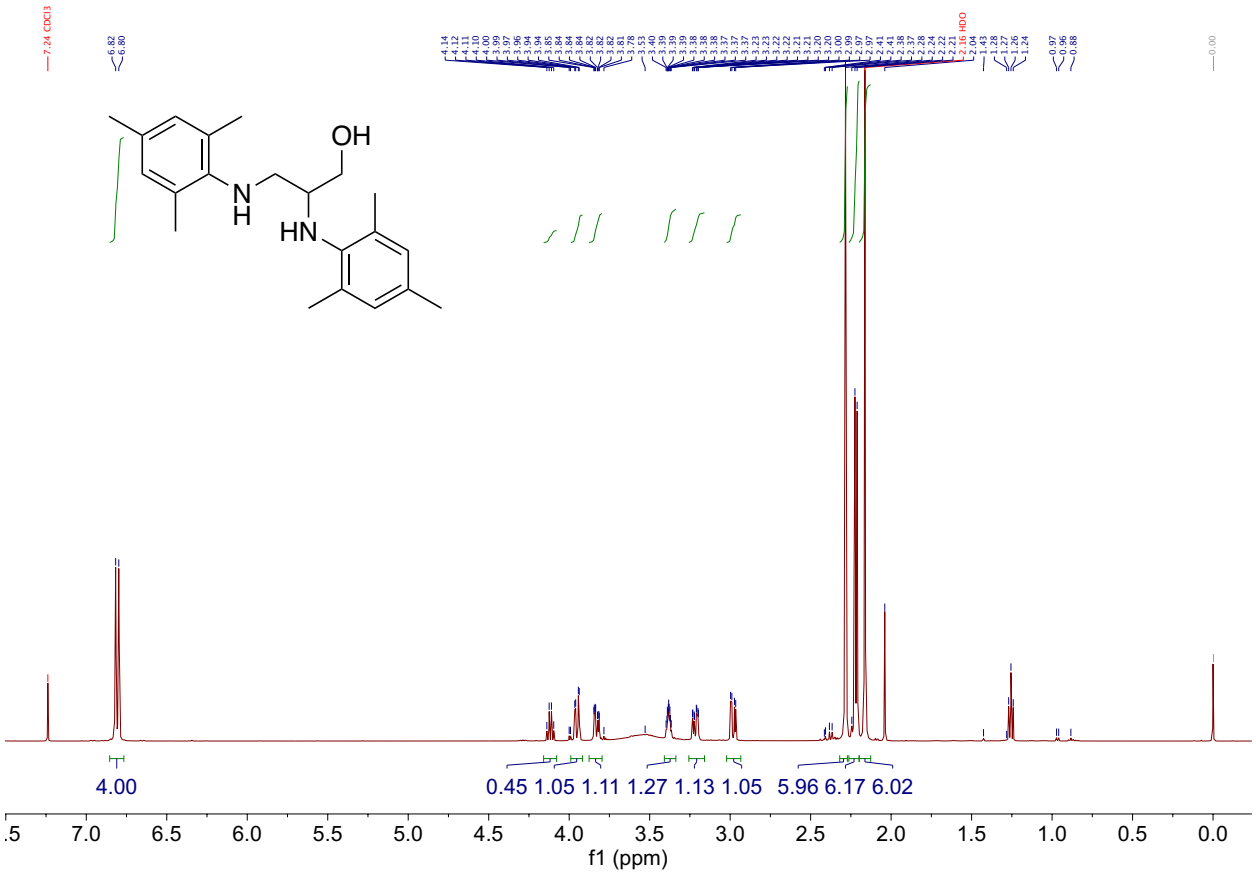

Figure A4 ^{1}H NMR of L3.1

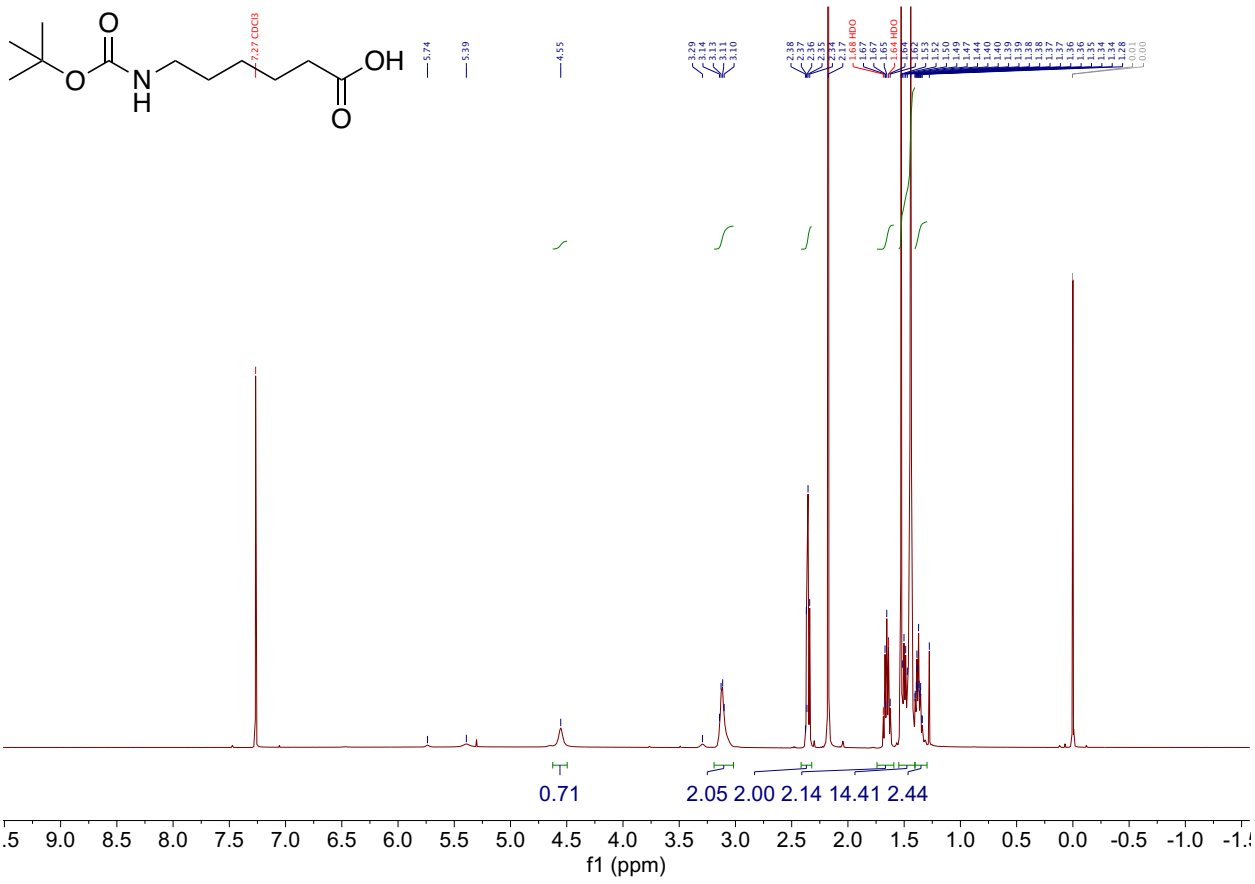

Figure A5 [1]H NMR of L3.2

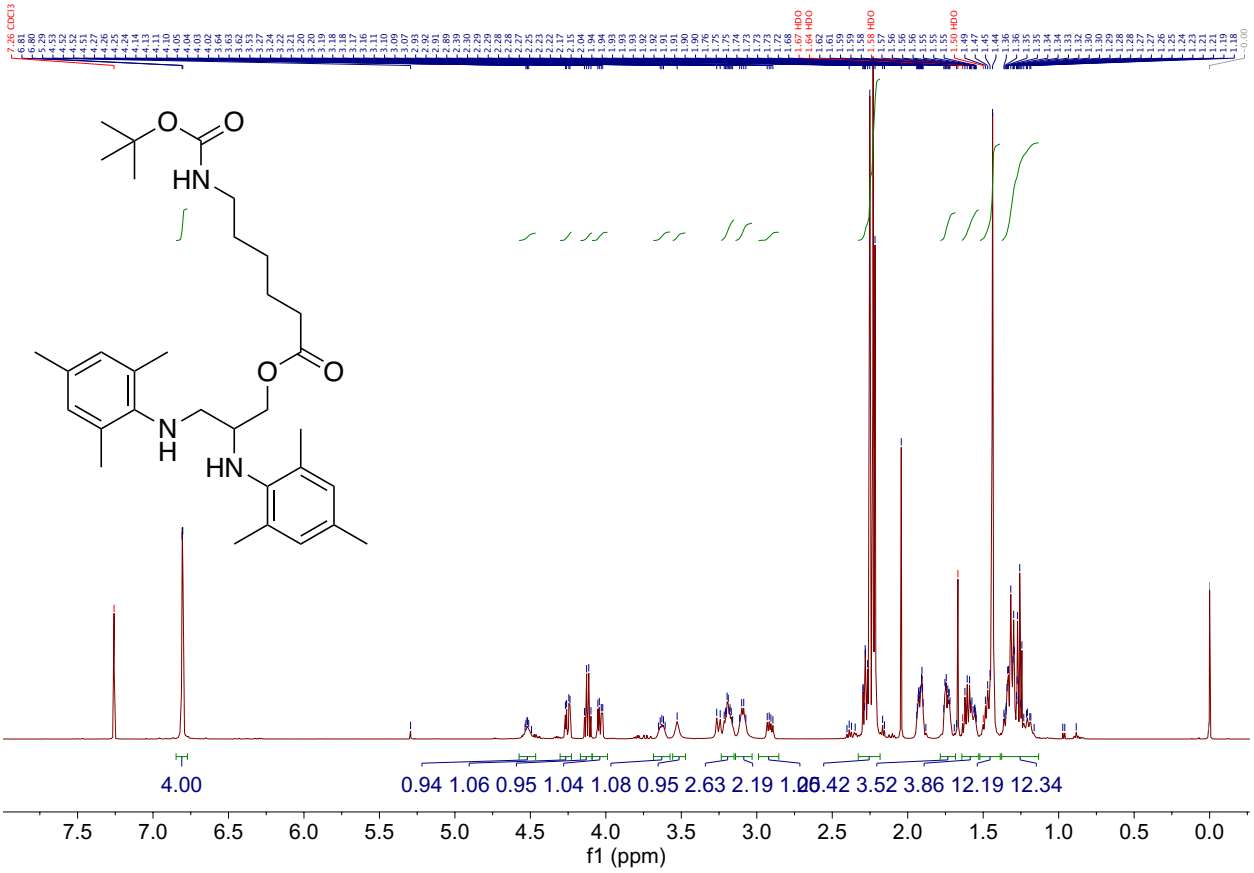

Figure A6 ^{1}H NMR of L3.3

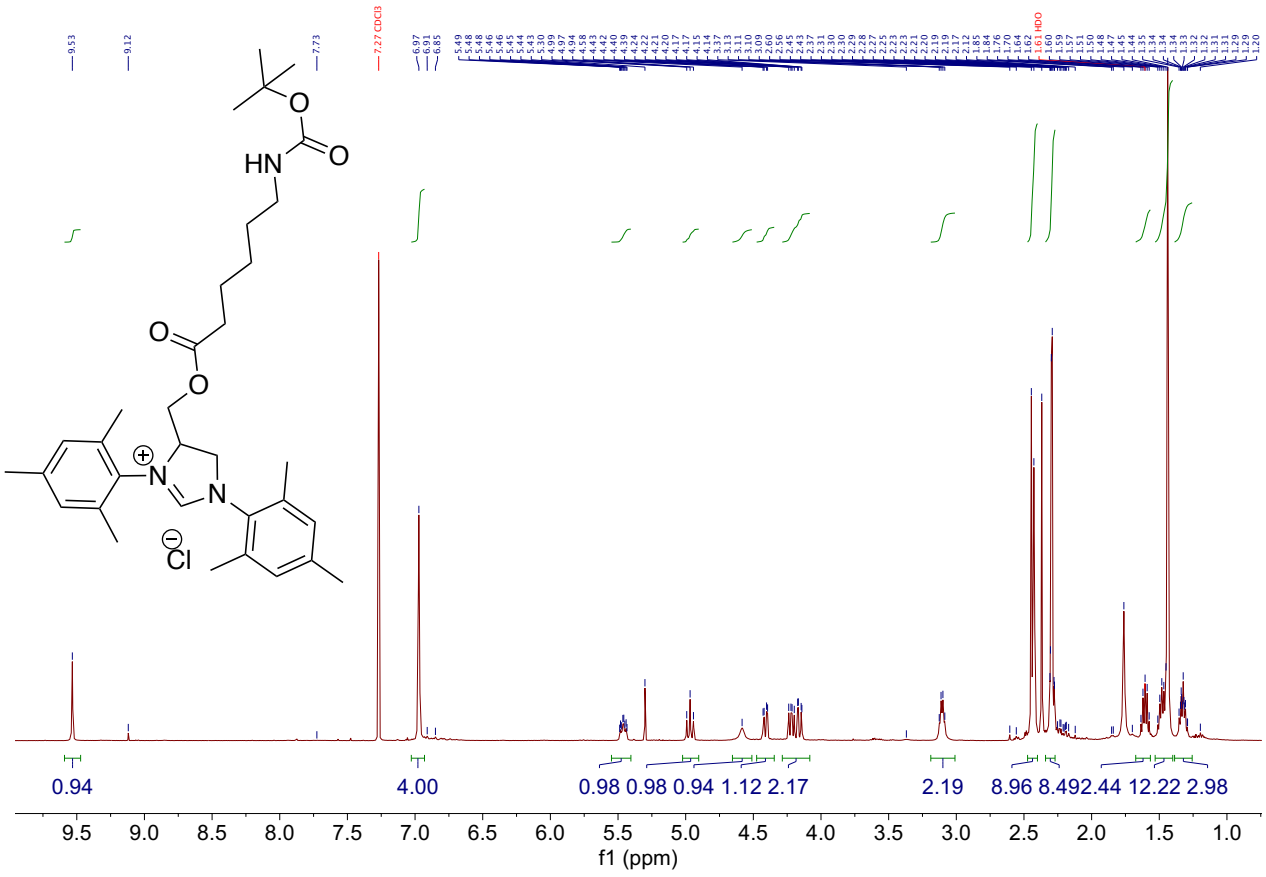

Figure A7 ^{1}H NMR of L3.4